

https://dspace.org/

Suction and shear strength relationships of granular materials

Katte, Valentine Yato

2016-03-17
http://hdl.handle.net/10539/20108

Downloaded from a DSpace repository. https://dspace.org/

SUCTION AND SHEAR STRENGTH RELATIONSHIPS OF GRANULAR MATERIALS

Valentine Yato Katte

A thesis submitted to the Faculty of Engineering and Built Environment, University of the Witwatersrand, in fulfillment of the requirements for the degree of Doctor of Philosophy.

Johannesburg, 2015

DECLARATION

I, Valentine Yato Katte, declare that this thesis is my own unaided work. It is being submitted for the degree of Doctor of Philosophy in the University of the Witwatersrand, Johannesburg. It has not been submitted before for any degree or examined in any other University.

----------day of ----------2015.

ABSTRACT

Unsaturated soils are the predominant soil type in moisture deficient areas of the world. These soils have the characteristic ‘suction’, which is the potential for a soil to absorb water. With more than one-third of the world located in moisture deficient zones, understanding the characteristics of these soils is important in enhancing engineering design and analysis.

Much of the research focus on unsaturated soils is centered on the formulation of the effective stress equation involving suction and its relevance to strength and volume change. Suction therefore is a key parameter linked to the behavior of these soils. It is made up of two components namely matrix and osmotic (solute) suction of which both are believed to influence soil properties. However, the exact role of each or both components in influencing the effective stress, strength and volume change behavior of unsaturated soils has not been fully verified. The hypothesis postulated is that osmotic or solute suction contributes to the shear strength of soils.

The focus of this research is experimentally to isolate the effect of osmotic suction and further evaluate its contribution as well as those of other capillary forces to the shear strength of granular soils.

The experimental method consisted in altering the suction characteristics of the pore matrix in granular soils by mixing it with various solutions. This was achieved by using distilled water, ionic solutions of NaCl and non-ionic solutions of detergent, and measuring the effects of these solutions on shear strength. In addition, surface tension measurements were made in a set of capillary tubes with these solutions and psychrometer tests were made on granular soils mixed with these solutions. Three sets of triaxial shear strength parameters and corresponding suction ranges were obtained from the verifications:

- Shear strength parameters and matrix suctions measured by the axis translation technique in the undrained triaxial test.
- Shear strength parameters measured in the drained triaxial test.

- Shear strength parameters measured in the undrained state on specimens exposed to different atmospheres in equilibrium with saturated salts solutions and others exposed to atmospheres in equilibrium with distilled water, ionic solutions of NaCl and non-ionic solution of detergent.

Results of the experiments revealed that though solute suction may indirectly influence the shear strength of granular soils, it does not contribute to it in a direct way. The Bishop equation appropriately describes the strength and deformable characteristics of unsaturated soils.

ACKNOWLEDGEMENTS

I am grateful to Professor G.E Blight who was my supervisor; I appreciate his guidance, support and advice. Unfortunately he could not live to see the end. I am grateful to Dr. Irvin Luker who has stepped in to help me go through. I also acknowledge Dr. Michelle Theron who acted as co supervisor while she was on staff in the School of Civil Engineering. I appreciate the advice of Professor Gerhard Heymann of the University of Pretoria. Mr. Norman Alexander assisted me in the laboratory and Ken Harman machined the triaxial bases. Mr. Bukhosi M Mathiya did most the drawings.

I appreciate the support and encouragement of the staff, especially those in the geotechnical group: Luis Torres and Charles MacRobert for support and encouragement.

I am grateful to the University of Witwatersrand for the some bursaries which enabled me to go through my research.

To the Minister of Higher Education of Cameroon and the Rector University of Dschang for granting me study leave.

I am grateful to Mr. Mufor Atanga who suggested South Africa as a possible study destination to me and enabled me to settle down. Also to the following families who opened their homes to me in South Africa: Ndoh, Nji, Mynhardt, Letsaol and the Cheyip's.

I found spiritual strength from folks within the Navigators, Redeemed Christian Church, Faith Bible Church and Roosevelt Park Baptist.

I appreciate numerous friends whom I cannot name here, my extended family and lastly to my wife Nji-Nkah and children Nsiyapnze-Katte, Aloh, and Chakunte who spent some lonely years without me.

TABLE OF CONTENTS

	PAGE
DECLARATION	ii
ABSTRACT	iii
ACKNOWLEDGEMENT	v
CONTENTS	vi
LIST OF FIGURES	xi
LIST OF TABLES	xv
1. INTRODUCTION	1
1.0 Background	1
1.1 Problem statement	2
1.2 Hypothesis	4
1.3 Objective of research	4
1.3.1 General Objective	4
1.3.2 Specific Objectives	5
1.4 Scope	6
1.5 Organisation of thesis	6
2. THE NATURE OF SUCTION IN SOILS	8
2.0 Introduction	8
2.1 The concept of suction	9
2.1.1 Air water interface and surface tension	10
2.1.2 Capillarity	15
2.2.3 Vapour pressure and humidity	18
2.2 Soil suction	21
2.3 Total suction	22
2.4 Matrix suction	23

2.5 Osmotic suction 24
2.6 Soil water potential 24
2.7 Components of soil water potential 25
2.8 Soil water characteristic curve 26
2.9 Methods of expressing suctions 34

3. THE BEHAVIOUR OF UNSATURATED SOILS 36
3.0 Introduction 36
3.1 Stress state in saturated soil 36
3.2 Stress state in unsaturated soil 38

4. SUCTION AND SHEAR STRENGTH MEASUREMENT IN UNSATURATED SOILS
PART 1 SUCTION MEASUREMENTS 55
4.0 Introduction 55
4.1 Direct matrix suction measurement 55
4.1.1 Suction plate 56
4.1.2 Tensiometers 57
4.1.3 Imperial college tensiometer 58
4.1.4 Osmotic tensiometer 60
4.1.5 Pressure plate 61
4.2 Indirect matrix suction measurement 63
4.2.1 Electrical conductivity sensors 63
4.2.2 Thermal conductivity sensors 65
4.2.3 Time domain reflectometry 67
4.2.4 In-contact Filter paper 69
4.3 Indirect osmotic suction measurement 71
4.3.1 Squeezing technique 71
4.4 Indirect total suction measurement 73

4.4.1 Thermocouple psychrometer 73
4.4.2 Transistor psychrometers (Relative humidity sensors) 76
4.4.3 Chilled –mirror hygrometer 77
4.4.4 Non-contact filter paper 79
4.5 Methods of controlling suction 79
4.5.1 Axis translation technique 80
4.5.2 Osmotic technique 80
4.5.3 Vapour equilibrium technique 81
4.6 Summary 82

PART II SHEAR STRENGTH MEASUREMENT 84
4.7 Introduction 84
4.8 Experimental techniques for testing unsaturated soils 84
4.9 Direct shear box testing 85
4.10 Triaxial Testing 87
4.11 The choice of equipment for research 90

5. EXPERIMENTAL SETUP AND RESULTS
5.0 Introduction 92
5.1 Materials 92
5.1.1 Limestone powder 92
5.1.2 Quartz powder 94
5.1.3 Fine glass beads 94
5.1.4 Particle size distribution 94
5.1.5 Specific gravity determination 95
5.1.6 Sample preparation 95
5.2 Surface tension measurement 96
5.2.1 Experimental theory 96
5.2.2 Surface tension measurement in sealed space 98
5.2.3 Results of surface tension measurement in sealed space 99

5.3 Measurement of total suction 99
5.3.1 Calibration of psychrometers 99
5.3.2 Set up for total suction measurements 101
5.3.3 Results of total measurements 101
5.4 Matrix suction and shear strength measurement 102
5.4.1 Calibration of triaxial cell 102
5.4.2 Consolidated undrained tests 103
5.4.3 Results of Consolidated undrained tests 104
5.5 Consolidated drained Triaxial on saturated specimens 104
5.5.1 Results of Consolidated undrained tests 105
5.6 Consolidated undrained tests on limestone specimens dried in salts solutions 105
5.6.1 Results of Consolidated undrained tests on limestone specimens dried in salts solutions 105

6. DISCUSSION OF RESULTS 106
6.0 Introduction 106
6.1 Discussion of surface tension measurements 106
6.2 Discussion of results of total suction measurements 109
6.3 Discussion of results of CU triaxial strength measurements 111
6.4 Discussion of results of CD triaxial strength measurements 118
6.5 Discussion of results of consolidated undrained tests on limestone specimens dried in salts solutions 121

7. SUMMARY, CONCLUSION AND RECOMMENDATIONS 124
7.0 Summary 124
7.1 Conclusions 124
7.2 Scientific relevance 126
7.3 Recommendations 127

8. REFERENCES 128

9. APPENDIX i

LIST OF FIGURES

FIGURE		PAGE
1.1	Isotropic stress on soil.	3
2.1	Soil hydrologic system and pressure profiles	9
2.2	Air water interphase	10
2.3	Surface tension phenomenon after Fredlund 1993.	13
2.4	Surface tension on a warped surface.	14
2.5	Behaviour of contact angle for a liquid on a solid.	15
2.6	Forces acting in a capillary tube	16
2.7	Capillary model of partly saturated porous material.	17
2.8	Relationship between total suction and Relative Humidity	23
2.9	Typical soil-water characteristic curves for sand, clay	27
2.10	McQueen and Miller conceptual model for SWCC.	28
2.11	An idealized hysteric soil water characteristic curve.	30
2.12	Hysteresis during consolidation (drying) and swelling	31
2.13	Drying and wetting characteristics found by Croney	32
2.14	A direct comparison of an oedometer consolidation curve and an atmospheric drying curve using a calibrated gypsum block to estimate suction.	33
3.1	Effective stress across a soil grain.	38

3.2 (a)	Three dimensional stress strain diagram for the swell of partly saturated soil under constant isotropic load.	44
3.2 (b)	Three dimensional stress-strain diagram showing contours of constant effective stress in partly saturated soils.	45
3.3 (a)	Semi quantitative validation of the closed-form equation for effective stress Group 1 soils: measure and fitted SSCCs for kaolin, Jossigny silt, Madrid clayey sand and sandy clay	51
3.3 (b)	Semi quantitative validation of the closed-form equation for effective stress Group 1 soils: (b) predicted SWCCs for these soils.	52
4.1	Suction plate	56
4.2	Soil moisture tensiometer	58
4.3	Imperial college tensiometer (Rideley et al., 2003)	59
4.4	Osmotic tensiometer (Bocking & Fredlund, 1979)	60
4.5	Pressure plate apparatus	62
4.6	Gypsum block	64
4.7	Thermal conductivity sensor	66
4.8	Pore fluid squeezer	72
4.9	Peltier type psychrometer	74
4.10	WP4 Chilled mirror psychrometer	77
4.11	Calibration characteristic curve for WP4	78
4.12	Shear box apparatus	85
4.13	Triaxial cell	88
5.1	Grain size distribution of granular materials	95
5.2	Experimental set up of glass capillary to measure surface tension	98
5.3	Calibration curve for psychrometer tip	100
6.1 (a)	Effects of ionic solute (NaCl) on the surface tension.	106

6.1(b) Effects of non-ionic solute (detergent) on the surface tension 107

6.2(a) Water content- total suction curves for Limestone Powder 109

6.2 (b) Water content- total suction curves for Quartz Powder 109

6.2 (c) Water content- total suction curves for Fine Glass Beads 110

6.3 (a) i Maximum deviator stress versus water content for limestone powder 112

6.3 (a) ii Matrix Suction versus water content for limestone powder 112

6.3 (b) i Maximum deviator stress versus water content for quartz powder 113

6.3 (b) ii Matrix Suction versus water content for quartz powder 113

6.3 (c) i Maximum deviator stress versus water content for fine glass beads 114

6.3 (c) ii Matrix Suction versus water content for fine glass beads 114

6.3 (d) s'-t' strength diagram showing the limits of measured strength for limestone powder 115

6.3 (e) s'-t' strength diagram showing the limits of measured strength for quartz powder 115

6.3 (f) s'-t' strength diagram showing the limits of measured strength fine glass beads 116

6.3 (g) s'-t' strength diagram showing the limits of measured strength for the soils mixed with 1 M NaCl at 2 % water content 118

6.4 (a): s´-t´ diagram for Limestone Powder in the CD test 119

6.4 (b): s´-t´ diagram for Quartz Powder in the CD test 119

6.4 (c): s´-t´ diagram for Fine Glass Beads in the CD test 120

6.5 (a) Plots of specimens dried over saturated salts, re- exposed to solutions of water, 1 M NaCl and detergent. 121

6.5 (b) Plots of total suction curves for limestone powder mixed with water (matrix suction) and limestone powder mixed with 1M NaCl (matrix + solute suction) 122

6.5 (c) Strength diagram plotted for Limestone powder in terms of ½(σ_1- σ_3) and ½(σ_1+σ_3) –u_w where σ_3 = 300 kPa and u_w = matrix suction for water content when tested. 123

LIST OF TABLES

TABLE		PAGE
2.1	Surface tension of contractile skin by (Kaye and Laby, 1973)	12
2.2	Vapour pressures of NaCl solutions by (Lang, 1967)	20
2.3	Vapour pressure of KCl solutions (Campbell & Gardner, 1971)	21
3.1	Soil descriptions and properties used to validate the Closed- Form Equation for Effective Stress.	51
4.1	Calibrations for estimating suctions by filter paper techniques	71
4.2	Summary of suction measurement methods	83
5.1(a)	Chemical properties of limestone powder.	93
5.1(b)	Physical properties of the limestone powder	93
5.1(c)	Chemical properties of the silica	94
5.1 (e)	Specific gravity of aggregates	95

APPENDIX

TABLE		PAGE
5.1	Grain size distribution of granular material	i
5.2(a)	Measurement of radii of glass capillaries	ii
5.2(b)	Surface tension measurements for distilled water and water diluted with ionic solute (NaCl).	iii
5.2(c)	Surface tension measurements for distilled water and water diluted with a non-ionic solute (detergent)	iv
5.3(a)	Results of calibration of psychrometer tips	v
5.3 (b)	Total suction values for Limestone Powder	viii
5.3 (c)	Total suction values for Quartz Powder	ix
5.3 (d)	Total suction values for Fine Glass Beads	x
5.4 (a-i)	Calibration of triaxial cell	xi
5.4 (a-ii)	Calibration of triaxial machines	xv
5.4 (b)	Results of triaxial strength parameters and suctions for Limestone powder	xvi
5.4 (c)	Results of triaxial strength parameters and suctions for Quartz Powder	vxiii
5.4 (d)	Results of triaxial strength parameters and suctions for Fine Glass Beads	xx
5.4 (e)	Results of s-t parameters Limestone Powder	xxii
5.4 (f)	Results of s-t parameters Quartz Powder	xxiv

5.4 (g)	Results of s-t parameters Fine Glass Beads	xxvi
5.5 (a)	Consolidated drained tests for Limestone powder	xxviii
5.5 (b)	Consolidated drained tests for Quartz powder	xxix
5.5 (c)	Consolidated drained tests for Fine Glass beads	xxx
5.5 (d)	The φ´ values of the consolidated drained tests soil.	xxxi
5.6	Shear strength parameters of limestone powder in different saturated solutions then exposed to atmospheres of distilled water, 1M NaCl and detergent. Initial water content 6%. total exposure time 6 months.	xxxii

APPENDIX

FIGURE		**PAGE**
5.3	Calibration curves for other psychrometers	vi-vii

CHAPTER ONE

INTRODUCTION

1.0 Background

The mechanics of unsaturated soils is a study that has been given considerable attention all over the world and more especially in regions where the average annual evaporation exceeds average annual precipitation as well as in areas which experience seasonal moisture deficits. Considering that more than one third of the world falls within the above described climatic zone (Barbour, 1999), unsaturated soil mechanics must, of necessity, be basic to geotechnical engineering. The engineering behavior of soil is intrinsically linked to a soil property termed suction. Suction simply defined is the potential of soil to absorb water. The suction concept was first developed in the field of soil science, which is considerably older than soil mechanics. The concept was originally developed for the soil-water-plant relationship at the beginning of the 1900's. It was in the mid twentieth century that soil suction was used to explain the mechanical properties of unsaturated soils at the Road Research Laboratory in England (Croney and Coleman, 1948, Croney, 1950). This marked the beginning of unsaturated soil mechanics, even though some years earlier Terzaghi investigated the effects of unsaturation in soil devoting a 12 page chapter to capillary forces in soils (Terzaghi, 1943).

The geo-professional has found it easier dealing with soils that are saturated than those that are unsaturated because, with the former, experimentation and formulations of the requisite equations are easier and more straight-forward than with unsaturated soil. This has therefore rendered designs in unsaturated soils to be conservative so as to avoid uncertainties. Still, there have been reported failures of compacted embankments, excavated and natural slopes and foundations using

unsaturated soils, but, with increasing scientific and technological advancement; there has been an improving degree of certainty in design, durability and use of this material in construction. Much research is still required in understanding how the shear strength of unsaturated soil relates with other soil parameters so as to increase reliability in design and construction. It is therefore important to evaluate how suction and shear strength relate so as to improve the knowledge base in this area resulting in confident interpretation of soil data, better design and construction with unsaturated soils and so limit potential hazards.

1.1 Problem statement

Much of the research interest in unsaturated soil mechanics revolves around the formulation of an effective stress equation for these materials and consideration as to whether, or under what circumstances, the principle of effective stress applies to unsaturated soils (Blight, 1982, Lu and Likos, 2006). Terzaghi (1936) originally stated the principle of effective stress and its relevance to saturated soils. The effective stress principle states that in an isotropic stress situation a change of volume is dependent on the difference between total stress and pore pressure as in figure 1.1 and expressed in equation 1.1. He recognized that the effective stress, as a stress state variable controls the shearing resistance and volumetric strains in soils.

$$\frac{\Delta \mathbf{V}}{\mathbf{V}} = \mathbf{c}\Delta\boldsymbol{\sigma}' \qquad \mathbf{1.1}$$

Through this concept, a rational approach at solving soil mechanics problems for saturated soils (previously very empirical) was born. The effective stress concept has proved workable in explaining

stress and volume changes that occur in saturated soils due to change in the applied external load.

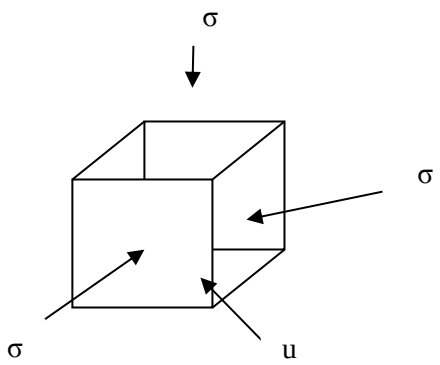


Figure 1.1 Isotropic stress applications on soil.

Extending this concept to unsaturated soils has been problematic because of the presence of pore fluid consisting of two phases; air and water.

At the inception of unsaturated soil mechanics, suction has been considered to be the combined effect of matrix and osmotic or solute suction. These concepts were developed in the disciplines of soil sciences for soil water and plant relationships, and so far no problems have been encountered with this concept within this discipline. The concept was taken over into unsaturated soil mechanics and perhaps it was assumed that since it worked very well in soil science, then the same must be true for shear strength and volume change of soils. Studies so far conducted within this discipline of soil mechanics have not given a precise and clear presentation how matrix and/or solute suction affect the shear strength of soils. For example, Sridharan & Venkatappa Rao, 1973 have asserted that osmotic suction plays a role in determining the behavior of soils, alluding that current formulations of the effective

stress equation do not account for osmotic suction. Still continuing in this thinking Allam & Sridharan, 1987 brought modifications to the effective stress and stress state variables approach to include osmotic suction and the contribution of the contractile skin stress. Also, studies carried out on marine soils indicate that the high salt content contributes to a high suction which in turn greatly influences the physical and volumetric changes of soil (Noorany, 1984 ., Barbour and Fredlund, 1989, Fredlund and Rahardjo, 1993, Feng et al., 2003). Sreedeep and Singh (2006) have concluded that most studies on suction wrongly approximate total suction to matrix suction. The basis of this conclusion is the assumption that the solutes present in the soil are dilute and hence the osmotic suction is negligible. On the other hand, Blight, (1982) in an attempt to revive the capillary model, quotes Casagrande's (1965) attempts to build a causeway across the Great Salt Lake in Utah. He mentioned that the clay forming the lake bottom has a shear strength gradient of only 6 kPa per metre depth. This is despite the fact that the clay contains crystalline salt and the pore fluid is therefore subject to a solute suction of the order of 40 000 kPa. Therefore the role of capillary and other intermolecular forces such as solute suction in the macroscopic stress, strength and volume change in the behavior of unsaturated soils have been uncertain. As such it is necessary to investigate the role of osmotic suction as it influences soil behavior, in particular the shear strength of soil.

1.2 Hypothesis

Osmotic suction significantly contributes to the shear strength of unsaturated soils.

1.3 Objective of the research

1.3.1 General Objective

The aim of this research was to experimentally isolate the effects of solute and matrix suction and evaluate them separately as well as examining other capillary forces, relative to matrix suction, while assessing the shear strength in a set of granular soils.

1.3.2 Specific Objectives

To attain the above general objectives the following specific objectives where set in place:

1. An array of capillary tubes to be set up to measure the surface tension of distilled water, water containing an ionic solute (NaCl) and a non-ionic solute, namely a detergent.

2. Total suction measurements to be made on samples of a number of different granular materials prepared with distilled water, dilute NaCl and detergent solutions.

3. Consolidated undrained shear strength measurements to be made on specimens prepared from the granular materials using the same solutions and determining their matrix suctions using the axis translation technique (ATT).

4. Consolidated drained shear strength measurements to be made on saturated specimens prepared from the granular materials using the same solutions.

5. Consolidated undrained shear strength measurements to be made on specimens prepared from the granular materials using the same solutions after equilibrating in controlled atmospheres of 90-98 % relative humidity for three months as well as in atmospheres in equilibrium with pure water, dilute salt and detergent solutions respectively for three months.

6. Pairs of capillary tubes to be set up side by side each within its own sealed air space, with one dipping into distilled water and the other into dilute solutions of NaCl and observing the equilibrium capillary rises.

1.4 Scope

Prior to carrying out the research, an exhaustive literature search was conducted to examine the work carried out so far on suction and shear strength relationships of soils. The scope of the work was primarily experimental with the objectives outlined above. As such, three granular materials were chosen for this work: limestone powder, quartz powder and fine glass beads. These were chosen to give aggregates with pH >7 (limestone), < 7 (quartz) and < 7 but also of uniform approximately spherical particles (glass beads). Suction and shear strength measurements were taken at various concentrations of pore fluids and at a range of moisture contents below 10 %.

1.5 Organization of thesis

The thesis has been arranged in the following manner:

Chapter one covers the introduction, problem statement, objectives, scope and, finally, the organisation of the work.

Chapter two covers the nature of suction in soils.

Chapter three covers the behaviour of unsaturated soils mentioning the historical developments of the effective stress equation.

Chapter four covers suction and shear strength measurement in unsaturated soils.

Chapter five describes the experimental set up and results obtained.

Chapter six covers the discussion of results of the experimental set up.

Chapter seven covers the summary, conclusions, relevance and recommendations.

CHAPTER TWO

THE NATURE OF SUCTION IN SOILS

2.0 Introduction

Soil is a particulate medium made of numerous discrete particles with a range of sizes, arranged in a complex geometry which leaves room for voids. The particle shape, origin, size, and voids influence the soil porous system. The soil porous system has been characterized as a two phase or a three phase medium. The two phase medium comprises either particle solids and water or particle solids and air while the three phase medium is made up of solid particles, water and air. An unsaturated soil is defined as one whose voids are filled with water and air, and as such is often called a three phase system. Fredlund and Morgenstern (1997) has called the air-water-interface or contractile skin on the liquid menisci, the fourth phase. It is this fourth phase which renders unsaturated soils particularly different from saturated soils in terms of engineering properties. Unsaturated soils are found in arid and semi-arid regions and where there is a deep groundwater. The climate in these areas is characterised by an annual evaporation greater than the annual precipitation. Since the presence of the least air in soils renders them unsaturated, then most of the soils used as construction materials are in the unsaturated state and may remain in that condition during the useful life of the structure. The behaviour of unsaturated soils then becomes very important in a diverse range of geotechnical and geo-environmental projects such as earth dams, embankments, waste containment facilities, slope stability problems and also in agricultural water application to crops in the unsaturated zone. Therefore phenomena like capillarity, suction and swelling/shrinkage become important parameters in understanding the behaviour of unsaturated soils.

2.1 The concept of suction

The soil profile acts as a reservoir for water which is stored within the soil porous system by adhesive, cohesive and capillary forces. Above the water table three distinct zones have been identified, namely the soil-water zone, the vadose zone and the capillary fringe. Below the water table is groundwater. The water table is the boundary at which the pore water pressure is zero. Above this boundary, the pore pressure is negative and below it, is positive.

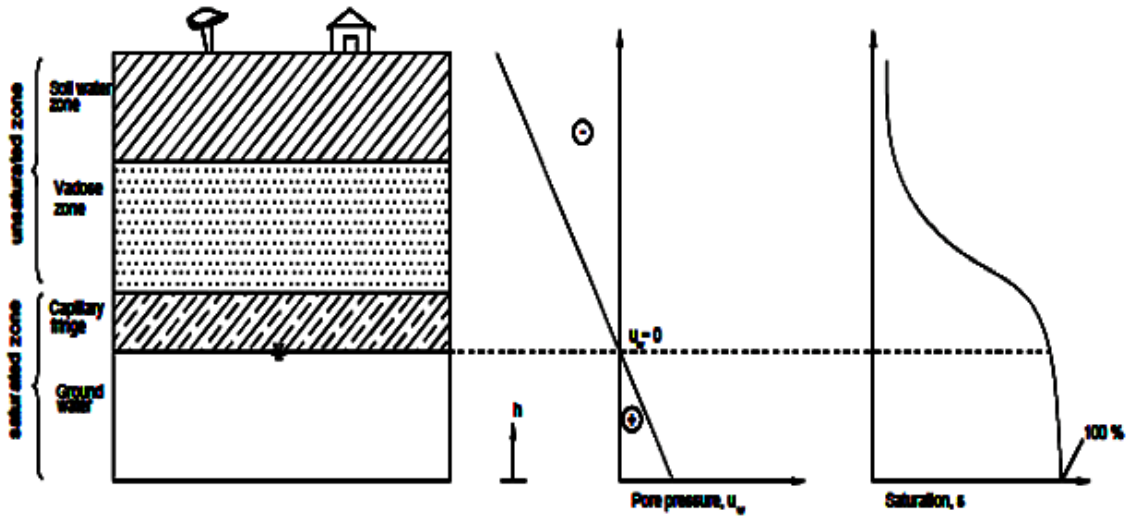


Figure 2.1 Soil hydrologic system and pore pressure profiles

The soil-water zone and the vadose zone contain pores that are partly filled with air and water and are referred to as the unsaturated zone. The capillary fringe is just below the vadose zone and is saturated but its pore pressure is negative or under tension. The unsaturated zone plays an important role in the biological, physical and chemical processes of the earth. This zone supports biological life and the intricate slow weathering processes. Both the saturated and unsaturated zones are influenced by climatic factors such as precipitation, evaporation and

transpiration. The soil in the unsaturated zone is characterised by a negative pore pressure referred to as suction. There are many other terms synonymous to suction such as soil moisture deficiency, soil water pressure deficiency, capillary suction, matrix suction, capillary potential, capillary water stress, pore water tension, soil water free energy and soil moisture tension. As you move from the point of zero atmospheric pressure towards the soil surface, there is increasing desiccation and the pore water pressure becomes increasingly negative. Curve liquid bridges can be observed linking soil particles. This curvature is due to the pressure difference between the air and water phase. The properties of the air water interface have an important bearing on the mechanical properties of unsaturated soils. Figure 2.2 below illustrates the air water interface

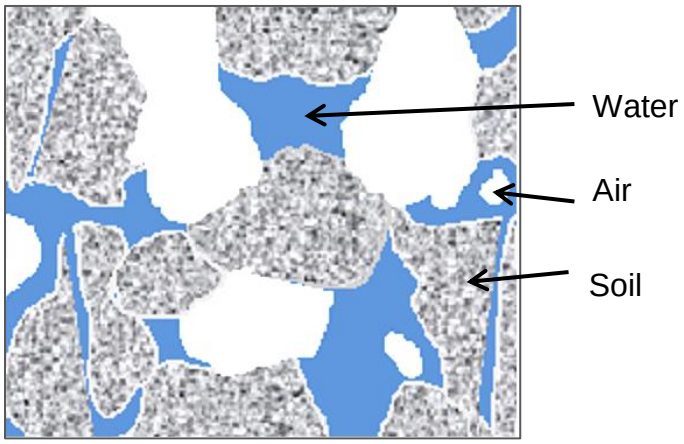


Figure 2.2 Air water soil interphase

2.1.1 Air water interface and surface tension

Surface tension is the phenomenon resulting from the physics of the contractile skin which results from an imbalance of forces acting on the molecules comprising the liquid phase and air phase. In the case of

water specifically, molecular attraction between water molecules (cohesion) exerts a stronger pull than the attraction between air and water molecules (adhesion). This is more evident for molecules located at the surface where the interaction is greatest, thus creating an imbalance toward the bulk of the water. For the system to remain in equilibrium an interfacial tension then develops across the air-water interface called surface tension. Therefore two distinct entities or properties are evident: the air-water interface and the bulk water. Davis and Rideal, (1963) discovered that the properties of the contractile skin are different from the contiguous water phase. They found that the contractile skin has reduced density, and increased heat conductivity while its birefringence data is similar to that of ice. Terzaghi made the same observation, noting that the properties of the contractile skin are different from water. The presence of the contractile skin is evident when an insect such as a water spider walks on top of the contractile skin and the back swimmer walks underneath it.

Surface tension can be defined thermodynamically as well as mechanically. Mechanically, surface tension is defined as the force per unit length required to enlarge the interfacial surface. (Lyklema, 1990, Adamson and Gast, 1997) Thermodynamically, surface tension has been defined by Lyklema (2000) as:

$$\mathbf{T_s} = \left(\frac{\partial \mathbf{F}}{\partial \mathbf{A}}\right)_{\mathbf{V,T,n}} \qquad \mathbf{2.1}$$

$$\mathbf{T_s} = \left(\frac{\partial \mathbf{G}}{\partial \mathbf{A}}\right)_{\mathbf{P,T,n}} \qquad \mathbf{2.2}$$

where T_s is the surface tension, A is area; F and G are the Helmholtz and Gibbs energies. The subscript P refers to pressure, T to temperature and n to the composition of the system. The units of surface tension are force/length or energy/area, i.e. Nm^{-1} or Jm^{-2}. The surface tension is tangential to the contractile skin surface therefore exerting a pull on it. At 20°C the surface tension of water is 72.8 x 10^{-2} Nm^{-1} or Jm^{-2}. Since surface tension is an intermolecular phenomenon, anything that influences the intermolecular arrangement will affect surface tension. As such, surface tension is influenced by temperature and solute concentration. An increase in temperature causes a decrease in surface tension. Table 2.1 gives the surface tension values for the contractile skin of pure water at different temperatures.

Table 2.1 Surface tension of contractile skin of pure water (Kaye and Laby, 1973)

Temperature T (ºC)	Surface tension T_s (N/m)
0	75.7
10	74.2
15	73.5
20	72.75
25	72.0
30	71.2
40	69.6
50	67.9
60	66.2
70	64.4
80	62.6
100	58.8

A mathematical relation for surface tension can be established by imagining a hypothetical curved water surface due to an imbalance of forces in the bulk of the water. The resulting effect of the imbalance of forces is a curved air-water interface as shown in the figure 2.3. As such, a relationship can be drawn between surface tension and radius of the curved surface.

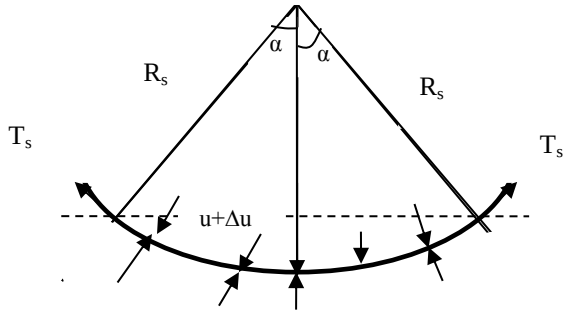


Figure 2.3 Surface tension phenomenon at the air water interface. Pressures and surface tension acting on a curved two dimensional surface (Fredlund and Rahardjo 1993)

The membrane has a radius of curvature R_s and the surface tension is T_s. The equilibrium of forces in the vertical direction leads to:

$$\mathbf{2}\boldsymbol{T_s}\mathbf{sin\alpha} = \mathbf{2\Delta u R_s sin\ \alpha} \qquad \mathbf{2.3}$$

2R sin α is the length of the membrane projected into the horizontal plane.

Rearranging equation 2.3 gives:

$$\Delta\mathbf{u} = \frac{\mathbf{T_s}}{\mathbf{R_s}} \qquad \mathbf{2.4}$$

Assuming that the shape of the contractile skin is also curved in the plane perpendicular to that of Figure 2.3 as shown in Figure 2.4. Equation 2.4 becomes:

$$\Delta \mathbf{u} = \mathbf{T_s}\left(\frac{\mathbf{1}}{\mathbf{R_1}} + \frac{\mathbf{1}}{\mathbf{R_2}}\right) \qquad \mathbf{2.5}$$

If the surface is hemispherical, $R_1 = R_2 = R_s$ and

$$\Delta \mathbf{u} = \frac{\mathbf{2T_s}}{\mathbf{R_s}} \qquad \mathbf{2.6}$$

where Δu = pressure increase [N/m^2]

R_s = radius [m]

T_s = surface tension of water [N/m]

α = subtended at the centre of curvature

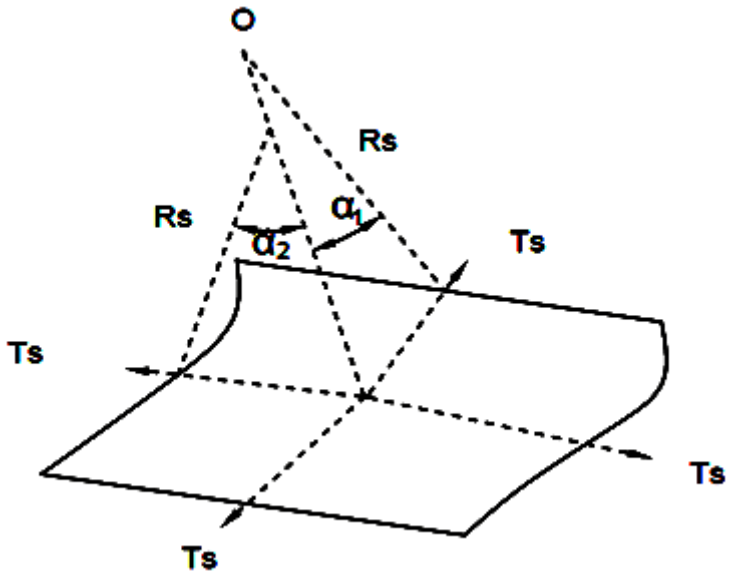


Figure 2.4 Surface tension on a warped surface

2.1.2 Capillarity

Capillarity is a phenomenon directly related to surface tension. When a liquid comes to equilibrium with its vapour and in contact with a solid surface, a contact angle θ is formed and is measured through the liquid as shown in figure 2.5 below. The contact angle results from equilibrium between the cohesive forces within the liquid molecules and the adhesive forces between solid and liquid molecules. For a contact angle θ = 0°, the surface is completely wet and the solid is perfectly hydrophilic. A partial wetting of the surface occurs for 0 < θ < 90° and the solid is partially hydrophilic and when θ ≥ 90° a non-wetting surface occurs and the solid is hydrophobic. Capillarity will cause water to rise up in a fine glass capillary because it wets the contact surface due to surface tension, producing a concave surface at the air-water boundary.

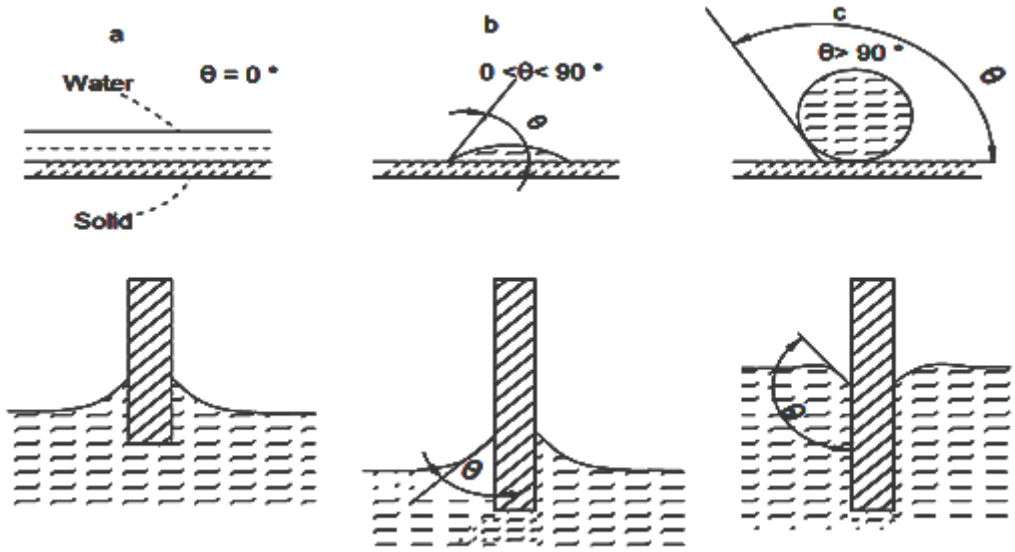


Figure 2.5 Behaviour of contact angle for a liquid on a solid

Figure 2.6 shows water raised to a height h_c in a fine capillary of radius r, then h_c, the height of water suspended in the bore is in equilibrium with the surface tension acting at the bore circumference. Resolving these forces leads to:

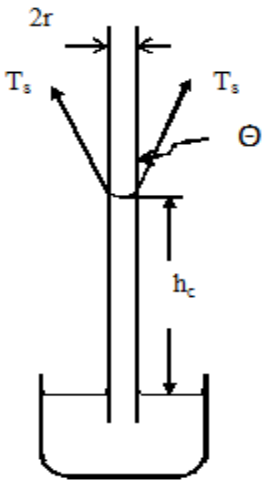


Figure 2.6 Forces acting in a capillary tube.

$$2\pi r \cos\theta \, T_s = h_c \gamma_w \pi r^2 \qquad 2.7$$

$$h_c = 2\frac{T_s \cos\theta}{r\gamma_w} \qquad 2.8$$

where: r = radius of fine capillary [m]

T_s = surface tension of water [N/m]

h_c = capillary height [m]

This phenomenon is responsible for soil water rising above the water table in soils. The soil pores act as tortuous capillary tubes with varying tube diameters. This is what has been termed the capillary model. A typical graphic presentation of this model for soil is given by (Marshall, 1959), shown in Figure 2.6. At the top of the capillary bore where the elastic film exists (contractile skin), the pressure difference across the film can be expressed by the Young – Laplace equation given as:

$$\Delta \mathbf{P} = (\mathbf{u_a} - \mathbf{u_w}) = \mathbf{2T_s}\left(\frac{\mathbf{1}}{\mathbf{r}}\right) \qquad \mathbf{2.9}$$

where T_s is the surface tension of the water and r is the radius of the capillary meniscus.

The Kelvin equation (Aitchison, 1965) represents the pressure difference as:

$$\Delta \mathbf{P} = \mathbf{-311 log_{10} H [MPa]} \qquad \mathbf{2.10}$$

where H is the relative humidity of the pore air above the meniscus.

Substituting the matrix suction (u_a-u_w) for ΔP in Equation 2.10 enables it to be expressed as a function of the relative humidity:

$$(\mathbf{u_a} - \mathbf{u_w}) = \mathbf{-311 log_{10} H\ [MPa]} \qquad \mathbf{2.11}$$

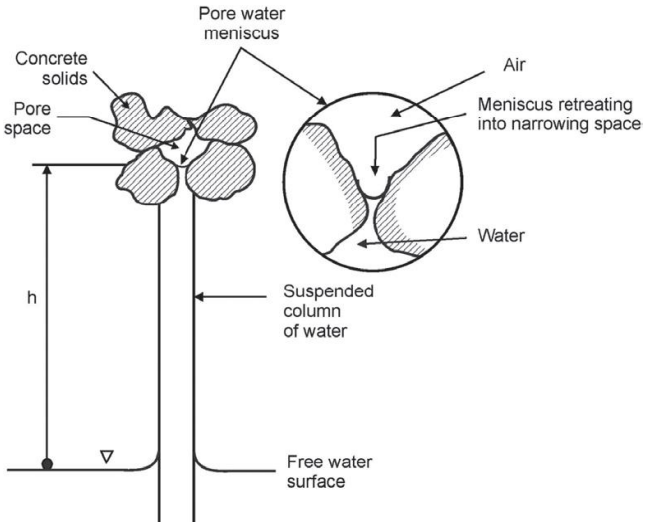


Figure 2.7 Capillary model of partly saturated porous material

2.2.3 Vapour pressure and humidity

At the air-water interphace there is the constant exchange of water molecules between the air and the bulk water. The water molecules that leave the bulk water form vapour and mix with the air above the air-water boundary. Some of the vapour condenses and returns to the bulk water. The kinetic theory offers an explanation of this phenomenon. Some of the water molecules have sufficient energy to overcome the cohesive forces and escape the bulk liquid.

Using the analogy of a vessel of air above water, enclosed by a moveable piston, we can understand better what goes on. If the piston is withdrawn creating some space above the water, then evaporation begins and water vapour fills the space. Initially more water vapour escapes and fills the space than returns into the liquid. Then after some time equilibrium is attained where the amount of water escaping equals the amount of water vapour entering. At this equilibrium state, the water vapour is at its optimum and is called the saturated vapour pressure. As the piston is withdrawn again further evaporation continues until an equilibrium state is again attained. Similarly pushing on the piston causes more water vapour to condense and return to the liquid. If the temperature of the system is raised, more molecules gain energy and escape, thus increasing the rate of evaporation and so also the saturated vapour pressure.

In an open system, similar to the real-life situation where water is exposed to the atmosphere, evaporation proceeds just as in a closed system. Dalton’s law of partial pressures becomes applicable. According to this law a mixture of gases exerts a pressure which is equal to the sum of the partial pressures of the separate gases.

Humidity is a measure of the amount of water vapour contained in the air. The maximum humidity is obtained at a given temperature when the partial pressure of water in the air equals the saturated vapour pressure of water at that temperature. Relative humidity is given as:

$$\textbf{Relative humidity} = \frac{\textbf{Partial pressure of water vapor}}{\textbf{Saturated vapor pressure of water}} \textbf{ x } \textbf{100}\% \quad \textbf{2.12}$$

In the atmospheric sciences condensation is reckoned as either the formation of dew or frost when the relative humidity attains 100 %. When air laden with water vapour is cooled sufficiently, condensation takes place. The temperature at which this condensation begins is the dew point temperature. This is what takes place at night as the temperature drops and cools the surrounding air resulting in dew formation. Applications of this principle have found relevance in some suction measuring equipment such as relative humidity sensors.

When non-volatile solutes (e.g NaCl) dissolve in pure water, the vapour pressure of the NaCl-water solution becomes less than that of the pure water. The addition of the solute has reduced the chemical potential of the salt solution relative to that of pure water. This reduced chemical potential is reflected in a reduced kinetic energy therefore less molecular transfer into the vapour phase occurs. Raoult's law states that for an ideal solution the partial vapour pressure of a component of the solution is equal to the mole fraction of that component times its vapour pressure alone. This law is expressed mathematically by the equation:

$$\mathbf{VP_{solution}} = \mathbf{VP_{pure\ solvent}} * \ \mathbf{M_{solvent}} \qquad \mathbf{2.13}$$

where $M_{solvent}$ = the mole fraction of the solvent

$VP_{pure\ solvent}$ = vapour pressure of pure solvent

$VP_{solution}$ = vapour pressure of solution

However, for a non-volatile component dissolving in another non-volatile solution, the partial pressure of any component equals the vapour pressure of that component multiplied by the mole fraction of the component.

The vapour pressures of salt solutions (e.g. NaCl and KCl) have found application in the calibration of suction measuring devices and are also used to induce suction in soil specimens. Tables 2.2 and 2.3 give values of (u_a-u_w) according to equations 2.11 to 2.13 taking into account different temperatures for NaCl and KCl respectively:

Table 2.2 Vapour pressures of an enclosed air mass over NaCl solutions by (Lang, 1967)

NaCl molality	Temperature								
	0°C	5°C	10°C	15°C	20°C	25°C	30°C	35°C	40°C
	Osmotic suction (kPa)								
0.05	214	218	222	226	230	234	238	242	245
0.1	423	431	439	477	454	462	470	477	485
0.2	836	852	868	884	900	915	930	946	961
0.3	1247	1272	1297	1321	1344	1368	1391	1415	1437
0.4	1658	1693	1727	1759	1791	1823	1855	1886	1917
0.5	2070	2115	2158	2200	2241	2281	2322	2362	2402
0.7	2901	2967	3030	3091	3151	3210	3270	3328	3385
1.0	4169	4270	4366	4459	4550	4640	4729	4815	4901
1.2	5032	5160	5278	5394	5507	5620	5730	5835	5941
1.5	6359	6529	6684	6837	6986	7134	7276	7411	7548
1.7	7260	7460	7640	7820	8000	8170	8330	8490	8650
2.0	8670	8920	9130	9360	9570	9780	9980	10160	10350

Table 2.3 Vapour pressure of an enclosed air mass over KCl (Campbell and Gardner, 1971)

KCl molality	Temperature						
	0°C	10°C	15°C	20°C	25°C	30°C	40°C
	Osmotic suction (kPa)						
0.0	0.0	0.0	0.0	0.0	0.0	0.0	0.0
0.1	421	436	444	452	459	467	474
0.2	827	859	874	890	905	920	935
0.3	1229	1277	1300	1324	1347	1370	1392
0.4	1628	1693	1724	1757	1788	1819	1849
0.5	2025	2108	2148	2190	2230	2268	2306
0.6	2420	2523	2572	2623	2672	2719	2765
0.7	2814	2938	2996	3057	3116	3171	3226
0.8	3208	3353	3421	3492	3561	3625	3688
0.9	3601	3769	3846	3928	4007	4080	4153
1.0	3993	4185	4272	4366	4455	4538	4620

2.2 Soil Suction

Suction is defined as the free energy state of soil water (Edlefsen and Anderson, 1943). This is the free energy state of soil water relative to a pool of pure water at the same temperature and pressure. Depending on their particle size and distribution, dryer soils may have a higher suction value than wetter soils. Suction is measured in Pascals = Nm^{-2} = Nmm^{-3} = Jm^{-3} i.e. energy per unit volume. Total suction is made up of two components: matrix suction, denoted by (ψ_m) and osmotic or solute suction, denoted by (ψ_o). The sum of these is called total suction. It is usually expressed as:

$$\psi_t = \psi_m + \psi_o \qquad 2.14$$

2.3 Total suction

At the soil review panel for the soil mechanics symposium, “Moisture Equilibria and Moisture changes in Soils’’ (Aitchison, 1964) adopted some definitions from the International Society of Soil Science which have been accepted in soil mechanics. Total suction is defined as ”The negative gauge pressure relative to the external gas pressure on the soil to which a pool of pure water must be subjected in order to be in equilibrium through a semi permeable membrane (permeable only to water molecules) with the soil water’’.

The relationship between total soil suction and the partial pore water vapour pressure is given by Kelvin’s equation below:

$$\psi_t = \frac{RT}{v_{wo} w_v} \ln\left(\frac{p}{p_0}\right) \qquad 2.15$$

where ψ_t = Total suction [kPa]

R = Universal gas constant [8.314 Nm/Kmol]

T = Absolute temperature [K]

v_{wo} = Specific volume of water [m^3/kg]

w_v = Molecular mass of water vapour [18.016 kg/kmol]

p = Partial pressure of water vapour in equilibrium with the soil water [kPa].

p_o = Partial pressure of the water vapour in equilibrium with an identical solution at atmospheric pressure [kPa].

The term (p/po) in the Kelvin equation is called the relative humidity, denoted as RH. The relationship between the relative humidity and suction is given in the figure 2.8 (below).

Total suction ranges from 0 kPa to the region of 1 GPa which corresponds to a virtually dry state of the soil.

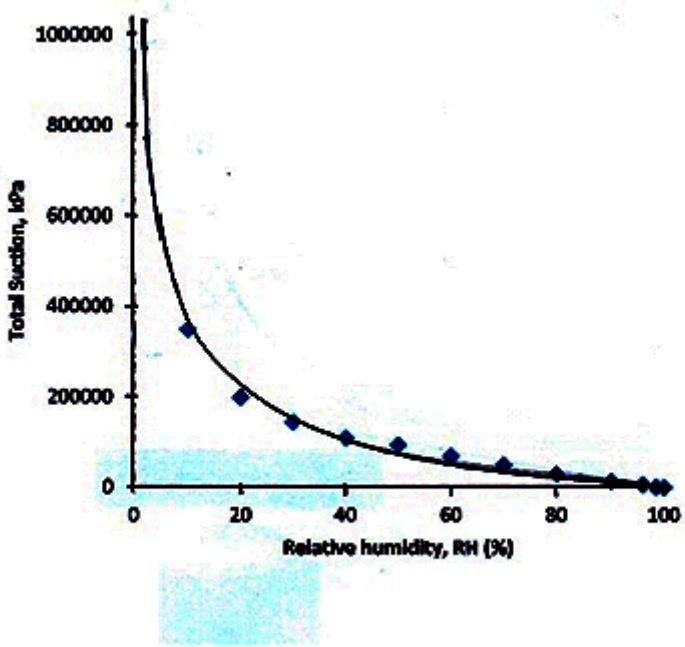


Figure 2.8 Relationship between total suction and relative humidity

2.4 Matrix suction

Matrix suction is defined as ‘‘The negative gauge pressure relative to the external gas pressure on the soil water to which a solution identical in composition with the soil water must be subjected in order to be in equilibrium through a semi-permeable membrane with the soil water’’. (Aitchison, 1965)

Matrix suction results from capillarity, texture and surface absorptive forces of the soil matrix. It is expressed as the pressure difference between the water and air across the air-water interface and is given by the relation below:

$$\psi_m = (u_a - u_w) \qquad 2.16$$

Referring to the previous chapter for equilibrium at the air water interface in a thin glass capillary inserted in a vessel containing water, the pressure difference across the air-water-interface can be expressed as:

$$(\mathbf{u_a} - \mathbf{u_w}) = \frac{\mathbf{2T_s}}{\mathbf{r}} \qquad \mathbf{2.17}$$

2.5 Osmotic suction

Osmotic suction is defined by Aitchison *et al*, (1965) as ‘‘The negative gauge pressure relative to the external gas pressure on the soil to which a pool of pure water must be subjected in order to be in equilibrium through a semi-permeable membrane (permeable only to water molecules) with free pure water’’.

Osmotic suction is also called solute component of free energy of free water. This arises from the differences in ion concentration of dissolved salts contained in the soil water.

2.6 Soil water potential

Water movement in soils is controlled by the difference in potentials or energy in the pores. This is what is referred to as soil water potential. The state of water in soils is characterized by the amount of water and its free energy. Three types of energy are involved - potential, kinetic and chemical. The difference in energy level from one point or state of soil (wet soil) to another, (dry soil) determines the direction of movement of water in soils. Soil water movement takes place from a higher potential to a lower potential. The standard reference is the potential of pure water in a free state, where the potential is taken as zero. In soils containing dissolved salts the potential is lower, so water will then flow into it until equilibrium is achieved. This concept is more used in the soil-water-plant relationship. In plant physiology positive work is being done as

plants take up water against the absorptive forces while negative work is being carried out when soil absorbs water from plants, causing them to wilt.

2.7 Components of soil water potential

Water in soil has many forces acting upon it, so its potential energy is variable within the soil matrix. These forces include:

i. Matrix forces resulting from the interaction of the solid, liquid and gaseous phases of the soil. The potential for work to be done by these forces is what is referred to as the matrix potential, ψ_m

ii. Osmotic forces resulting from the differences in the chemical composition of the soil water. The potential for work to be done by these forces is referred to as the osmotic or solute potential, ψ_o

iii. Gravitational forces (and other forces such as (centripetal forces) are due to their position within those force fields. The potential for work to be done by the gravitational force is referred to as gravitational potential energy, Ψ_p.

The algebraic sum of the energy components of the system is referred to as total potential and is given by:

$$\boldsymbol{\psi_t = \psi_p + \psi_o + \psi_m} \qquad \mathbf{2.18}$$

where ψ_t = total potential

Ψ_p = pressure potential

ψ_o = osmotic potential

ψ_m = matrix potential

The proportional effect of the components summed in equation 2.18 may not equal their numerical proportion, e.g if $\psi_o = 2\ \psi_m$, it may not be twice as effective in its action on soil behaviour.

In soil science only the matrix potential and osmotic potential are considered because only near surface soils within the root zone are of interest, since the availability of water for plant growth is the major concern, therefore $\psi_p = 0$. Because the flow rate in soils is very low the kinetic energy is also negligible, therefore the energy state of soil water is defined only by virtue of its matrix and osmotic components. Assuming that the dissolved salts are insignificant, the total potential is expressed in terms of the matrix potential:

$$\boldsymbol{\psi_t = \psi_m} \qquad \mathbf{2.19}$$

The matrix potential is given by:

$$\boldsymbol{\Psi_m \equiv (u_a - u_w) \equiv p'' \equiv s} \qquad \mathbf{2.20}$$

Where ≡ means identical, $(u_a\text{-}u_w)$ = pore water suction.

Though soil mechanics and soil science use the same soil-water terminologies for potential, their interests vary. In soil mechanics the focus is on strength and volume change, which are controlled by the effective stress of which some types of potential are a component.

2.8 Soil water characteristic curve (SWCC).

The soil water characteristic curve is a function of the suction in soil and the water content. It describes the thermodynamic potential of soil relative to the free water that the soil system tries to absorb. At low water contents the forces and energy required to move water within the soil system are high resulting in high suction values. The reverse is the case with soils having high water contents. Figure 2.9 shows a typical SWCC

for sand, silt and clay. The shape and behavior of the SWCC is influenced by the type of soil, grain size distribution, void ratio, density, organic matter content, clay content and mineralogy. For example, a sandy soil has larger pores than a clay soil, so during drying out the amount of water at a given suction value will be far greater in the clay soil than in the sandy soil due to the smaller pore diameter which ensures greater water retention.

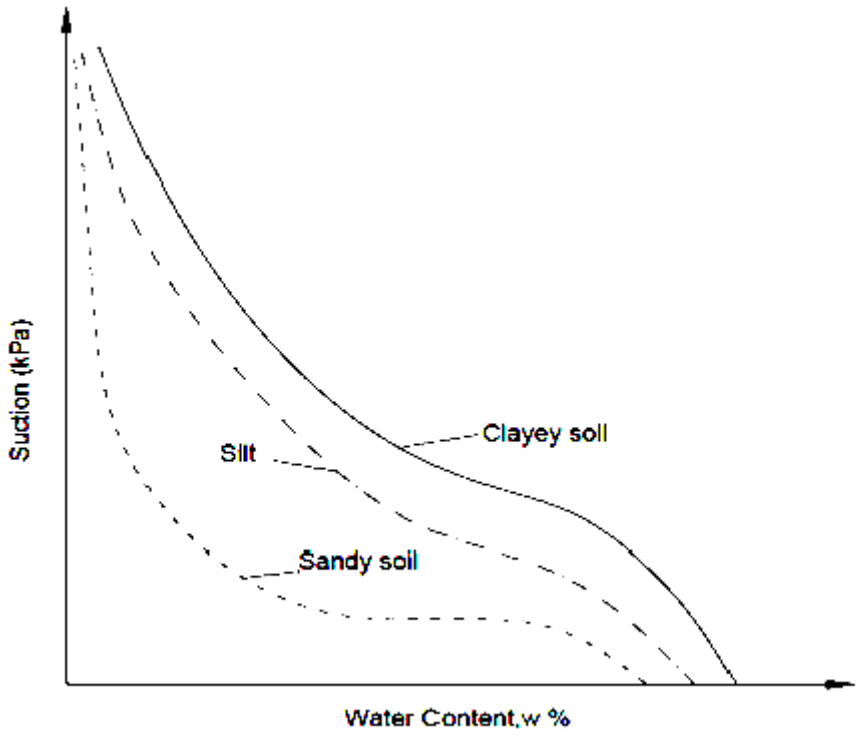


Figure 2.9 Typical soil-water characteristic curves for sand and clay

The soil moisture characteristic has been approximated from limited data as a composite of segments that are simple logarithmic relations by McQueen and Miller (1974). This is a simple conceptual model which describes the shape and behavior of the soil water characteristic curve for sand and is shown in figure 2.10. The line segment from 10^6 to 10^4 kPa signifies the region of the tightly adsorbed water regime. The line segment from 10^4 to 10^2 signifies the adsorbed film regime while the line

segment from 10^2 to 0 designates the capillary regime.(Lu and Lukos, 2004) have given an exhaustive description of the various water regimes in soil, following the McQueen and Miller (1974) model. These are the tightly adsorbed film segment, adsorbed film segment and the capillary regime.

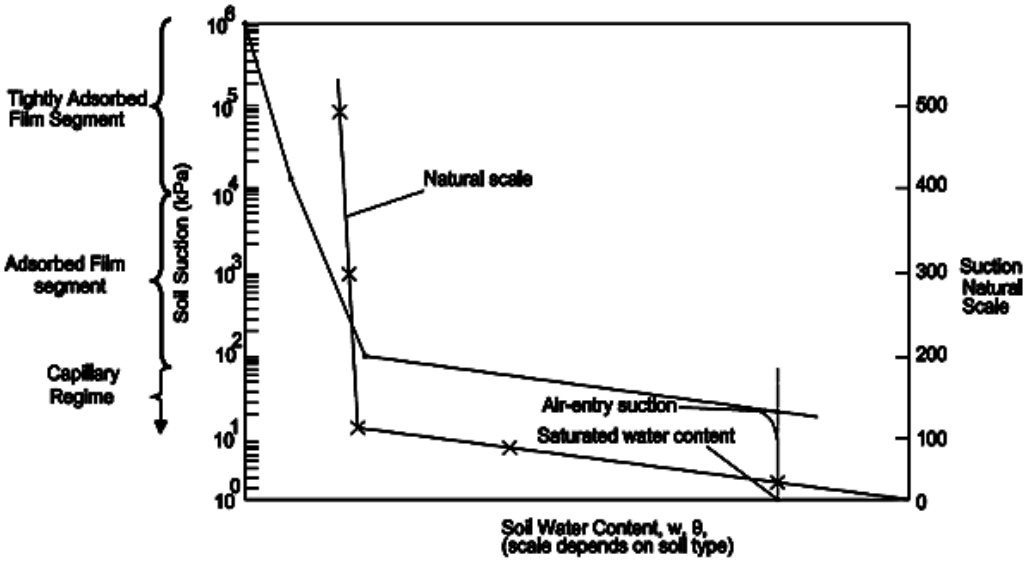


Figure 2.10 McQueen and Miller conceptual model for SWCC

In the tightly adsorbed water regime water is held by molecular bonding mechanisms, primarily hydrogen bonding with the exposed O^{2-} or OH^- on the surfaces of the soil mineral. In the adsorbed water regime water is held in the form of thin films on the particle surfaces under the influences of short range solid–liquid interaction mechanisms (e.g. electrical field polarization, van der Waal attraction and exchangeable cation hydration). The water content of the first two water regime is dependent on the soil surface area, surface density and the valency of the adsorbed exchangeable cations. Once the adsorbed water film becomes thicker than could be influenced by adsorption effects, then capillary forces dominate. However, the practical range for suction in soil does not exceed 3000 kPa and using a log scale for suction distorts

the relationship between suction and water content. This is shown when the McQueen and Miller (1974) data are plotted on both log and natural scales in figure 2.10. The air entry point is seen to be a function of the log scale rather than a real changing point on the soil water characteristic curve. The air entry point is defined by Fredlund and Rahardjo, 1993 as the matrix suction value that must be exceeded before air recedes into soil pores.

The degree of saturation (S_r) or gravimetric water content (w) or volumetric water content (θ) can be used to define the soil water characteristic curve. The relations between volumetric water content θ_w, gravimetric water content, w, and degree of saturation, S_r are given by the relation below:
In a saturated soil:

$$\theta_w = \frac{v_w}{v_w + v_s}$$

$$w = \frac{M_w}{M_s} = \frac{v_w \rho_w}{G_s \rho_w v_s} = \frac{v_w}{G_s v_s} = \frac{e}{G_s} \quad e = wG_s \qquad 2.21$$

$$\theta_w = \frac{S_r e}{1 + e} = \frac{wG_s}{1 + wG_s}$$

In an unsaturated soil:

$$e = \frac{wG_s}{S_r}$$

$$\theta_w = \frac{wG_s}{1 + wG_S/S_r} = \frac{S_r wG_s}{S_r + wG_s} \qquad 2.22$$

Where e = void ratio, G_s = specific gravity, ρ_w = density of water, M_s = mass of soil solids and M_w = mass of water.

Equations 2.21 and 2.22 are just some useful theoretical relationships. For practical purposes the soil water characteristic curve is always measured in terms of the gravimetric water content, w.

The relationship between suction and moisture content is not unique for a particular soil type. This is due to the significant variation in the water content for a given suction value which is caused by the history of wetting and drying of the soil. The main drying cycle is obtained by taking an initially wet soil sample and subjecting it to increasing suction by drying and measuring the moisture content while the main wetting cycle is obtained by taking an initially dry soil sample and wetting it and measuring the moisture content. The main cycles yield continuous curves which are not identical and separated from each other by w_i as shown in Figure 2.11.

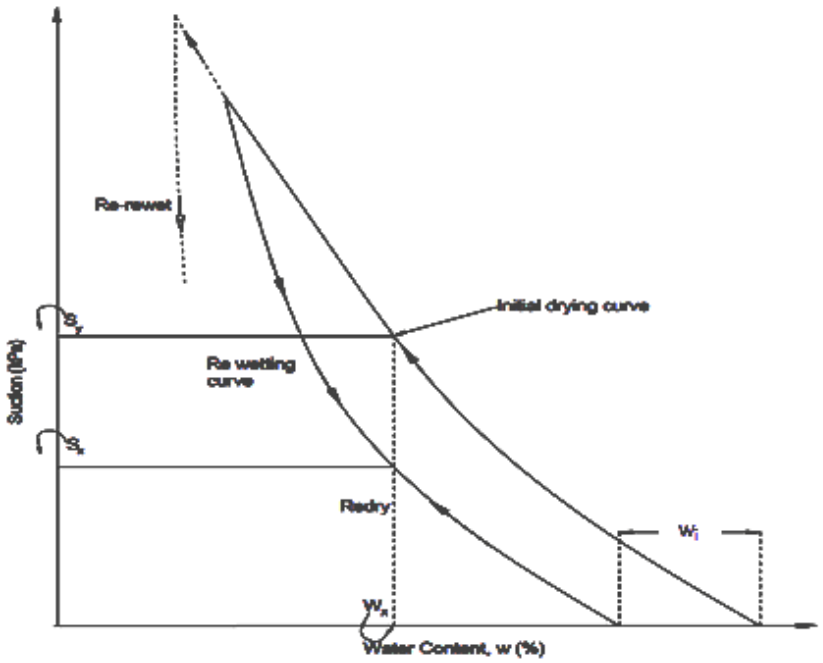


Figure 2.11 An idealised hysteretic soil water characteristic curve

From the graph it is evident that the suction value at given moisture content is greater for the main drying leg than the wetting leg. This phenomenon is called hysteresis in unsaturated soils. Hysteresis can significantly alter soil behaviour since two different suction values can be obtained for the same water content depending on which cycle, either drainage or wetting, is taking place.

Blight (2013), has attributed hysteresis to non-recoverable energy consumed by compression of the soil. His explanations come from figure 2.12. This figure shows the consolidation pressure and void ratio plotted together with their corresponding water contents for saturated Boston blue clay. Taylor, (1948) had the following as clay parameters: percentage clay size fraction < 2 μm, PL=20, LL=40 and PI= 20. The clay was dried by increasing the compression in an oedometer, then re-wetted by unloading and re-dried again by loading.

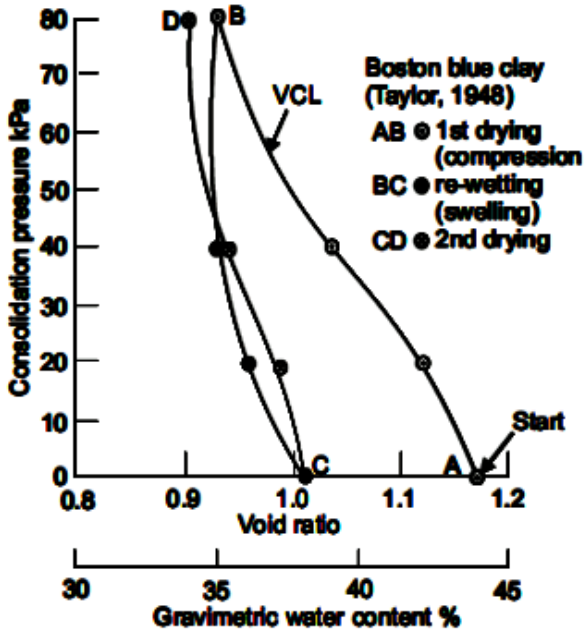


Figure 2.12 Hysteresis during consolidation (similar to drying) and swelling (similar to re-wetting) in saturated clay (Blight, 2007)

The area enclosed by the hysteresis loop will have units of w.kN.m/m^3 {since the water content is a dimensionless quantity} Area = kN.m/m^3 = 1kJ/m^3. The hysteresis loop ABC is the energy loss upon loading, to 80 kPa and unloading which is approximately 3.2 kJ/m^3. While BCD is the area enclosed by rewetting, curve BC and the second drying, CD, whose enclosed area is approximately 0.5 kJ/m^3, if closure DB is assumed. Since the area BCD is not zero, CD and BC do not coincide.

Once a saturated soil is consolidated by drying, it can wet up only along the rebound curve (see fig 2.11). As a consequence, it is impossible to have scanning curves. These may be possible only in rigid porous materials such as ceramics.

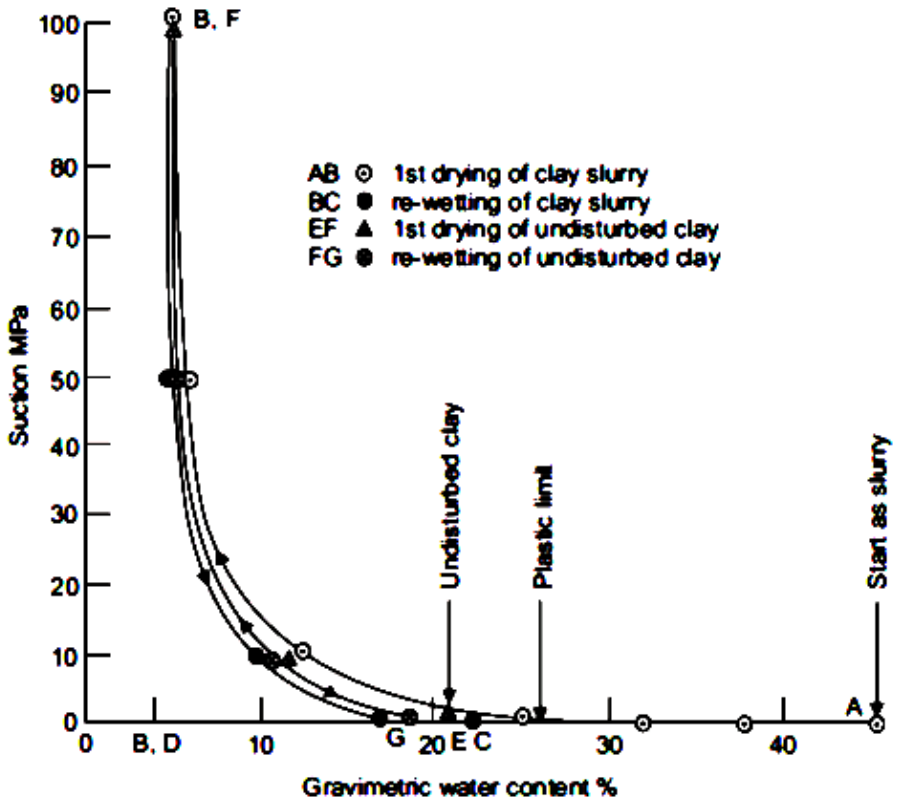


Figure 2.13 Drying and wetting characteristics found by Croney, Coleman and Bridge (1952) for a heavy clay

Hysteresis also occurs in natural soils as well as in compacted soils. In natural soils, hysteresis occurs between the virgin drying line (VDL) and the subsequent re-wetting limb. Figure 2.13 illustrates experiments by Croney, Coleman and Bridge (1952) showing undisturbed clay and clay slurry reaching suctions of up to 100 MPa. As the clay slurry dries from a water content of 45 % to 5 % and then re-wets to 17 %, the resultant loop, ABC, demonstrates an energy consumption of approximately 1300 kJ/m^3. In an undisturbed clay specimen, drying from 21% to 5% and re wetted to 19 %, the EFG loop shows no energy consumption. This implies that for natural soils that are over consolidated or over-dried, little or no hysteresis occurs.

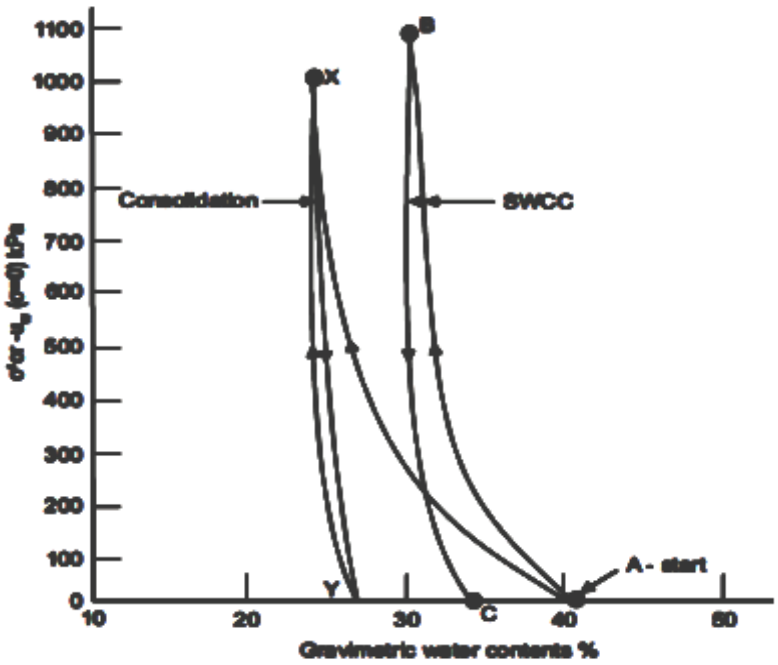


Figure 2.14 A direct comparison of an oedometer consolidation curve and an atmospheric drying curve using a calibrated gypsum block to estimate suction Blight 2013

This is what is experienced by near surface soil deposits in water deficient climates with repeated wet and dry cycles.

The soil water characteristic curve is simply a pressure consolidation curve. Since these graphs have axes with similar units, these two curves can be compared. Figure 2.14 shows a comparison of these curves for saturated silty clay (Blight, 2013). The loop ABC shows the SWCC while AXY is the pressure consolidation curve. The silty clay was consolidated from a water content of 41 % to 24 % at a vertical stress of 1000 kPa, while atmospheric drying caused the clay to attain a suction of 1100 kPa at a water content of 30 %. Therefore, the consolidation of a saturated soil is a more effective approach to dewater a soil than by surface evaporation. However, consolidation entails more energy consumption (loop AXY- 40kJ/m^3) than surface drying (loop ABC- 20 J/m^3)

2.9 Methods of expressing suctions

The terms suction and soil water potential are used interchangeably by both soil physicists and geotechnical engineers. Soil water potential is often expressed as the energy per unit quantity of water. This unit quantity of water could either be mass, volume or weight so the energy per unit mass of water is Jkg^{-1}, and is also called chemical potential in $kgmol^{-1}$. The energy per unit volume is Jm^{-3} which is equivalent to pressure, Nm^{-2}. This is a pressure potential. The energy per unit weight is JN^{-1} which is equivalent to [m], i.e. a measure of length or head. In geotechnical engineering, soil pore water potential units of head [h] or pressure, [ψ], are used in describing stress and deformation in unsaturated soils. These relationships are summarized in equations 2.23 and 2.24.

$$\Psi = [Nm^{-2} = Nm.m^{-3} = Jm^{-3}] \qquad 2.23$$

$$\rho_w gh = [kg.m^{-3}\ m.s^{-2}.m = kg.ms^{-2}.m^{-2} = Nm^{-2} = Jm^{-3}] \qquad 2.24$$

where:

ψ is the pressure [N/m^2]

h is the head [m]

g is the gravitational acceleration [m/s^2]

ρ_w is the density of water [kg/m^3]

CHAPTER THREE

THE BEHAVIOUR OF UNSATURATED SOILS

3.0 Introduction

This chapter presents some historical perspective on the behaviour of unsaturated soils but with focus on the evolution of shear strength and/or effective stress equations. The behaviour of unsaturated soils has received attention from many researchers whose common objective has been to develop an appropriate expression which adequately models the shear strength of soil. The choice of appropriate state variables necessary to describe unsaturated soil behaviour has not been the same from these researchers. This chapter reviews the historical development of the equations describing the state of stress in saturated and unsaturated soils.

3.1 Stress state in saturated soil

According to Lu and Likos (2006) the definition of the concept of effective stress was formulated by Terzaghi in 1936, though evidence of its earliest use by Terzaghi dates back to 1926 with the equation:

$$\boldsymbol{\sigma' = \sigma - u_w} \qquad \mathbf{3.1}$$

Through this concept a rational approach to solving soil mechanics problems for saturated soils, which previously was very empirical, was born. Terzaghi's concept links deformation and strength uniquely to a change in the effective stress. It has proven to be practically relevant in current geotechnical practice where stress, volume, strain and deformation are analysed for saturated soils. Other researchers like Rendulic (1936), Bishop and Eldin (1950), Henkel (1960) and Lu and

Likos (2006) proposed similar expressions for saturated soils. Skempton (1960) refined the Bishop and Eldin (1950) effective stress expression, asserting that volume change and shear strength be separated with respect to effective stress and thus proposed two expressions for the effective stress equation. The first one is the effective stress equation for shear strength given as:

$$\boldsymbol{\sigma' = \sigma - \left(1 - \frac{a\tan\psi}{\tan\phi'}\right) u_w} \qquad \mathbf{3.2}$$

where $\boldsymbol{\sigma'}$, σ = Effective and total applied stresses

ψ = angle of intergranular friction

$\boldsymbol{\phi'}$ = angle of shearing resistance

$\boldsymbol{a = \frac{A_s}{A}}$ = contact area ratio

$\boldsymbol{A_s}$ = contact area between two particles on a statistical plane

A= gross area in a plane parallel to the contact

$\boldsymbol{u_w}$= pore water pressure.

For all practical purposes ‘a’ is close to zero and therefore

$$\boldsymbol{\sigma' = \sigma - u_w}$$

The second is the effective stress equation for volume change given as:

$$\boldsymbol{\sigma' = \sigma - \left(1 - \frac{C_s}{C}\right) u_w} \qquad \mathbf{3.3}$$

where C = compressibility of the soil particles

C_s = compressibility of the soil structure

Here also, C_s/C is close to zero and for all practical purposes

$$\sigma' = \sigma - u_w$$

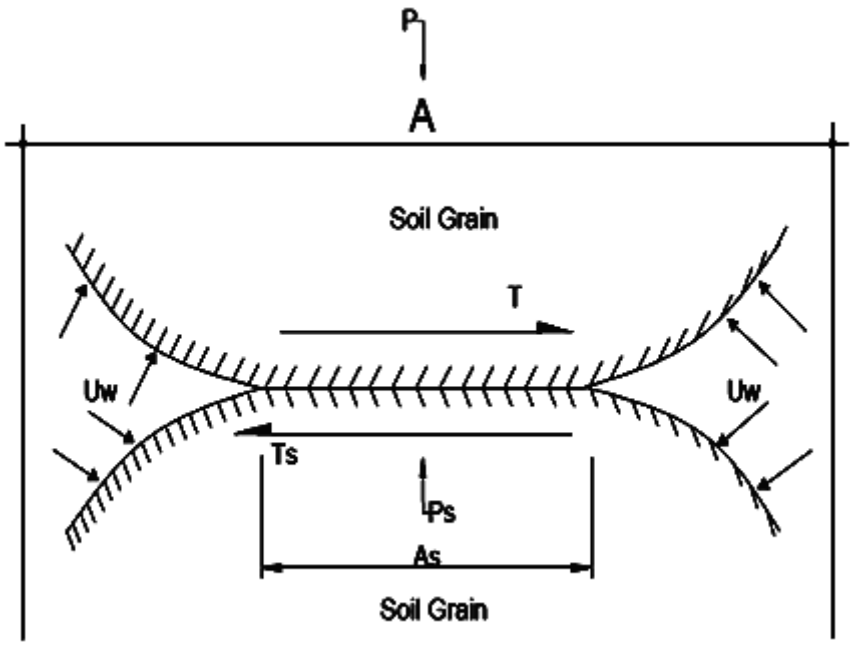


Figure 3.1 Effective stress across a soil grain

3.2 Stress state in unsaturated soil

At the first unsaturated soil conference in 1960 four proposed versions of the effective stress in unsaturated soil were presented. This marked the beginning of what has been termed the 'modified effective stress approach'. This name is attributed to Bishop (1959, 1961), who proposed the equation:

$$\sigma' = (\sigma - u_a) + \chi(u_a - u_w) \qquad 3.4$$

Where u_a and u_w are the pore air and pore water pressures respectively and χ is an empirical factor called the coefficient of effective stress. Its value varies between 0, for extremely dry soil and 1, for saturated soil.

Aitchison (1961) proposed the equation:

$$\boldsymbol{\sigma' = \sigma + \psi p'} \qquad \mathbf{3.5}$$

where p' is the suction or pressure deficiency which is the equivalent of (u_a-u_w). The Aitchison equation is a special case of the Bishop equation when the air pressure is zero (atmospheric).

Jennings (1961) proposed an equation similar to that of Aitchison using a different symbol, β, in place of either χ or ψ. This equation was dated in 1958 though it was in the 1960s that it was made public.

$$\boldsymbol{\sigma' = \sigma + \beta p'} \qquad \mathbf{3.6}$$

The fourth equation, presented at that same conference by Croney (1958) is given as:

$$\boldsymbol{\sigma' = p - \beta' u} \qquad \mathbf{3.7}$$

where p is the equivalent of σ and u is the pore water pressure and β is the bonding factor which is a measure of the effectiveness of the pore pressure contribution to soil strength. This fourth equation is similar to the Bishop equation when the air pressure is zero.

The discussions at the 1960 conference on pore pressure and suction in soils concluded that the equations presented were similar to

each other and the Bishop equation was adopted as the equation of reference for unsaturated soils.

The adoption of the Bishop equation did not close the discussion on this topic since within a year Lambe (1960) suggested a modified form of the effective stress equation as given below:

$$\boldsymbol{\sigma = \bar{\bar{\sigma}} a_m + u_a a_a + u_w a_w + R - A} \qquad \mathbf{3.8}$$

where $\bar{\bar{\sigma}}$ is the mineral to mineral contact stress, a_m is the fraction of total cross sectional area that consist of mineral to mineral contact, a_a and a_w are the fraction of total cross sectional area occupied by air or water respectively and R and A are the repulsive, (R), and attractive, (A), electrical forces. The Lambe equation can be simplified to the following:

$$\boldsymbol{\bar{\bar{\sigma}} a_m + R - A \equiv \sigma'}$$
$$\boldsymbol{a_w \equiv x \text{ and } a_a \equiv 1 - x}$$

From the above relations, it is evident that the Lambe (1960) equation is equivalent to the Bishop equation.

In 1963, Bishop and Blight published the results of some experiments to validate the Bishop equation where they demonstrated that the shear strength and volume change characteristics are unchanged with effective stress changes when $(\sigma\text{-}u_a)$ and $(\sigma\text{-}u_w)$ are kept constant. Three years later Richard (1966) also suggested another equation for the effective stress, where he included a contribution due to the effect of osmotic (or solute) suction:

$$\boldsymbol{\sigma' = (\sigma - u_a) + \chi_m (u_a - u_w)_m + \chi_s (u_a - u_w)_s} \qquad \mathbf{3.9}$$

in which σ' and σ are respectively the effective and total stresses and χ is Bishop's effective stress parameter. The subscripts m and s denote ''matrix'' and ''solute or osmotic suction''.

Other more recent equations similar to the Bishop's has been proposed by other researchers such as Allam & Sridharan (1987); Oberg & Sallfor (1997) and Sheng et al. (2002).

Allam & Sridharan (1987) proposed the following equation.

$$\boldsymbol{\sigma' = (\sigma - u_a) + \chi(u_a - u_w) - R' + \gamma T} \qquad \mathbf{3.10}$$

Where R' is the osmotic suction which tends to disperse soil particle, γ is the interphase perimeter and T is the surface tension. Since Richard's 1966 equation which included the effects of solute suction, Sridharan & Venkatappa Rao (1973) had suggested an osmotic suction addition to the existing current formulations of the effective stress equation.

Oberg & Sallfors, 1997 proposed the following equation for shear strength expressed as.

$$\boldsymbol{\tau = c' + \{(\sigma - u_a) + S_r(u_a - u_w)\} \tan \theta'} \qquad \mathbf{3.11}$$

S_r is equivalent to χ and the equation is similar to the Bishop equation.

Sheng *et al.* (2002) proposed another equation for the effective stress expressed as.

$$\boldsymbol{\sigma' = \sigma - \delta_{ij}(S_r)u_w, u_a = 0} \qquad \mathbf{3.12}$$

When the $u_a > 0$ then the equation is exactly Bishop's and is given as

$$\boldsymbol{\sigma' = (\sigma - u_a) - \delta_{ij}(S_r)(u_a - u_w)} \qquad \mathbf{3.13}$$

Matyas and Radhakrishna (1968) used the concept of constitutive 'state surfaces' to relate void ratio, e, and degree of saturation, S_r, with the net normal stress $\sigma_a = (\sigma - u_a)$ and the matrix suction $u_c = (u_a - u_w)$. The assumption here was that the principle of effective stress was inadequate to explain changes in the volumetric behaviour of unsaturated soils subjected to external loads. They used mixtures of 20% kaolin and 80 % flint powder giving clay of medium plasticity, compacted to densities of 14 kN/m^2. Samples of about 101.2 mm diameter by 101.2 mm height were made by statically compacting the kaolin mixture in four layers at the rate of 1.9 mm/min using a compression machine. The compacted specimen was mounted on a modified triaxial apparatus having a fine pored ceramic disk, with an air entry value of 310 kPa. This was the beginning of what has been termed the 'two stress method'. They called the equations used to express the unique relationship between different state parameters 'state functions'. In these a physical quantity, for example θ, associated with an element of a material is uniquely determined by the state of the element and this gives a unique function as:

$$\boldsymbol{\theta = f(J_1,\ J_2,\ J_3,\ S_1, \ldots)} \qquad \boldsymbol{3.14}$$

where J_1, J_2 … are the stress parameters

S_1, S_2 … are other state parameters

θ is the 'state point' function

Furthermore they hypothesized that in the triaxial compression testing of saturated soils the void ratio and degree of saturation can be expressed as dependent quantities by the following equations:

$$\boldsymbol{e = F(p_a, q, u_c, e_o, S_{ro})} \qquad \boldsymbol{3.15}$$

$$\mathbf{S = \phi(p_a, q, u_c, e_o, S_{ro})} \qquad \mathbf{3.16}$$

Where p_a, q and u_c are the stress parameters and e_o and S_{ro} are the initial void ratio and degree of saturation respectively.

Blight (1965) represented the stress parameters in a three-dimensional rectangular coordinate system by generating some surfaces using unsaturated effective stress variables (σ-u_a) and (u_a-u_w) with respect to volume change for swelling and collapsing soils. These were based on experimental measurements and are illustrated in figure 4.2 (a) and (b). Figure 4.2 (a) shows the stress strain diagram for the swell of partly saturated soil under constant isotropic load. For a constant (σ-u_a) stress situation, a reduction matrix suction (u_a-u_w), will cause swelling along line AB. If the grain structure of the soil is stable, swelling will continue until (u_a-u_w) = 0 and the soil attains saturation at B. Swelling will continue further than B along BC' if (σ) is reduced because the soil is in a saturated state and u_a = 0. If the grain structure is unstable collapse settlement may occur when suction falls below a critical value of the applied stress-path DEF. Once the grain structure stabilizes, swelling resumes along FG, provided that suction continues to decrease and the soil behaves normally

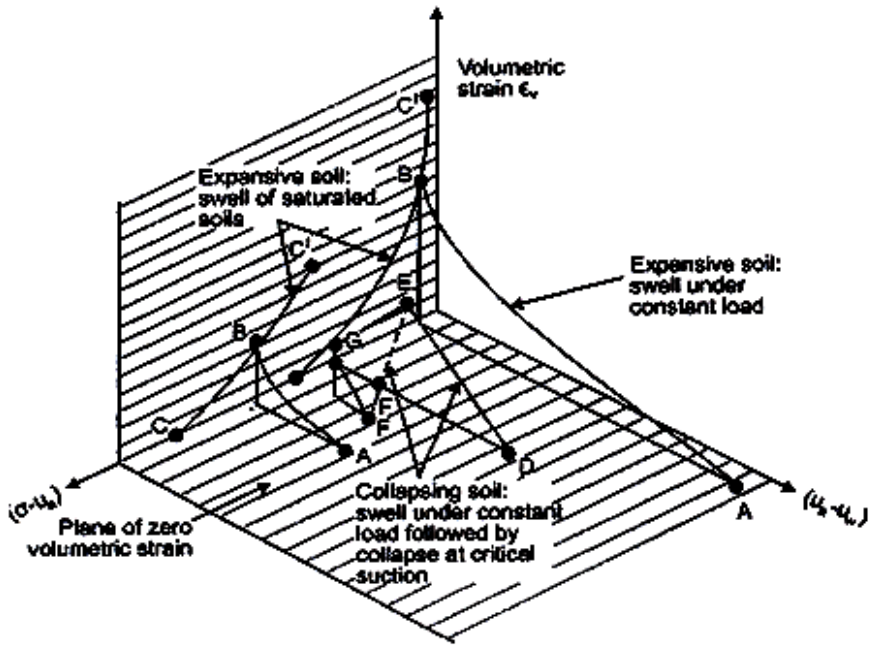


Figure 3.2 (a) Three dimensional stress strain diagram for the swell of partly saturated soil under constant isotropic load.

Figure 3.2 (b) shows the constant volume swell process of an unsaturated soil where the suction is reduced by wetting the soil and the applied stress (σ-u_a) is adjusted to prevent swelling or shrinkage from occurring.

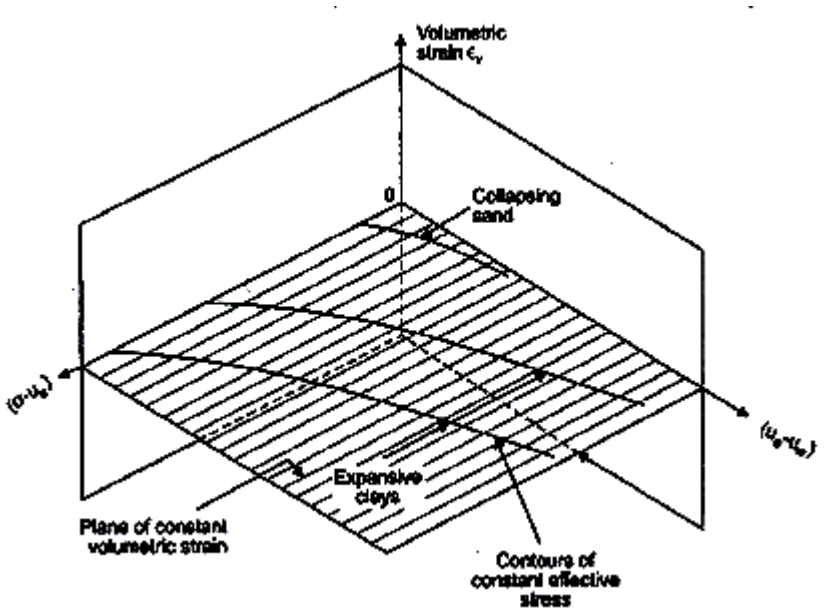


Figure 3.2 (b) Three dimensional stress-strain diagram showing contours of constant effective stress in partly saturated soils.

Aitchison (1969) continued along the same line of reasoning with the two independent stress variable method and later, Brackley (1971) carried out some studies on the partial collapse of unsaturated expansive clays where he independently measured stress variables (σ-u_a) and (σ-u_w). He encountered some difficulties in applying the Bishop equation, describing the volume change behaviour as a function of the independent stress variables. Fredlund et al (1977) consolidated and popularised this method. They argued that introducing the χ factor of the Bishop equation renders it a constitutive relation because χ depends on the soil characteristics. The possible stress combinations proposed to describe the stress strain behaviour of unsaturated soils are:

- $(\boldsymbol{\sigma} - \mathbf{u_a}), (\mathbf{u_a} - \mathbf{u_w})$
- $(\boldsymbol{\sigma} - \mathbf{u_w}), (\mathbf{u_a} - \mathbf{u_w})$
- $(\boldsymbol{\sigma} - \mathbf{u_a}), (\boldsymbol{\sigma} - \mathbf{u_w})$

In 1978, Fredlund, Morgenstern and Widger proposed three shear strength equations in terms of pairs of the three independent stress state variables. These were expressed following the Mohr-Coulomb failure criterion. The first of these expressions is given as:

$$\tau = c' + (\sigma - u_w)\tan\phi' + (u_a - u_w)\tan\phi'' \qquad 3.17$$

where

c' = effective cohesion parameter

ϕ'= friction angle with respect to changes in (σ-u_w) when (u_a-u_w) is held constant

ϕ'' = friction angle with respect to changes in (u_a-u_w) when (σ-u_w) is held constant

Equation 3.17 is advantageous in that it provides for a smooth transition from the unsaturated to the saturated state. The disadvantage comes when the pore water changes because the two stress state variables change.

The second expression is given as:

$$\tau = c'' + (\sigma - u_a)\tan\phi^a + (u_a - u_w)\tan\phi^b \qquad 3.18$$

where

c'' = cohesion intercept when the two stress variables are zero

ϕ^a= friction angle with respect to changes in (σ-u_a) when (u_a-u_w) is held constant

ϕ^b = friction angle with respect to changes in (u_a-u_w) when (σ-u_a) is held constant.

The advantage of Equation 3.18 is that only one stress variable is affected when the pore water pressure changes. Regardless of the combination of stress variables used to describe the shear strength, the

value of the shear strength obtained is the same for a given soil provided that σ, u_a and u_w remain unchanged.

The third expression for shear strength is given as:

$$\tau = c' + (\sigma - u_a)\tan\phi' + (u_a - u_w)\tan\phi^b \qquad 3.19$$

Equations 3.17 and 3.19 will give the same value of shear strength therefore equating them will result in an expression relating the various angles of friction given as:

$$\tan\phi' = \tan\phi^b - \tan\phi'' \qquad 3.20$$

Fredlund, Morgenstern and Widger however, favoured Equation 3.19 for engineering practice.

A third approach to describe the stress state in unsaturated soils is called the suction stress characteristic curve (Lu and Likos, 2006). They proposed a form of suction stress that is similar to Terzaghi's effective stress for saturated soils (Terzaghi, 1943) and Bishop's effective stress for unsaturated soil (Bishop, 1954, 1959). The aim of this approach is to propose a single stress variable that can model the mechanical behaviour of earth materials. Forces such as the van der Waals, double layer forces, surface tension and adhesive forces are said to interact at the soil solid surface, generating energy which results in suction stress. Consequently, the suction stress characteristic curve is a thermodynamic approach. The following reasons were given why this approach is better than the other two mentioned above:

- Suction stress is solely a function of soil suction and therefore does not require that the effective stress coefficient χ be used to define effective stress.

- The suction stress characteristic curve is similar to the soil water characteristic curve so a single valued function is uncalled for.
- Hysteresis can also be conveniently handled in the suction stress characteristic curve.

The effective stress equation by the suction stress characteristic curve is expressed as:

$$\boldsymbol{\sigma' = (\sigma - u_a) - \sigma^s} \qquad \mathbf{3.21}$$

where u_a is the pore air pressure, σ is the total stress, σ' is the effective stress and σ^s is the suction stress characteristic curve of the soil, where $\sigma^s = -(u_a - u_w)S$ and S = saturation proportion and $(u_a - u_w)$ is the matrix suction.

Using thermodynamic justifications Lu *et al.,* (2010) also evaluated the tensile stress from the virtual work of increasing the volume of the soil system with bound residual water. They arrived at an expression for the suction stress characteristic curve as:

$$\boldsymbol{\sigma^s = -(u_a - u_w)S_e} \qquad \textbf{for} \quad \mathbf{V_w > V_r} \qquad \mathbf{3.22}$$

where S_e = effective saturation, $(u_a - u_w)$ is the matrix suction, V_w is the total water volume and V_r is the residual water volume.

From equation 3.21, Lu *et al*. (2010) proposed an effective stress equation as an extension of Bishop's equation and an expansion of Terzaghi's equation for all saturations by modifying the contribution to effective stress as:

$$\boldsymbol{\sigma' = (\sigma - u_a) - [-S_e(u_a - u_w)]} \qquad \mathbf{3.23}$$

$$\boldsymbol{= (\sigma - u_a) — \frac{S - S_r}{1 - S_r}(u_a - u_w) \; = \; (\sigma - u_a) - \sigma^s} \qquad \mathbf{3.24}$$

Where S_r is the residual saturation

The above equation is different from Bishop's equation with respect to the degree of saturation but can become Terzaghi's effective stress equation, $\sigma' = \sigma - u_w$, when it is saturated. An additional extension can be carried out by applying the relationship between normalised volumetric water content or the degree of saturation and matrix suction. Using van Genuchten's (1980) soil water characteristic curve model, the normalised degree of saturation is expressed as:

$$\boldsymbol{S_e = \left\{\frac{1}{1 + [\alpha(u_a - u_w)]^n}\right\}^{1-1/n}} \qquad \mathbf{3.25}$$

where n and α are empirical fitting parameters of unsaturated soil properties, n being the pore size distribution parameter and α the inverse of the air entry pressure of water saturated soil.

A closed-form expression for the suction stress for a full range of saturation is obtained by substituting equation 3.25 into equation 3.22 and eliminating matrix suction:

$$\boldsymbol{\sigma^s = \frac{S_e}{\alpha}\left(S_e^{\frac{1}{1-n}} - 1\right)^{\frac{1}{n}}} \qquad \mathbf{0 \leq S_e \leq 1} \qquad \mathbf{3.26}$$

A similar closed-form equation for the suction stress for the full range of matrix suction is obtained by substituting equation 3.25 into equation

3.22 and eliminating the degree of saturation giving equation 3.27 and 3.28 for saturated and unsaturated soils respectively:

$$\sigma^{s} = -(u_a - u_w) \qquad u_a - u_w \leq 0 \qquad 3.27$$

$$\sigma^{s} = -\frac{(u_a - u_w)}{(1 + \alpha[u_a - u_w]^{n})^{n-1/n}} \qquad u_a - u_w \geq 0 \qquad 3.28$$

Substituting the equations 3.27 and 3.28 into 3.24 yields equation 3.29 (for saturated soils) and 3.30 (for unsaturated soils):

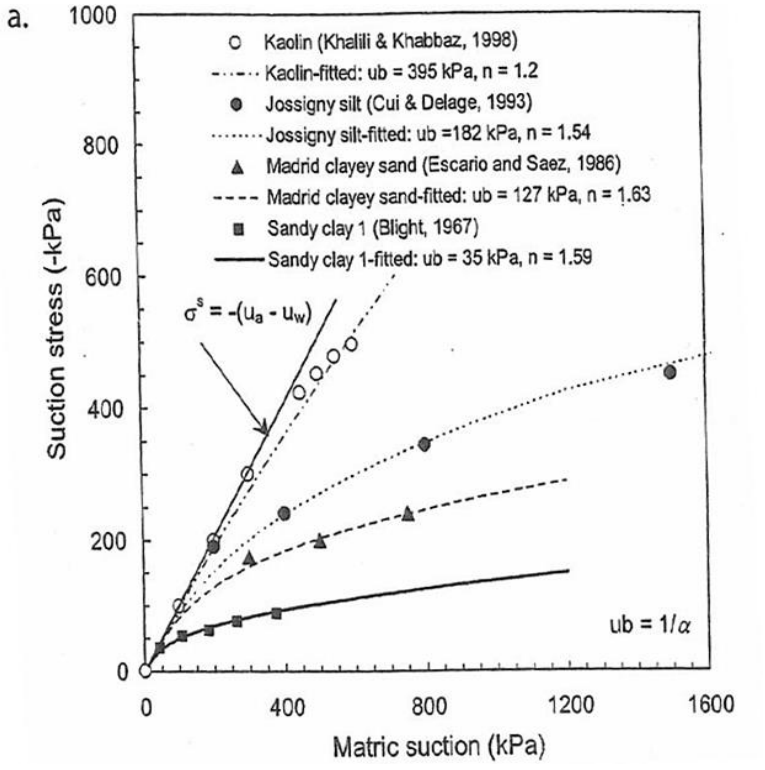
$$\sigma' = \sigma - u_a + (u_a - u_w) \qquad u_a - u_w \leq 0 \qquad 3.29$$

$$\sigma' = \sigma - u_a + \frac{(u_a - u_w)}{(1 + \alpha[u_a - u_w]^{n})^{n-1/n}} \qquad u_a - u_w \geq 0 \qquad 3.30$$

Due to the scarcity of data for SWCC and SSCC for same soils Lu *et al,* 2010 used existing data to validate this model. For soils which have both the SWCC and SSCC their data was validated by comparing them with equations 3.25 for SWCC and equations 3.27 for SSCC. Table 3.1 gives some characteristics of these soils used while figure 3.3 gives semi quantitative validation of the closed form equation for effective stress.

Table 3.1 Soil descriptions and properties used to validate the Closed-Form Equation for Effective Stress. (Group 1 soils) (Lu *et al.,* 2010).

Name	Soil properties	ub=1/α	n	φ'	c
Kaolin	LL=63 %, PI =33 % Percent finer than 3 μmm =70, γ_{dmax} =1.4 g/cm^3	395	1.20	22	24
Jossigny Silt	LL=37 %, PI =18 % clay fraction =34, γ_{dmax} =1.7 g/cm^3	182	1.54	22	25
Madrid clay	LL=32 %, PI =15 % clay fraction =17, γ_{dmax} =1.91 g/cm^3	127	1.63	38	0
Sandy clay	No Data	35	1.59	37	0



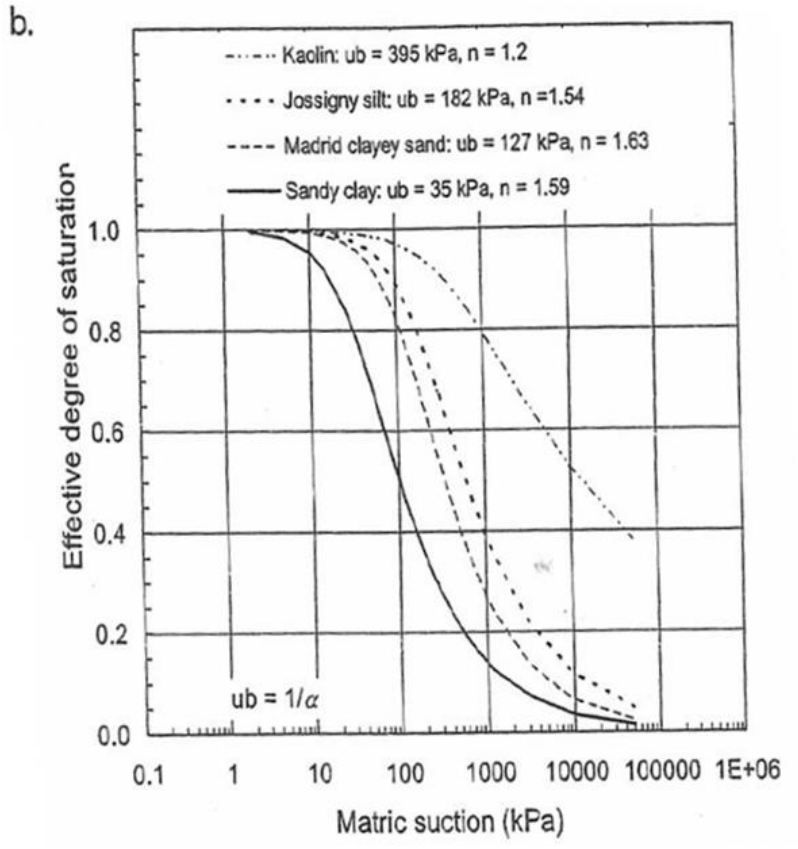


Fig 3.3 Semi quantitative validation of the closed-form equation for effective stress Group 1 soils: (a) measure and fitted SSCCs for kaolin, Jossigny silt, Madrid sandy sand and sandy clay and (b) predicted SWCCs for these soils. (Lu *et al.,* 2010)

From available geotechnical literature it is evident that three schools of thought have been established with regards to unsaturated soil behaviour. The modified effective stress approach attributed to Bishop, the two independent stress approach attributed to Fredlund and Morgenstern (1977) and the suction stress characteristic curve, Lu and Likos (2006), Lu *et al*., (2010).

Bishop's approach has received some criticism especially concerning the use of χ which some researchers call an elusive parameter. For example, Coleman (1962) pointed out that χ is related to soil structure and that no correlation can be found between χ and a volumetric parameter such as the degree of saturation. However, Khalili and Khabbaz (1998), Khalili *et al.* (2004) obtained a unique relationship upon analysis of 14 different unsaturated soils thus establishing a relationship between χ and a volumetric parameter and therefore expressed Bishop's parameter as:

$$\chi = \left[\frac{(u_a - u_w)}{(u_a - u_w)_b}\right]^{\eta} \qquad 3.31$$

where χ is the effective stress coefficient, (u_a-u_w) is the matrix suction in the soil samples at failure conditions, $(u_a-u_w)_b$ is the air entry value of the soil and η = -0.55. This parameter was based on the analysis of data from 13 soil samples.

Nuth and Laloui, (2008) have also validated Bishop's equation as an appropriate constitutive framework for critical state soil mechanics.

While the two independent stress variables approach is popular and has been able to handle elastoplasticity, critical state soil mechanics and couple yield limits with some success, (Alonso *et al.*,1990, Wheeler and Sivakumar 1995, Gallipoli *et al.* 2003), it is plagued with having to measure separate material properties whose determination in the laboratory is slow and time consuming. Lu (2008) has also questioned whether matrix suction is a stress variable and also the physical basis for the additional shear strength parameter φ^b. In addition, the two independent stress states approach cannot be reconciled within the context of classical soil mechanics for saturated soils. However it can be

said that the two independent stress state equations proposed by Fredlund *et al.* 1978, are not different from Bishop's equation. The relationship between ϕ^b and χ is given by the relation:

$$\tan\phi^b = \chi \tan\phi' \qquad 3.32$$

CHAPTER FOUR
SUCTION AND SHEAR STRENGTH MEASUREMENT IN UNSATURATED SOILS

PART I SUCTION MEASUREMENTS

4.0 Introduction

Suction measurement is very challenging both in the field and in the laboratory. With recent technological advancements many instruments have been developed that can be used for this purpose. However, there are still limitations regarding cost, reliability, range of operation and suitability for use within either field or laboratory settings. Suction measurements can be divided into two broad categories, the direct and indirect methods.

4.1 Direct matrix suction measurement.

In this method, matrix suction is measured by applying capillarity principles thereby measuring the negative pore water pressure using a porous material. The porous material has a range of pore sizes which allows water and solute movement but stops air at the suction desired. The main aim is to have control of the water pressure separately from the air pressure. The maximum value of the matrix suction that can be measured corresponds to the air entry value of the porous material. Typical porous materials used are sintered glass, sintered bronze and ceramics. The various techniques available to measure matrix suction directly include the suction plate, tensiometers, pressure plate and Imperial college tensiometer or suction probe.

4.1.1 Suction plate

This consists of a saturated high air entry ceramic disk attached to a water reservoir connected to a U tube to which is attached a vacuum gauge or manometer. Figure 4.1 below shows a sketch of the suction plate. The suction plate can measure suction between 20–30 kPa. Higher values of suction between 80-85 kPa can also be attained using multiple water hanging columns. Beyond this value cavitation occurs and air enters the system. The equilibrium time of the suction plate is in hours.

It is operated by placing a soil sample on the saturated ceramic disk. Water flows from the reservoir into the soil sample, thereby causing a change in the meniscus which is read off on the scale. The meniscus is then adjusted to its original position by applying a vacuum. By placing several soil samples of different moisture contents on the saturated ceramic plate, various suction values can be obtained and a suction versus water content curve for the soil sample can be constructed.

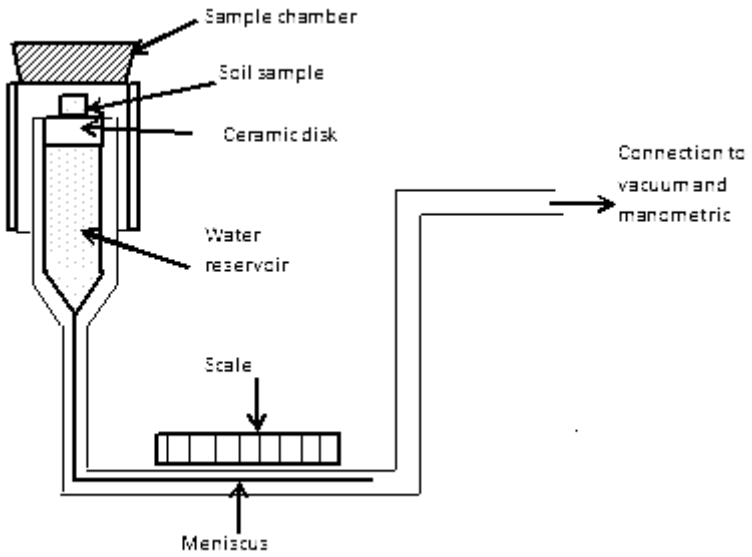


Figure 4.1 Suction plate

4.1.2 Tensiometers

The tensiometer consists of a water filled tube (reservoir) having a high air entry ceramic disk at one end and at the opposite end, is attached a pressure sensing device. The ceramic tip allows the movement of water between the soil with which it is in contagct and the tube containing the water (reservoir). The ceramic tip allows the movement of water including the solutes. However the tensiometer reading is not affected by the presence of solutes hence it only measures matrix suction and not osmotic suction. The equilibrium time of the tensiometer is in minutes and depends on the hydraulic conductivity of the ceramic material, its thickness and the hydraulic conductivity of the contact soil. Figure 4.2 shows a tensiometer commonly used in the field.

Prior to using the tensiometer, the reservoir is filled with de-aired water and a vacuum is applied to remove any trapped air bubbles. The tensiometer works by allowing the flow of water between the water reservoir and the soil in contact with the tip. When equilibrium is attained which is usually in a small number of minutes, the stress holding the water in the reservoir is equal to the stress in the soil. The water stress in the reservoir is read off on the sensing device attached to the reservoir. Tensiometers are limited to a suction value of about 100 kPa at sea level. At higher elevations their range may drop to between 70-80 kPa. Also, dust particles, dissolved gases and air bubbles, which get trapped within the instrument, often cause a reduction in the readings since these serve as possible nucleation sites for cavitation to occur. They can be used both in the field and in the laboratory.

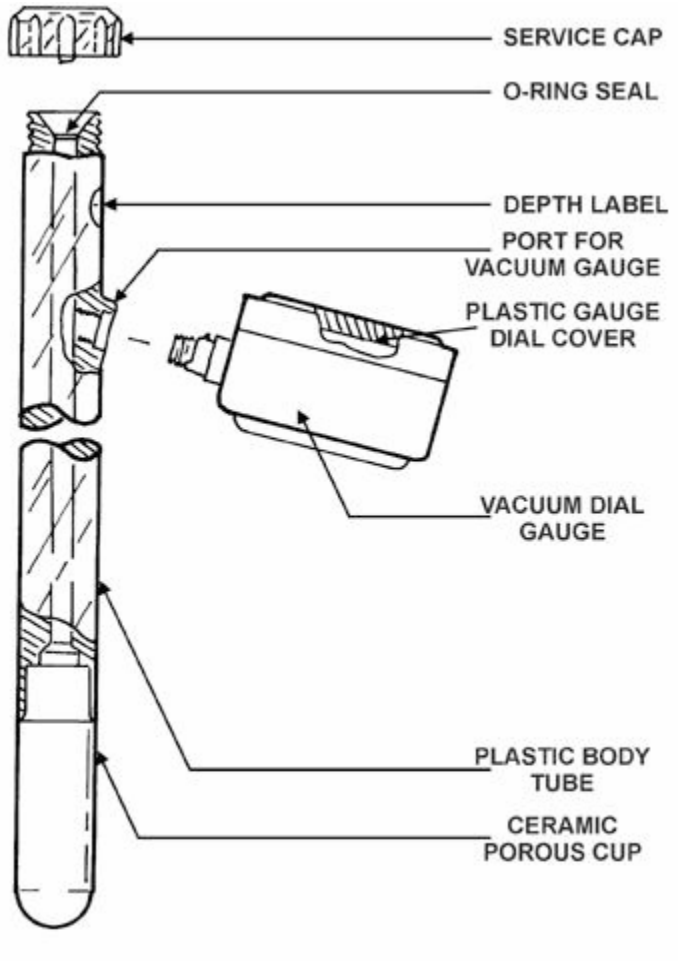


Fig 4.2 Soil Moisture Tensiometer (Soil Moisture Corporation, 1998)

4.1.3 Imperial college tensiometer (suction probe)

These are miniature tensiometers, which were first developed by Ridley and Burland (1993) at Imperial College. They are high capacity tensiometers capable of measuring suctions of 1500 kPa. They consist of a high air entry ceramic disk of 100 kPa attached at the tip of a transducer. The other end has a diaphragm to which a sensor is attached. The thin space between the porous disk and the diaphragm is a water reservoir containing de-aired water. See figure 4.3. When the probe comes in contact with soil, water flows from the reservoir into the

soil due to suction. Consequently the pressure drop in the reservoir is sensed by the strain guage sensor attached to the diaphragm. Similar varieties of the suction probe have been developed by Guan and Fredlund (1997), as well as Tarantino and Mongiovi (2001). Toker *et al.* (2004) developed the MIT tensiometer with a face diameter of 38 mm for use in triaxial soil testing. Subsequently, miniature probes have been developed by Meilani *et al.* (2002) and Rahardjo and Leong, (2006) for direct measurement of matrix suction within the range of 100-500 kPa, though their range can be extended to 1500 kPa.

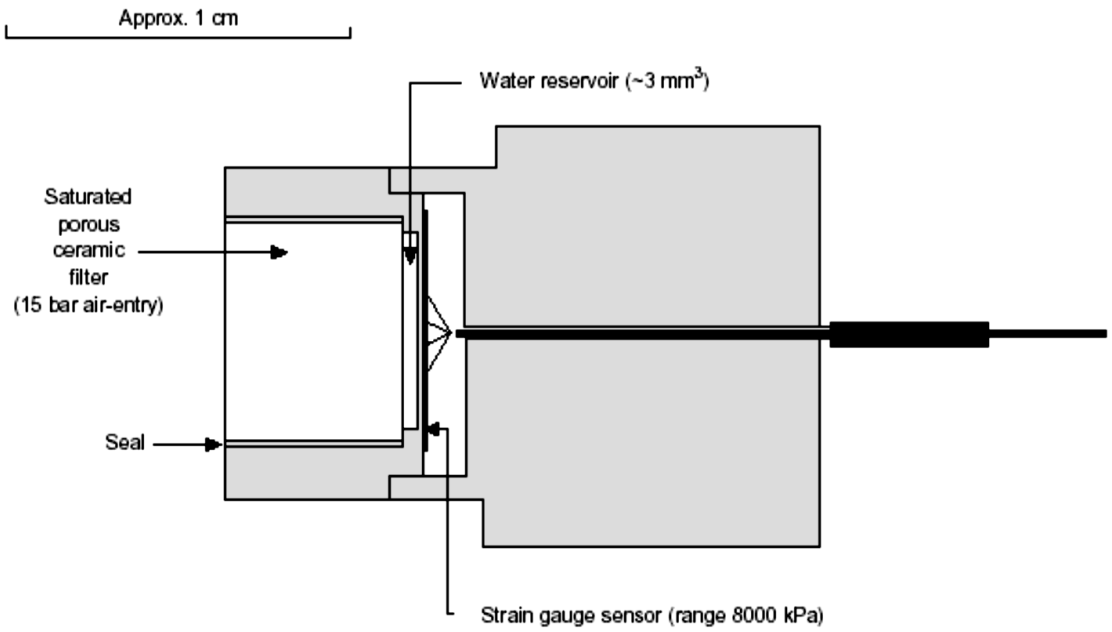


Figure 4.3 An Imperial College tensiometer or suction probe (Ridley *et al.,* 2003)

4.1.4 Osmotic Tensiometer

The Osmotic tensiometer was first developed by Zur (1966), Peck and Rabbidge (1969) and Kassif & Ben Shalom (1971). It makes use of an aqueous solution of polyethylene glycol PEG (20000) to transmit an osmotic pressure which is used to measure soil suction. Bocking & Fredlund (1979) have developed the one shown in Figure 4.4.

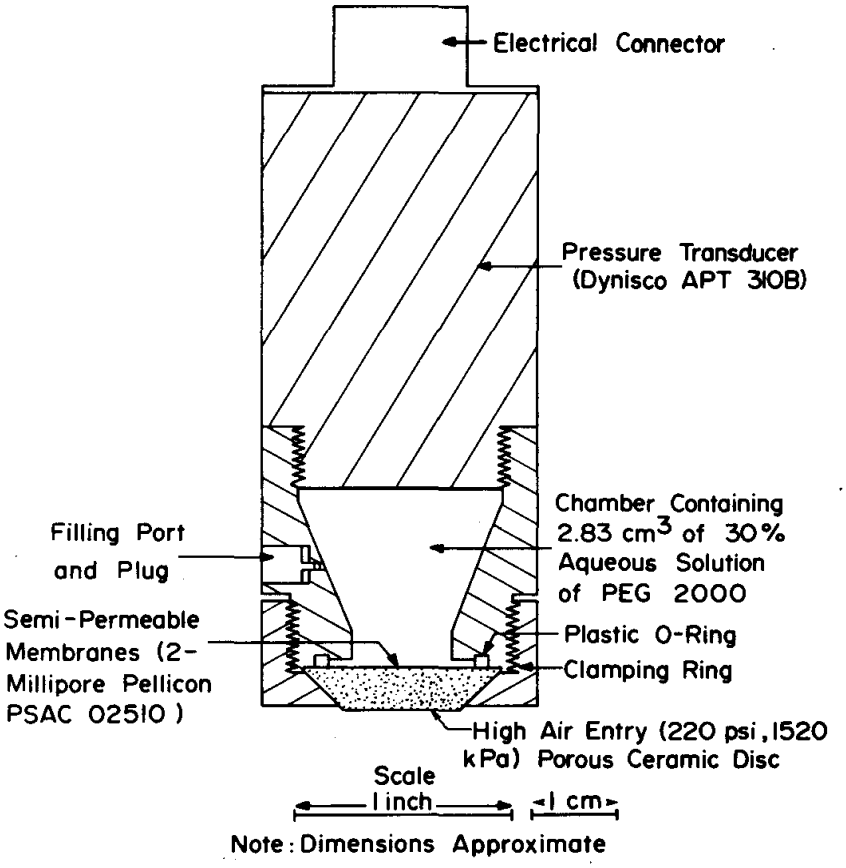


Figure 4.4 Osmotic tensiometer (Bocking & Fredlund, 1979)

This instrument is operated by maintaining a high chamber pressure of between 1380-2070 kPa through the process of osmosis. This is achieved by immersing the tensiometer in distilled water where a positive pressure is created in the chamber as water molecules pass through the

semi permeable membrane into the chamber but it stops the PEG from moving out. When the Osmotic tensiometer now comes in contact with unsaturated soil, the suction causes a net flow of water from the chamber until equilibrium is attained with the soil. The reduced chamber pressure is recorded by a pressure transducer which in turn reflects the suction in the soil. Bocking & Fredlund have found that the pressure response of the osmotic tensiometer is erratic due to the following reasons:

- The amount of flow into and out of the pressure chamber may be large enough to significantly affect the soil suction being measured.
- The osmotic pressure may change during the period of flow because of the change in the osmotic coefficient, molar concentration or temperature of the chamber fluid (PEG).
- The compressibility of the fluid in the chamber and the expansibility of the chamber may not be constant.
- Flow may cause some solution stratification resulting in a change in the reflection coefficient.

Bocking & Fredlund (1979) also found that the pressure response of the osmotic tensiometer is a function of the soil properties such as permeability and compressibility. Hence the osmotic tensiometer has limited applications in the field and little reference is made of it in geotechnical literature.

4.1.5 Pressure plate

This consist of a pressure vessel enclosing a saturated high air entry ceramic disk below which is a small water reservoir mounted on a stand. The water reservoir is connected to a pressure transducer lying outside the pressure vessel. Also a drainage pipe is connected to the water

reservoir which also vents outside the pressure vessel. A typical representation of a pressure plate is given figure 4.5.

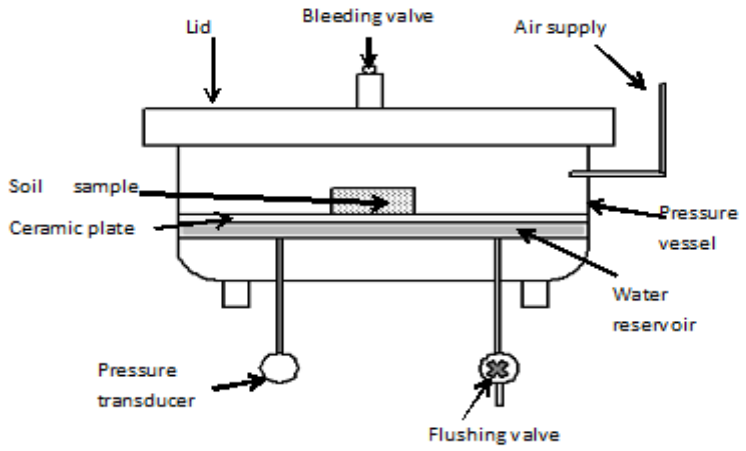


Figure 4.5 Pressure plate apparatus.

The high air entry ceramic disk separates the air phase from the water phase and stops air from flowing through but allows water. To carry out measurements, several soil specimens prepared at the same density and moisture contents are placed on the ceramic disc. A slight suction is placed in the chamber such that the soil specimens absorb some water from the reservoir through the ceramic disc. The air pressure in the chamber is increased to a given desired value and drainage is permitted. When the drainage is over, the pressure chamber is opened and one of the samples is removed for water content determination. This reading is the first point on the water content suction curve. Subsequent increments of air pressure are carried out concurrently with their water content

determinations of the other specimens to establish other points on the water content suction curve.

The maximum range of matrix suction measured on the pressure plate is 1500 kPa. The equilibrium time takes several hours to days and is convenient only for laboratory determination of matrix suction.

4.2 Indirect matrix suction measurement

In this method matrix suction is measured by calibrating the physical property of the porous material such as the thermal and electrical conductivity against matrix suction. This is achieved by equilibrating the porous material with the matrix suction in the soil so that the water content of the porous material corresponds with the magnitude of matrix suction of the soil. The methods available to measure matrix suction indirectly include electrical conductivity sensors, thermal conductivity sensors, time domain reflectometry (TDR) and in-contact filter paper.

4.2.1 Electrical conductivity sensors

This equipment consists of two concentric electrical electrodes embedded in a porous block usually made of gypsum. It measures the electrical resistance of the porous block in contact with the soil whose suction is to be determined. The electrical resistance of the porous block decreases with an increase of the water content of the porous block. A diagram of a typical electrical conductivity sensor (Gypsum block) is shown in figure 4.6.

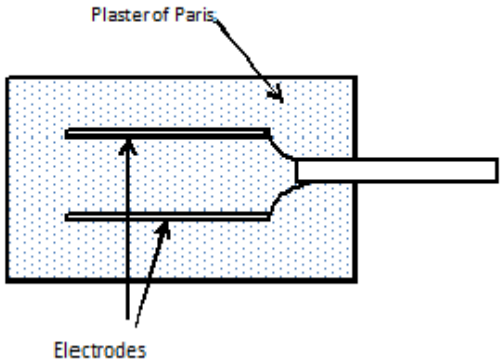


Figure 4.6 Gypsum block

A calibration curve is established between the electrical resistance of the block and the moisture content which is indirectly related to suction. Some of the disadvantages of the porous block include:

- The porous block has a long equilibration time of between 2-3 weeks. The equilibration time also varies with matrix suction ranging from about 6h for a matrix suction of about 50 kPa to about 2 days for matrix suction of about 1500 kPa.
- The sensitivity drops when the matrix suction is greater than 300 kPa.
- The salt concentration of the soil affects the electrical resistance of the block and the readings obtained may not be a true reflection of the moisture content of the porous block.
- The block may be soluble in water leading to an increase in the salt content of the soil.
- The block experiences hysteresis upon wetting and drying.

Some of its advantages include:

- It is easy to use and handle.

- It is useful for suction determination in non-saline soils and can measure suction within the range of 30-1500 kPa.
- It is good for field and laboratory applications.

4.2.2 Thermal conductivity sensors

These were first proposed by Shaw and Baver (1939). Figure 4.7 shows a design by Fredlund *et al.* (1994). It consists of an electric heater and a temperature sensor embedded in a porous ceramic block. The thermal conductivity of the ceramic porous block is directly proportional to the thermal conductivity of the ceramic solid and the pore fluid (air and/or water). The thermal conductivity of water is 25 times that of air, so a change in thermal conductivity of the block varies directly with changes in moisture content.

When the porous block is brought in contact with a soil sample, water flow is established and at equilibrium the suctions in block and soil are the same. The water content is measured by generating heat at the centre of the block using the heating element and measuring the temperature rise. As the moisture content increases more heat will be dissipated. The undissipated heat will result in a rise in the temperature of the block which is inversely proportional to moisture content. The rise in temperature can be calibrated against suction.

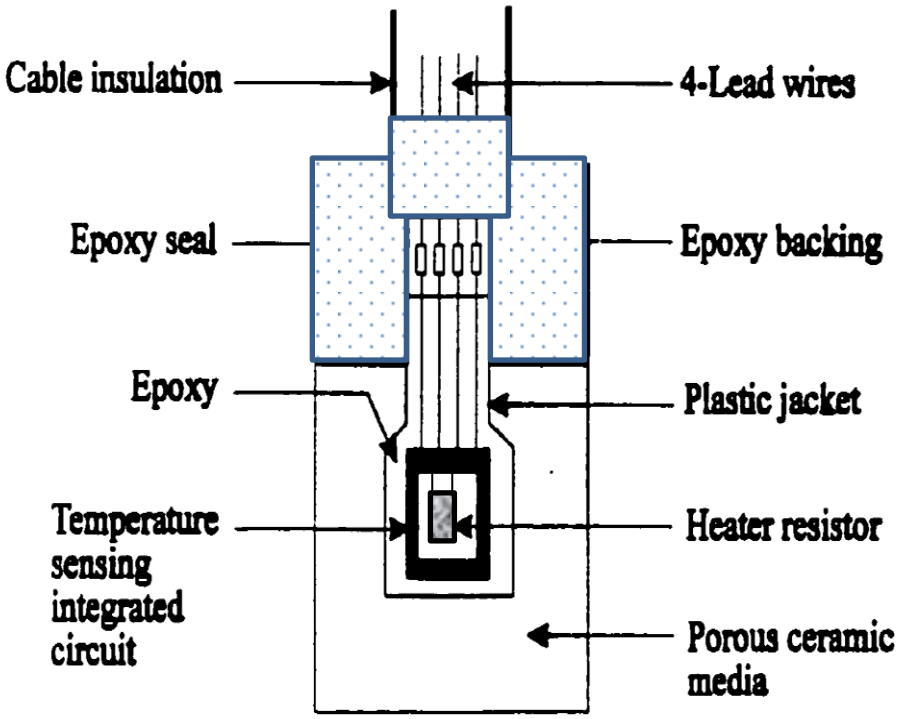


Fig 4.7 Cross section of thermal conductivity sensor after Fredlund *et al.,* 1994

Due to the variation in the properties of individual ceramic porous blocks calibration is required for optimum functioning. This is achieved by using a pressure plate and applying different matrix suctions to a soil in direct contact with the sensors. A correlation can now be obtained between the measured temperature or its related voltage readings and the matrix suction. The thermal conductivity sensor is used for both laboratory and field determinations of matrix suction. It is advantageous in that its readings are not affected by the amount of salt concentration present in the soil. However the porous ceramic block is influenced by hysteresis and takes a long time to respond to a change in suction.

4.2.3 Time Domain Reflectometry (TDR)

TDR is used for an indirect determination of matrix suction. It was first used to measure the dielectric properties of materials. The use of TDR for soil moisture measurements is fairly recent (Topp et al., 1980). Since then many others have used it, for example Dalton *et al.* (1984); Kalinski and Kelly (1993); Benson and Bosscher (1999); Amente et al. (2000) and Yu and Drneich (2004).

The working principle behind the TDR is based on the travel time of an electromagnetic wave emitted from a material of electric discontinuity. The dielectric constant is evaluated from the travel time of the electromagnetic wave and the length of the waveguide. When the travel time varies with a change in the characteristics of the material around the waveguide, its dielectric constant will also vary. The speed of the wave through the waveguide embedded in the soil can be given with respect of the dielectric property of the bulk soil as:

$$\varepsilon_b = \left(\frac{c}{v}\right)^2 = \left(\frac{c\,t}{2L}\right)^2 \qquad 4.1$$

Where v = velocity of the electromagnetic wave.

c = speed of light in vacuum (3×10^8 m/s).

L = Length of conductor or waveguide length.

t = time of traverse of the electromagnetic pulse to travel between wave guide length 2L.

ε_b = Soil bulk dielectric constant.

Water has a very high dielectric constant which ranges between 80-81 compared to say air with a value of 1, ice 4, and soil 3-5. This large disparity of the dielectric constants makes the method relatively insensitive to soil composition and texture and thus adequate for liquid

soil water measurement. The dielectric property of the soil is inversely proportional to the waveguide length L and is expressed as:

$$\varepsilon_b \propto \left(\frac{1}{L}\right)^2 \qquad 4.2$$

A relationship can then be established between the dielectric property of bulk soil and that of water content of the soil, whereby its dielectric property can be determined by the expressions below.

$$\frac{\varepsilon_w}{\varepsilon_b} = \left(\frac{L}{L_w}\right)^2 \qquad 4.3$$

$$\varepsilon_w = \varepsilon_b \left(\frac{L}{L_w}\right)^2 \qquad 4.4$$

Where L and L_w is the travel of the wave in bulk soil and wet soil respectively.

Calibration of the TDR can be carried out using the relationship between soil bulk dielectric constant, ε_b and the volumetric water content θ_w for water contents less than 50 %. The relationship is given by Topp et al. (1980) as:

$$\theta_w = -5.3x10^{-2} + 292x10^{-2}\varepsilon_b - 5.5x\,10^{-4}\varepsilon_b^2 + 4.3x10^{-6}\varepsilon_b^3 \quad 4.5$$

Calibration can also be established by relating the volumetric water content and suction measured with a pressure plate apparatus, from which a relation can be drawn with the dielectric constant of the soil.

The TDR measures suction in the range of 0-1500 kPa and is excellent for both laboratory and field measurements. The equilibration time is in hours. The advantages of the TDR include:

- They are excellent for measurement of volumetric water content to an accuracy of within 1-2 %.
- Enable measurements to be carried out quickly.
- Calibration requirements are minimal - in many cases soil-specific calibration is not needed.
- Since the TDR has a very narrow response area perpendicular to the waveguides, the volumetric water contents can be obtained at very high degrees of vertical resolution and continuous assessment of soil water measurements is possible through automation and multiplexing.

The disadvantages include:

- It requires sophisticated electronic devices.
- There is a high possibility of signal attenuation in saline soils.
- It is not recommended for water logged soils or soils having high organic contents. In such cases the TDR must be calibrated for these.

4.2.4 In-contact filter paper

This may be classified as the simplest method of measuring soil suction. It was first used by Hansen (1926) in Denmark, though Gardner (1937); Fawcett and Collis-George (1967) McQueen and Miller (1968); Al-Khafar and Hanks (1974) may be credited with having made it popular for suction measurements. Attempts at using filter paper for measuring suction in geotechnical engineering are credited to (McQueen (1968); Ho (1979); Tang (1978); Khan (1981); Gallen (1985); Chandler and Gutierrez (1986).

The filter paper method exploits the water absorptive characteristics of filter paper. When filter paper is exposed to a soil environment it will either absorb or desorb moisture until the suction in the soil and filter paper is equalized. The soil suction is then obtained from determination of the water content of the filter paper. Two types of filter papers are commonly used for suction determination: the Whatman No. 42 and the Schleicher & Schuel No. 589 WH.

The in contact filter paper method is used for the indirect determination of matrix suction. A filter paper of known weight is brought in direct contact with the soil specimen and placed in a container which is sealed with an electric tape and placed in an insulated temperature controlled box. After equilibration has been attained (after about 7-14 days) the filter paper is weighed and its moisture content determined. The accuracy of the method depends on the quality of the filter paper used, the sensitivity of the weighing balance and the accuracy of the established calibration curve.

The calibration curve for the filter paper is done by equilibrating the filter paper in a pressure plate apparatus (or suction plate) at various applied suction pressures and the moisture content of the papers is determined separately.

A number of researchers such as Chandler *et al.* (1992); Leong *et al.* (2002) and Power *et al.* (2008) have carried out the calibrations of Whatman No. 42 filter paper for both the contact and non-contact filter. They are shown in table 4.2.

Table 4.1 Calibrations for estimating suctions by filter paper technique

Filter paper	**Reference**	**Calibration equations (s in Pa)**	
Whatman No 42	Chandler *et al.,* 1992	Matrix suction log.s =4.84-0.062 w log.s=6.05-2.48 log w	 w < 47% w > 47%
		Total suction log.s =4.84-0.062 w log.s=5.31-.088 w	 w < 47% w > 47%
	Leong *et al.,* 2002	Matrix suction log.s =2.91-0.023 w log.s=4.95-.067 w	w ≥ 47% w < 47%
		Total suction log.s =8.78 -0.22 w log.s=5.31-0.088 w	w ≥ 26% w < 26%
	Power *et al.,* 2008	Contact log.s =1.51-0.944 log w log.s=6.71-2.93 log w	37≤ w ≥ 38 w < 26%

4.3 Indirect osmotic suction measurement

Osmotic suction may be present in both saturated and unsaturated soils. In saturated soils, the osmotic suction remains constant except if there is an inflow of contaminated water. Osmotic suction increases in unsaturated soil as it dries due to the increase in the concentration of the solutes as the water content decreases. An indirect approach to measure osmotic suction is by using the squeezing technique.

4.3.1 Squeezing technique

The osmotic suction is measured indirectly by determining the electrical conductivity of an extract of the pore fluid. The pore fluid squeezer

technique enables the entire range of osmotic suction to be measured and is said to give reasonable measurements of suction (Brackley, 1971, Morgenstern, 1976). This method consists of extracting the pore fluid from soil samples sandwiched between a compressing piston and a set of disks at one end, and at the other end another disk, filter paper and a cylindrical base where a syringe is used to extract the pore fluid. An example of a pore fluid squeezer is that given by Manheim (1966) shown in figure 4.8

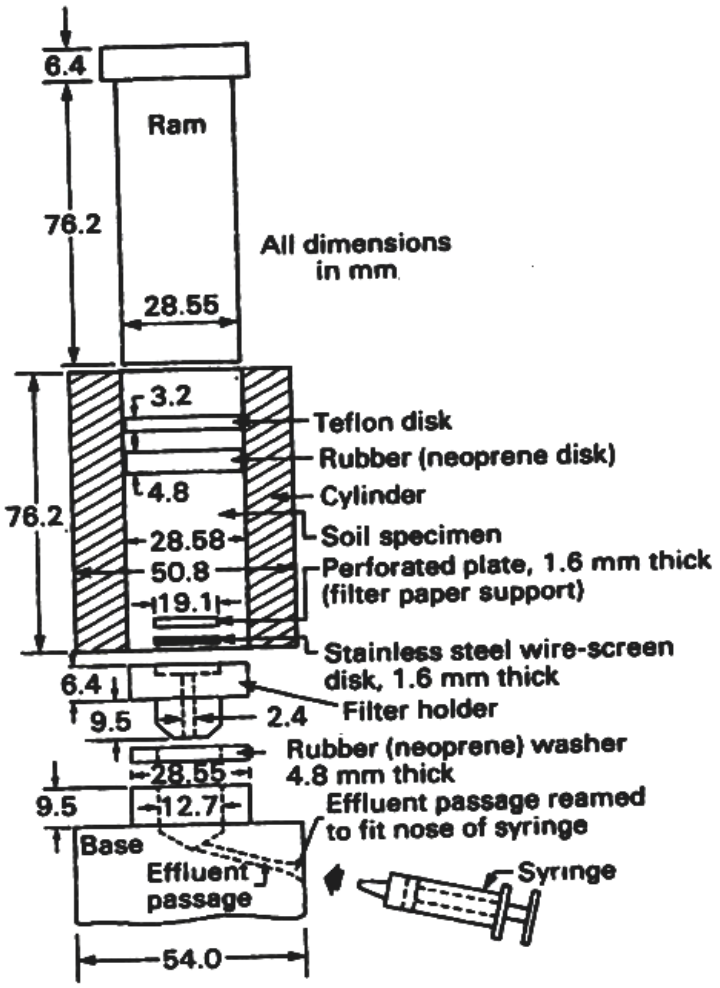


Figure 4.8 Pore fluid squeezer (Manheim, 1966).

By using an osmotic suction versus conductivity curve, the electrical signals are converted to osmotic suction (Fredlund and Morgenstern, 1977). The results obtained using the squeezing technique by Krahn and Fredlund (1972) have been reported to be influenced by the magnitude of the extraction pressure. Experiments carried out on glacial till and Regina clay required a squeezing pressure of about 34.5 MPa. The osmotic suctions obtained are shown to agree closely with the total suction using a psychrometer minus matrix suction measurements from pressure plate. From their tests, Krahn and Fredlund (1972) attest to the reliability of the osmotic squeezing technique for osmotic suction measurement.

4.4 Indirect total suction measurement

Indirect suction measurement techniques require the measurement of the moisture equilibrium condition of the soil. In this method the total suction is obtained from the measurements of the vapour phase which is in equilibrium with the soil sample. Some of the instruments used to measure total suction indirectly include the thermocouple psychrometers, relative humidity sensors, chilled mirror hygrometer and non-contact filter paper. Each of these methods is described below:

4.4.1 Thermocouple Psychrometer

The thermocouple psychrometer is an instrument that is used to determine soil suction by measuring the relative humidity within the soil. There are two types of thermocouple psychrometers: the Peltier type (Spanner, 1951) and the wet loop type (Richards and Ogata, 1958) . Both types are similar in their mode of functioning which is dependent on the temperature difference between an evaporating junction and a non-evaporating junction. They differ from each other in how the evaporating

junction is wetted to induce evaporation. A typical Peltier type thermocouple psychrometer is shown in figure 4.9.

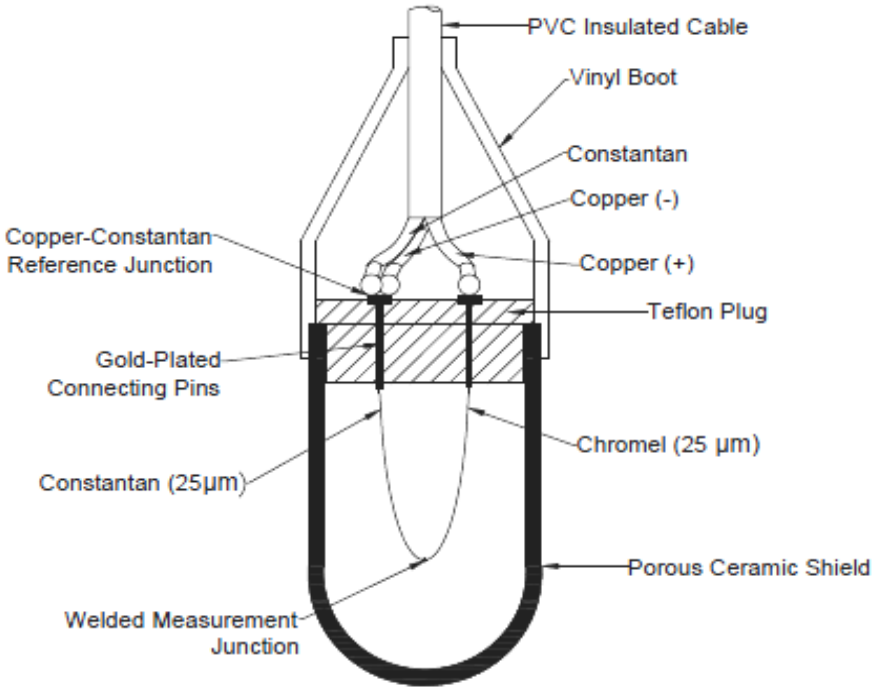


Figure 4.9 Peltier type thermocouple psychrometer

It is made up of a loop of two dissimilar thin wires of about 0.0025 mm enclosed in a porous ceramic or stainless steel mesh. The two thin wires comprising the circuit are made of constantan (copper–nickel alloy) and chromel (chromium–nickel alloy) joined together to form a measuring junction. The separate ends of the dissimilar wires are connected to copper connectors, called reference junctions, which then lead to a voltmeter.

If the measuring junction of the thermocouple, T, is at the same temperature as the reference junctions there is no voltage generated and

the voltmeter reading is zero. If the temperature of the junction, T, is increased relative to that of the reference junctions then a positive voltage is induced in the circuit which will be recorded on the voltmeter. Similarly, decreasing the temperature of junction, T relative to the reference induces a negative voltage. The Seebeck effect is the phenomenon of an induced electromotive force in a closed circuit made up of two dissimilar metals when the two junctions have two different temperatures.

The Peltier effect involves passing an electric current through the two dissimilar wires; the measuring junction cools the air below the dew-point temperature resulting in the condensation of water onto the junction. When the current dies down, the condensed water evaporates, causing a further drop of the temperature at the junction of the dissimilar wires. This drop in temperature of the junction is a function of the rate of evaporation which is also affected by the amount of atmospheric water vapor. A Seebeck effect voltage is then induced which is measured by the voltmeter.

Prior to the use of the psychrometers, these must be calibrated using salt solutions of known molarity. The psychrometer tips are suspended in the salt solutions for an hour in a temperature controlled environment and thereafter the voltage readings are taken. A regression curve between salt molar solutions and voltage readings is established. These now can be used to determine suction in soils. The magnitude of induced output voltage depends on the suction of the soil (relative humidity) and the temperature. The output voltage is temperature dependent and, as such, the results can be adjusted to a temperature of 25 °C by using the formula below after (Brown, 1970; Wiebe et al., 1970).

$$\textbf{Corrected reading} = \frac{\textbf{measured reading}}{(0.325+0.027t)} \qquad 4.6$$

Where t = temperature in °C

4.4.2 The transistor psychrometer (Relative Humidity Sensors)

The transistor psychrometer consists of a thermally insulated container containing two bulbs – the wet and dry transistor probes which act as the wet and dry thermometers. The sensors measure the relative humidity of the air space which is in equilibrium with the soil specimen. The wet transistor holds a standard size of distilled water drop. When an electric current passes through the circuit, the water on the wet transistor evaporates resulting in a drop of the temperature of the wet transistor. The difference in temperature between the wet and dry thermometers gives the measure of the relative humidity after an equilibrium period of 1 hour, which is related to the soil suction. Its range of suction measurement is between 100-10,000 kPa. Bulut *et al.* (2000) have shown that the transistor psychrometer has a better capability of measuring total suction at lower moisture levels, compared with other psychrometric methods.

The transistor psychrometers are calibrated with salt solutions (just like the thermocouple psychrometers). They are very sensitive to temperature fluctuations, hysteresis and the size of the water drop. The voltage reading for zero total suction is obtained when the probes are exposed for about 4 hours over distilled water and the output adjusted to an initial zero voltage reading before calibration. Thereafter different voltage readings at various salt concentrations are recorded, after an equilibration time of one hour. Thereafter the Kelvin equation 2.15 on page 22 is used to obtain the total suction.

4.4.3 Chilled-mirror hygrometer

This equipment is similar to the thermocouple psychrometer and it measures total suction between 150 kPa and 60 MPa with an equilibration time of 5 minutes. Its principle of functioning is based on equilibrating the liquid phase of water in a soil sample with the vapour phase of the water in the air space above the soil specimen in a sealed chamber (Bulut & Leong, 2008). The sealed chamber contains a fan, a mirror, an optical sensor, an infrared sensor, a thermocouple and a soil specimen. An example of the device is shown in figure 4.10. The thermocouple attached to the mirror measures the dew point temperature, while the fan circulates the air in the sealed chamber and speeds up vapour equilibrium.

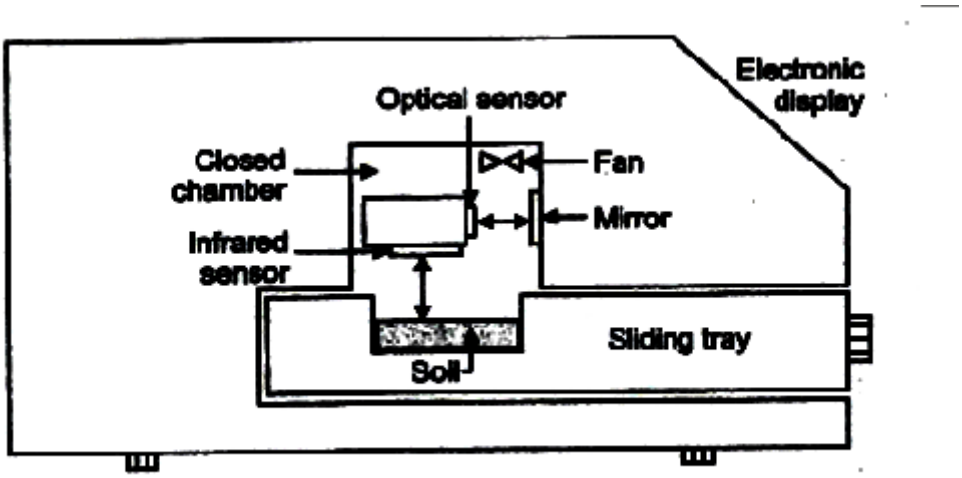


Figure 4.10 Schematic diagram of WP4 chilled mirror psychrometer and characteristic curve at low suction range

An applied Peltier effect cools the mirror until dew is formed and then heats it to evaporate it. The temperature of the specimen, which is equal to the temperature of the vapour space, is measured by the infrared sensor. The temperature of the soil sample and the dew point temperature are used to determine the relative humidity, from which the soil suction can be calculated using the Kelvin equation.

A calibration curve is established using standard salt solutions of known concentrations against their osmotic suctions. Figure 4.11 shows one established by Bulut *et al* (2002).

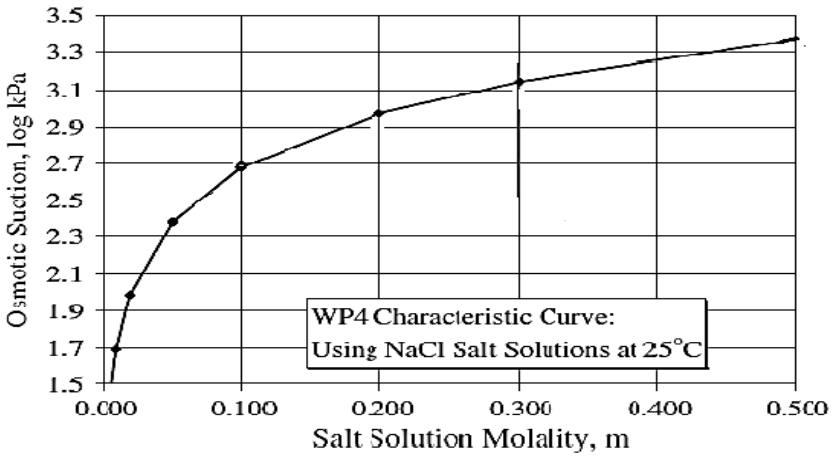


Figure 4.11 Calibration of WP4 chilled mirror psychrometer

Leong *et al.* (2003) evaluated the accuracy of a chilled mirror dew point device using compacted soil samples. A thorough calibration of the instrument using several standard salt solutions was performed.

The equilibration time during calibration and total suction measurement was short, less than 15 min. The total suction measurements on the compacted samples were compared to the sum of matric and osmotic suctions of the same soils that were measured independently. The matric suction of the soils was measured with the null-type axis-translation apparatus and the osmotic suction of the samples was estimated from electrical conductivity measurements of the soil water solution obtained from a pore fluid squeezer device. The test results showed that total suctions obtained using the chilled mirror dew point device were always greater than the sum of the matric and osmotic suctions measured independently.

4.4.4 Non-contact filter paper

The non-contact filter paper method measures the total suction of soil. In this method the vapour phase separates the filter paper and the soil which acts as barrier, therefore exchange of solutes is impossible. The calibration procedure is carried out as given above in 4.3.4. Given, therefore, an established calibration curve the suction of soil can be computed from the curve equation using the obtained water content.

The non-contact filter paper method has been used in the field to measure total suction (Fredlund 1989). It is also suitable for laboratory conditions and the practical range of suction measurement is between 50 kPa - 30 MPa or higher.

4.5 Methods of controlling suction

These are methods used to control suction in the laboratory. They are often used in apparatuses such as the triaxial cell, shear box and odeometer. The three methods available for controlling suction are the axis translation technique, the osmotic technique and the vapour equilibrium technique.

4.5.1 Axis translation Technique (ATT)

This technique was proposed by Hilf (1956), to control matrix suction in unsaturated soils. The basic principle of the axis translation technique (ATT) is to raise the pore air pressure such that positive values of the pore water pressure are measured. The technique enables the negative pore water pressure to be measured without cavitation. Since the negative pore water pressure is also raised, the pressure difference between the pore air pressure and the pore water pressure is the matrix suction and its value remains the same. The matrix suction obtained is limited by the air entry value of the ceramic disks and values of high air entry ceramic disks of 1500 kPa are readily available in the market. Usually the water pressure in the water reservoir is kept as close as possible to zero with no flow permitted. This is what has been called to as the null axis translation technique.

The main advantage of ATT is that no chemical is used in the process to control suction therefore the risk of changing the chemistry of the pore fluid is eliminated. The disadvantages include the possible diffusion of air through the high air entry discs into the pore water pressure system. The diffusion of air leads to the formation of air bubbles in the water thereby influencing measurements. A flushing system is needed to overcome this (Bishop and Donald 1961; Fredlund 1975; Sivakumar 1993). Also the air and water phases must be continuous in order to characterize actual suction within the soil sample.

4.5.2 Osmotic Technique (OT)

This technique has been used to control suction in oedometers (Delage *et al.,* 1992; Dineen and Burland, 1995; Delage, 2002), the shear box (Boso *et al.,* 2005) and the triaxial apparatus (Delage *et al.,* 1987; Cui and Delage, 1996; Ng *et al.,* 2007). The matrix suction is controlled by allowing the pore water to equilibrate with a salt solution of known osmotic potential, separated from the soil specimen by a semi permeable

membrane (Zur, 1966). The semi permeable membrane is permeable to water molecules but not the salt molecules. Different values of suction are applied using different concentrations of polyethene glycol (PEG) which is a salt with large molecules. This generates an osmotic pressure gradient across the membrane enabling the movement of water from the soil until the suction and osmotic pressure are equal. The advantages of using the osmotic control technique include:

- The real conditions of suction can be reproduced without resort to using air pressure on the sample.
- As a result of not applying air pressure diffusion problems are eliminated
- It is very adaptable to triaxial soil testing since there is no need to impose high values of the confining stress to maintain the constant net total stress (σ-u_a) at the elevated pressures needed to impose high suctions. Cui and Delage (1996) have applied suctions as high as 1500 kPa using this technique. Comparably, ATT has a better adaptability to triaxial testing than OT.
- The osmotic technique is also very adaptable to oedometer tests since the bottom porous stone is replaced by a semi permeable membrane.

The disadvantage of the osmotic technique is the perishable nature of the semi permeable membrane. When it fails, suction cannot be controlled and more especially very high suctions.

4.5.3 Vapour equilibrium technique (VET)

This method was developed by soil scientists for controlling suction in soils. There are two approaches to achieving this, which are the isopiestic (or same pressure) approach and the two pressures method. The two pressures approach relies on attaining the required relative humidity by either varying pressure or by mixing the vapour pressure

saturated gas with dry gas. The isopiestic approach is achieved by attaining vapour equilibrium for acid or salts in a closed thermodynamic system. According to Delage *et al.* (1998), the vapour equilibrium technique was first used in geotechnical engineering by Esterban and Saez (1998).

In the vapour equilibrium method the soil specimen is placed in a thermodynamically sealed system connected to a desiccator containing aqueous salt solutions of known concentrations. Equilibrium is attained by the exchange of water with the vapour until the suction in the soil specimen is equal to the partial vapour pressure.

The vapour equilibrium technique can be attributed all the advantages of the osmotic technique with the additional advantage that the testing times can be significantly reduced by using an air circulation technique employing an air pump (Blatz and Graham, 2000; Cunningham *et al.,* 2003; Lloret *et al.,* 2003; Dueck 2004; Oldecop and Alonso, 2004; Alonso *et al.,* 2005). The main disadvantage is the extremely long time required for equilibrium to be attained, in some cases 1-2 months.

4.6 Summary

There are so many methods of measuring suction that they cannot be all mentioned. Just the common ones have been described here, which are widely used in engineering practice and in research. The table 4.3 gives a summary of the various methods described, their advantages, disadvantages, suitability for laboratory or field use and their equilibration time.

Table 4.2 Summary of suction measurement methods

		Method/Technique	Suction range (kPa)	Equilibrium time	Laboratory (L) or field application (F)
Direct suction measurement	Matrix suction	Tensiometer	0-1,500	Minutes	L & F
		Suction probe			
Indirect suction measurement	Matrix suction	Electrical conductivity sensor	50-1,500	6-50 hours	L & F
		Thermal conductivity sensor	0-1,500	Hours – days	L & F
		In – contact filter paper	All	7-14 days	L & F
		TDR	0-1500	Hours	L & F
	Osmotic suction	Squeezing technique	0-1,500	days	L
	Total suction	Thermocouple Psychrometer	100-10,000	1 hour	L & F
		Transistor Psychrometer	100-8000	Hours-days	L
		Chilled-mirror hygrometer	150-30,000	10 minutes	L
		Non-contact filter paper	All	7-14 days	L & F

PART II SHEAR STRENGTH MEASUREMENTS

4.7 Introduction

The shear strength of soil is the maximum resistance to shear that the soil can sustain. When this is exceeded the soil is said to fail. This usually occurs in the form of slip surfaces. The internal friction angle of the soil and the cohesion contribute to shear strength of soil. The internal friction angle is a measure of resistance to interlocking of the soil particles while cohesion is a measure of the forces which tend to bind the soil particles together. These two contributions form the Mohr-Coulomb shear strength equation for saturated soils which has been extended for unsaturated soils as explained in chapter three.

4.8 Experimental techniques for unsaturated soil testing

The extension of the Mohr-Coulomb shear strength criterion to unsaturated soils requires that the shear strength parameters c’ and φ’ be determined. For saturated soils these are determined using the conventional triaxial and direct shear apparatus. However for unsaturated soils these apparatuses must be slightly modified to make room for pore air and pore water pressure measurements simultaneously. Several challenges to the experimental determination of the shear strength of unsaturated soils have been identified (Blight 2013) such as:

- The need to make a large number of tests to establish the variation of shear strength with matrix suction.
- The long time required to achieve equilibrium in soil samples before testing.
- Specialized equipment for unsaturated soil testing is complicated and expensive.

4.9 The Direct Shear Box Testing

The direct shear apparatus consists of a horizontally split open metal box. The soil material is placed into the box and one half of the box moves relative to the other. Vertical forces are applied through a load frame acting through the top half of the box, while horizontal forces are applied through a motor driven device. The diagram below gives a simple illustration of the shear box apparatus.

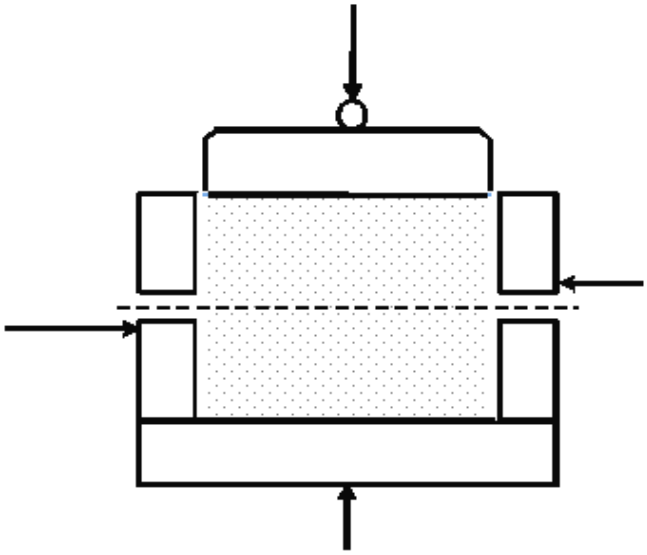


Fig 5.12 Shear box apparatus

The direct shear apparatus has been modified to be able to test unsaturated soils. Donald (1956) modified the traditional direct shear box and reported a series of shear tests on unsaturated fine sands and

coarse silts. In his modification the top of the shear box was exposed to atmospheric pressure while the pore water pressure was controlled. Escario (1980) also modified the traditional shear box making room for measurement of both the pore air and water pressures and allowing suction to be controlled through the axis translation technique. Gan *et al.* (1988) have described another modification where the shear box is enclosed within an air pressure chamber allowing control of the air pressure in the specimen. The control of pore water pressure was through a high air entry pressure disk located at the base of the specimen. The following results can be obtained from a shear box apparatus:

- The peak and residual angles of shearing resistance.
- The peak and residual cohesion intercepts.
- The volume change response of the soil to shearing (dilatant or contractant).

The advantages of the direct shear box test are:

- The test is relatively simple and quick to perform.
- During testing, large shear displacements can be applied enabling the determination of the soils residual strength.
- The time required for specimen consolidation and drainage is small, because of a small drainage path length equivalent to half the specimen thickness.
- Shearing takes place along a predetermined plane.

Some of the disadvantages and limitations of the direct shear box include:

- Impossible to control drainage, so the soil sample is normally assumed or tested either as drained or undrained.

- The stress conditions during test are indeterminate so only an approximation can be given because they are not uniform. Hence a stress path cannot be established.
- Shear stress failure may develop progressively during testing.
- Specimen saturation for example by back pressuring is not possible therefore specimen must be inundated.
- The area of the shearing surface changes continuously, so a correction for this change of area is needed.

4.10 The triaxial testing

The first triaxial apparatus was developed by Bishop and Henkel (1962) and up to now only minor improvements have been done on it, such as the replacement of the mechanical measuring systems with electronic control systems and data logging facilities. The triaxial equipment can be used to determine the triaxial strength, stiffness and characteristic stress (k_o) ratio of soils. An illustration of a triaxial cell is given in figure 4.13. In the testing of unsaturated soils, the triaxial cell has been coupled to various suction controlling apparatuses. The most common uses the axis translation technique. The use of the osmotic control technique in triaxial testing has been reported by Cui & Delage (1996) while the vapour control technique has also been reported (Blatz & Graham 2000, Chavez *et al.,* 2009). Some triaxial testing devices have also been developed using psychrometers (Tang *et al.,* 2002 and Thom *et al.,* 2008) as well as high capacity tensiometers (Colmenares & Ridley, 2002; Meilani *et al.,* 2002 and Jotisankasa *et al.,* 2007).

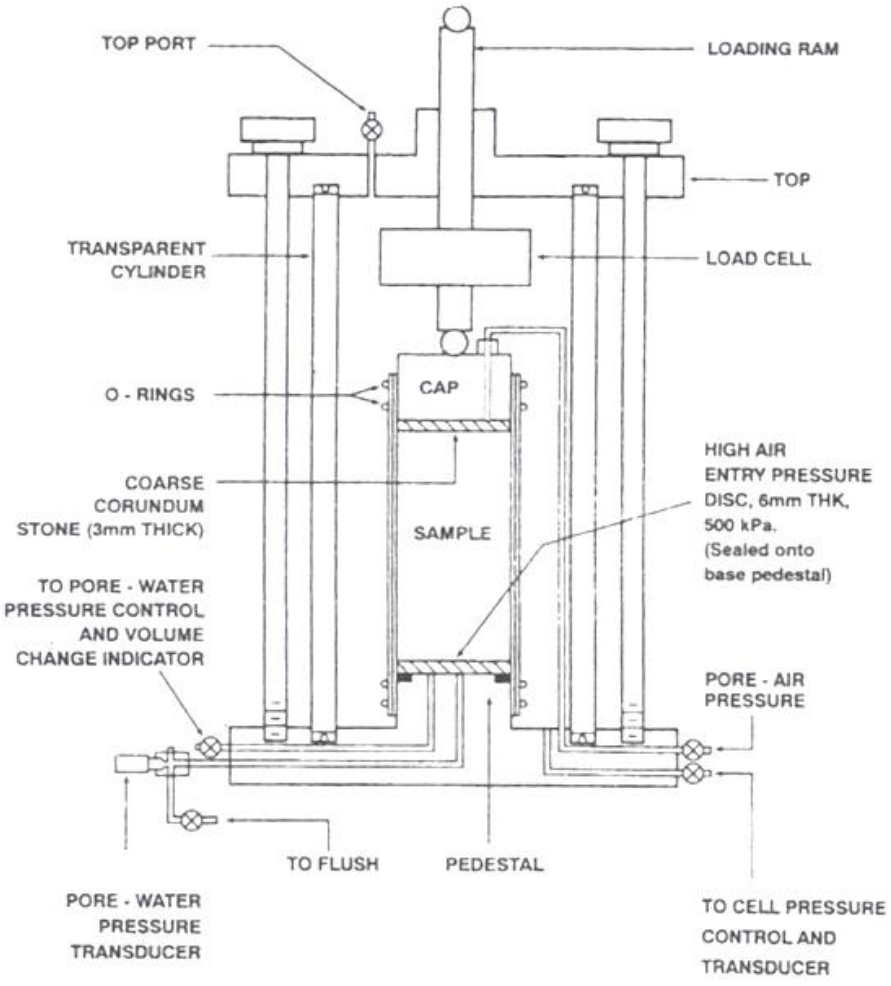


Figure 4.13 Triaxial cell

In present practice the following types of triaxial tests are carried out.

- Unconsolidated undrained tests denoted (UU) with or without pore pressure measurement.
- Isotropically consolidated undrained compression (CIU) test with or without pore pressure measurement.
- Isotropically consolidated drained compression (CID) test.

In compression triaxial testing the soil specimen is acted upon by three stresses. The vertical axial stress is the major principal stress σ_1, while the intermediate stress σ_2 and the minor principal stress σ_3 are equal and corresponds to the cell pressure. (Brenner *et al.* 1997)

The following types of results can be obtained from triaxial soil testing (Brenner *et al.* 1997):

- The strength envelope with peak angle of sharing resistance and cohesion intercept (either in total or effective terms)
- The pore pressure response to shearing (in undrained tests)
- The volume change response to shearing (in drained tests on saturated soils and drained and undrained in unsaturated soils)
- Tangent and secant moduli (or corresponding unloading and reloading moduli) for the soil
- Consolidation characteristics
- Air and water permeability under different confining pressures and flow gradients

The advantages of the triaxial shear include (Brenner *et al.* 1997):

- Control of drainage is possible as well as the measurement of pore pressures.
- Stress conditions in the soil sample remain more or less constant and are more uniform than in direct shear test. They are controllable during test and their magnitude is known with fair accuracy.
- Volume changes during sharing can be determined accurately

The disadvantages and limitations of the triaxial tests include (Brenner *et al.* 1997):

- The influence of the intermediate principal stress σ_2 cannot be evaluated. In certain practical problems which approximate the

conditions of plain strain σ_2 may be higher than σ_3. This will influence c' and φ'.

- The principal stress direction remains fixed, and conditions where the principal stresses change continuously cannot be simulated easily.
- Influence of the end restraints (end caps) causes non uniform stresses, pore pressures and strains in the test specimens and barrel shape deformation, all of which must be considered and corrected for where possible.

4.11 Choice of equipment for research

The resistance of a soil specimen to deformation at the macro scale is closely linked with the soil particle arrangement and interactions at the micro scale. The choice of equipment was to specifically replicate what seems to take place at the micro level which in turn affects the macro scale.

At the micro scale the intermolecular forces were modelled using capillary tubes with varying pore fluid concentration. The suction response of the varying pore fluid was obtained using a psychrometer. The motivation for using these two tests above is because of their simplicity and availability. Meanwhile at the macro scale the interest was measuring the shear strength. The triaxial equipment was preferable for this because both the saturated and unsaturated soil tests could be performed on them with very minimal adaptations. The axis translation technique (ATT) was easily applied on the specimens. The consolidated drained test is best carried out on triaxial equipment. The shear box was also available but it needed an enclosure so that air pressure could be applied. Using the shear box for unsaturated soil testing would require more challenging techniques in measuring drainage as well as pore

pressures. Different combinations of axial stress and cell pressure are possible only on the triaxial test.

CHAPTER FIVE

EXPERIMENTAL SETUP AND RESULTS

5.0 Introduction

This chapter describes the materials used, the sample preparation, the equipment calibration and the experimental procedure adopted to study the relationship between suction and shear strength in unsaturated soils.

5.1 Materials

In keeping with the objective of investigating the role of suction in the shear strength of soil, aggregates were selected which will not react (or will have as little reaction as possible) with the mixing fluids. Clayey soils were avoided because of the possible reaction of the clay minerals with ionic and non-ionic solutes. The materials ranged from slightly inert (limestone powder) having a pH > 7 to inert (quartz powder) pH < 7 and to completely inert (fine glass beads) pH < 7.

5.1.1 Limestone powder

The limestone powder was sourced from a specific calcrete deposit in the Northern Province where it has been obtained for more than 50 years. The cream colored limestone went through a well-controlled milling process. The chemical and physical properties of the limestone powder are given in tables 5.1(a) and 5.1(b).

Table 5.1(a) Chemical properties of limestone powder.

Chemical composition	Percentage (%)
SiO_2	8
Al_2O_3	1
Fe_2O_3	0.4
CaO	49
MgO	1
Na_2O_3	0.1
K_2O	< 0.1
CO_2	40
Total	99.5

Table 5.1(b) Physical properties of the limestone powder.

Property	Putty Limestone
Natural colour	Light cream
Reflectance (Photovolt)	< 70
Colour in oil	Dark cream
Oil absorption	13-15 %
Moisture	1-2%
pH	9
SG	2.67
Bulk density	0.95-1.2

5.1.2 Quartz powder

The quartz powder was sourced from a supplier in Johannesburg and the chemical properties of the silica are given in table 5.1 (c).

Table 5.1(c) Chemical properties of the silica

Chemical composition	Percentage (%)
SiO_2	98.01
Al_2O_3	0.3
Fe_2O_3	0.2
TiO_2	0
ZnO_2	0
MgO	0.01
CO_2	0.12
Total	98.64

5.1.3 Fine glass beads

The fine glass beads were available in the laboratory. These were preferable since they were smooth and rounded and were within the range of fine sand fraction.

5.1.4 Particle size distribution of Aggregates

The particle size distributions of the aggregates were determined in accordance with ASTM 422 on dry aggregates. The particle size distributions obtained for the three aggregate materials are given on table 5.1 found in appendix pp. i and their grain size distribution curves are shown in figure 5.1. All these materials consist predominantly of particles the size of fine sand.

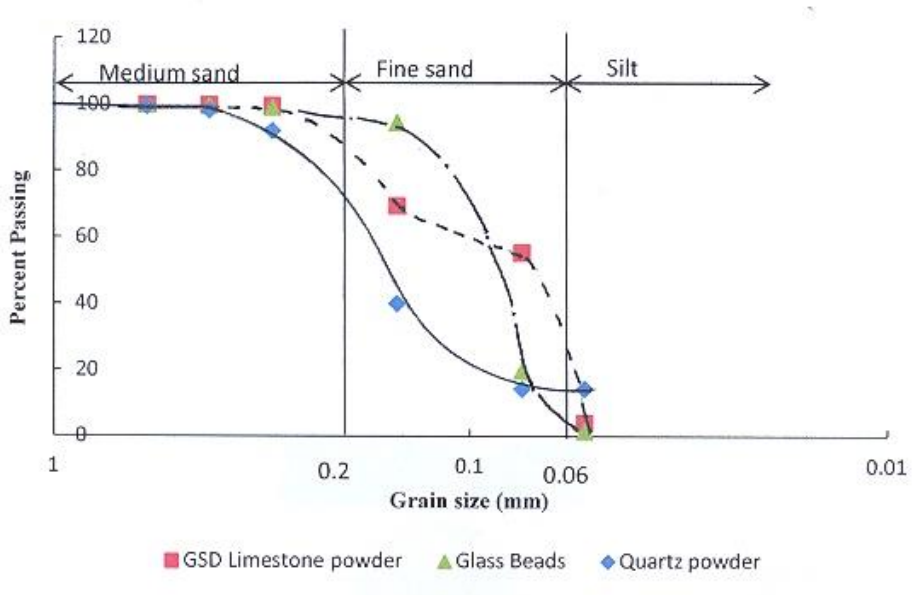


Figure 5.1 Grain size distribution of granular material.

5.1.5 Specific Gravity Determination

The specific gravity of the aggregates was determined in accordance with ASTM 854-00. The results of the specific gravity of the aggregates are given in table 5.1 (e)

Table 5.1 (e) Specific gravity of aggregates

Aggregates	Specific gravity
Limestone powder	2.67
Quartz powder	2.65
Fine glass beads	2.48

5.1.6 Sample preparation

The mixing fluids used in preparing the sample were distilled water, molar solutions of NaCl and detergent solutions. The molar solutions were obtained by dissolving molar quantities of NaCl in one litre of distilled water. 1 kg each of the aggregates were weighed into a mixing

bowl. The corresponding mixing fluid at moisture contents of 2, 4, 6, 8 and 10 % by mass was added to it and these were thoroughly mixed and kept in plastic containers which were sealed and kept for 48 hours for moisture equilibration. These were carried out for distilled water, various molar solutions of NaCl and detergent solutions. The specimens were statically compacted in a cylindrical mould of diameter 38 mm and 76 mm high in three layers. For each layer 50 g of moist aggregate mix was used. The void ratios of the specimens were estimated from the relation.

$$\mathbf{e = G_s(1 + w)\frac{\gamma_w}{Mass/volume} - 1} \qquad \mathbf{5.1}$$

The limestone powder was compacted to a bulk density of 1741 kg/m^3 giving void ratios ranging from 0.56 at 2 % moisture content to 0.69 at 10 % moisture content respectively. Quartz powder was compacted similarly to the same bulk density giving void ratios of 0.55-0.67 at 2% to 10 % moisture contents respectively. The fine glass beads were compacted to a density of 1671 kg/m^3 by weighing 48 g compacted in three layers, giving void ratios of 0.51 at 2 % moisture content to 0.63 at 10 % moisture content.

5.2 Surface tension measurements

5.2.1 Experimental Theory

The phenomenon of capillarity which is responsible for water rising above the water table has been exploited in order to measure surface tension. This is what has been termed the capillary model. A typical presentation of this model for soil is given by Marshall (1959), shown in Figure 2.6, in section 2.1.2. Equation 2.8 can be re- arranged to give equation 5.2 for the surface tension force in terms of the water rise in a capillary tube

$$T_s = \frac{\gamma_w h_c r}{2} \qquad 5.2$$

The surface tension was estimated from the height of water in the capillary assuming that the contact angle was zero since a clean glass was used.

The capillary tubes were clamped vertically and concentrated sulphuric acid was used to clean the glass by injecting the acid slowly through the capillary. Water was used to rinse the capillaries several times and then they were dried in an oven at 105 ºC for ten minutes. After cooling to room temperature, the radius of the capillaries was measured by injecting a known weight of water from a syringe. The radius of the capillary was estimated from the density volume relationship given below

$$v = \frac{m}{\rho} = \pi r^2 h \qquad 5.3$$

$$r = \left(\frac{m}{\rho \pi h}\right)^{1/2} \qquad 5.4$$

The temperature of the water used was recorded as well the laboratory temperature and the relative humidity of the air in the laboratory. The results of measurement of the radius of the capillaries are given in Table 5.2 (a) in appendix pp. ii.

The surface tension was measured by clamping two clean capillary tubes vertically over two beakers containing various molar concentrations of pure sodium chloride (0, 0.25M, 0.5M, 0.75M and 1M) and a non-ionic detergent at concentrations 0, 0.5 g/l, 1g/l and 2g/l. These capillaries were open to the 20˚C temperature-controlled laboratory. The relative humidity inside the laboratory was 61%. The capillary rise h_c in each

case was measured and three separate experimental repetitions were carried out. The surface tension was calculated from the relation in Eq. 5.1

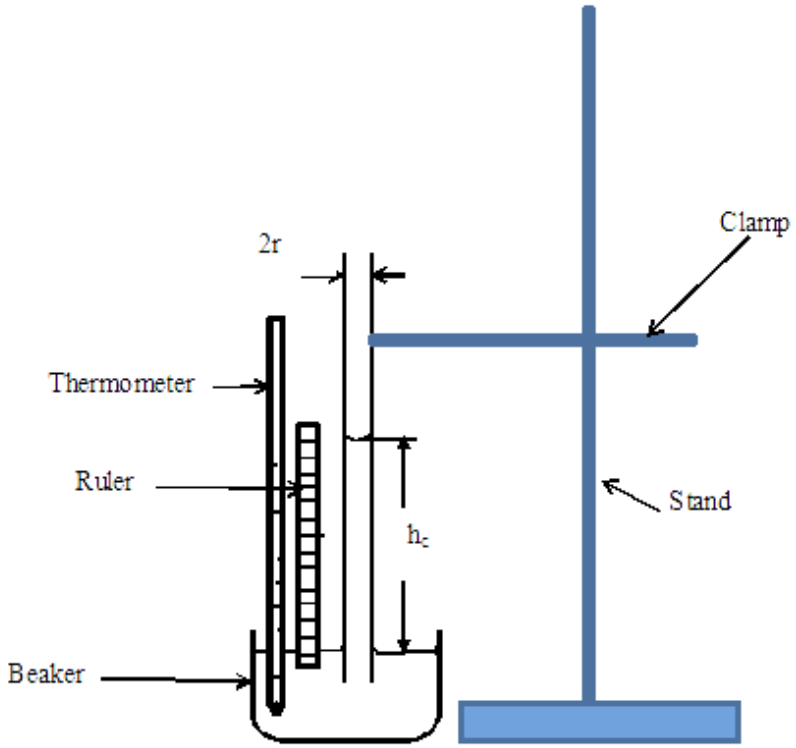


Figure 5.2 Experimental set up of glass capillaries to measure surface tension

5.2.2 Surface tension measurements in sealed space

A second experimental set up was made with the capillary tubes, side by side as before, but each within its own sealed air space, with one tube dipping into a beaker of pure water and the other into a 1M NaCl solution. These were left for four weeks to see if, with time, the capillary

rises would change as the humidity of the air above the menisci equilibrated with the liquid forming each meniscus.

The capillary tubes were left untouched and the two containers of liquid swapped, so that the capillary tube filled with pure water was now dipping into a beaker of salt solution and vice versa. Both remained within the same sealed air space for four weeks.

5.2.3 Results of Surface tension measurements in sealed space

The results of the surface tension measurements for distilled water, water diluted with ionic solute (NaCl) and water diluted with a non-ionic solute (detergent) for the first set of experiments are given in the Table 5.2 (b) and (c) in appendix pp. iii-iv. While for the second set of experiments no change in the meniscus levels were observed in either case.

5.3 Measurement of Total Suction

5.3.1 Calibration of psychrometers

The psychrometers were calibrated to obtain the regression equation unique for each of the psychrometer tips. The calibration procedure was as follows:

1. Holes were drilled in the lid of a container.
2. The psychrometers' tips were passed through these holes to an appreciable length and the holes were properly sealed with a silicon sealant and allowed to dry.
3. A salt solution of known molarity was placed in the container and the lid attached such that the psychrometers' tips was suspended over the solution.
4. The container was placed in a water bath and the temperature maintained at 25° C for a period of 1 hour

5. The leads of the psychrometer were connected to an HR 33 T voltmeter and three measurements of the total suction value in microvolts were carried out.
6. The process was carried out for different salt solutions.
7. The psychrometer tips were washed and dried after each set of measurements before re-use.
8. The results of the calibrations of the psychrometers are given in table 5.3 (a) in appendix pp. v.
9. The calibration curve for one of the psychrometer tips is shown below while the rest is in the appendix pp. vi-vii.

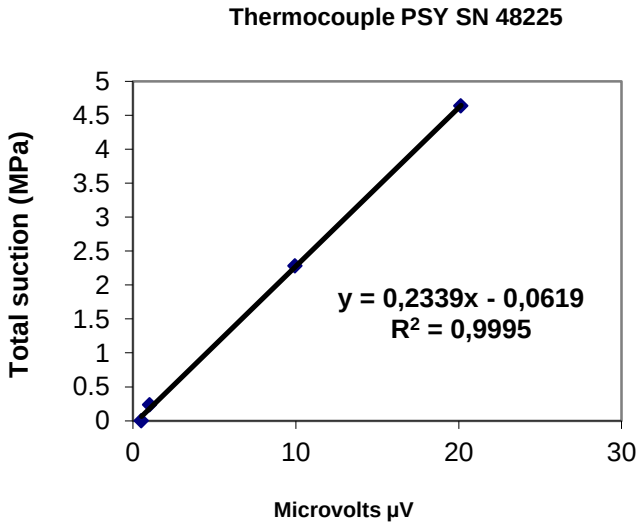


Figure 5.3 Calibration curve for psychrometer tip

5.3.2. Set up for total suction measurements

1. Specimens of the granular soil materials were mixed with distilled water, NaCl solution or 2g/l detergent solution at gravitational moisture contents of 2, 4, 6, 8, and 10 % and cured in sealed plastic containers for moisture equilibration for a period of 48 hours.
2. The prepared samples were then sealed in test tubes with the calibrated psychrometer tips suspended in the sealed air space above the soil materials for one hour before the suction measurements were taken.
3. The sealed test tubes were inserted in a water bath having a controlled temperature of 25 °C. The leads of the psychrometers were connected to a WESCOR HR-33T DEW POINT MICROVOLTMETER.
4. The results obtained were corrected for each of the psychrometers tips using the calibration regression curves established.

5.3.3 Results of total suction measurements

The results of thermocouple psychrometer measurements carried out on limestone powder, quartz powder and glass beads at a range of solution contents of (1-10%) using distilled water (control), 0.25 M, 0.50 M, 0.75 M, 1 M NaCl solutions and 2g/l detergent are given in Tables 5.3 (b), (c) and (d) in appendix pp. viii-x. ‘Real Mc’ stands for the target moisture content expected while ‘Lab Mc’ stands for the moisture content obtained after the aggregates have been mixed, cured for 48 hours and the suction determined using a psychrometer.

5.4 Matrix suction and Shear Strength Measurement

5.4.1 Calibration of triaxial cell

1. Brass pedestals 38 mm diameter with a recess 4mm deep and 35 mm diameter were made.
2. 500 kPa high air entry ceramic disks were sealed into the recess using an epoxy adhesive.
3. These were placed in beakers containing warm distilled water and vacuumed at 70 kPa until air bubbles were no longer coming out of the disks.
4. These were then mounted on the triaxial cell base and the cell was filled with de-aired water.
5. The triaxial cell was pressurized incrementally and the cell expansion and the pore water pressure were recorded.
6. A regression curve was established between applied pressure and cell expansion also another regression curve between applied pressure pore water pressures for each of the triaxial cells.
7. Readings of the calibration are presented in Table 5.4 (a)-(i) in appendix pp. xi-xv.
8. Pressure was maintained at 700 kPa and the ceramic disks were repeatedly purged by opening and closing the valves quickly to release trapped air.
9. Limestone powder was mixed with water at 2 % moisture content and kept to equilibrate for 48 hours in sealed plastic bags.
10. Triaxial specimens of diameter 38 mm and 76 mm long were prepared by compacting the material in three 50 g layers in a triaxial mould.
11. The specimens were quickly extruded and mounted on the triaxial base, enclosed with a rubber membrane and sealed from the environment at the triaxial base and the top cap with O-rings.

12. The triaxial jacket was replaced and filled with de-aired water and its pressure raised to 500 kPa. A 200 kPa air pressure was simultaneously applied through the top cap.
13. After 8-10 hours of consolidation the shearing was carried out at the rate of 2 %/ hour over 10 hours.
14. The effective confining pressure used was 500-200 = 300 kPa so the value of cell expansion at this pressure was used in the calculations of the deviator stresses.
15. The pore water pressure at each instant during testing was recorded u_w.
16. The suction at failure is obtained by (u_a-u_w)
17. A summary of sample calibration for 2% limestone powder is shown on table 5.4 (a)-ii on appendix pp. xv.

5.4.2 Consolidated undrained tests

These were carried out on limestone powder, glass beads and quartz powder. The aggregates were separately mixed with distilled water (control), 0.25 M, 0.50 M, 0.75 M and 1M NaCl solution and 2g/l detergent solutions and sealed in separate plastic bags for 48 hours to allow moisture equilibration. Specimens of 38 mm diameter and 76 mm height were made by statically compacting 150 g (fine glass beads 144 g) of aggregates in a cylindrical mould. The specimens were sealed using a rubber membrane onto de-aired ceramic disks having an air entry value of 500 kPa. The axis translation technique (Hilf, 1956) was used with an air pressure, $u_{a,}$ of 200 kPa, applied through the top cap and a confining pressure, $\sigma_{3,}$ of 500 kPa. Consolidation was achieved within 8-10 hours. Thereafter each specimen was sheared at constant water content at a rate of 2 % /hour, giving a time to failure of 10 hours. The pore water pressures were measured via a system filled with pure water, and represent matrix suction only. This is so since no semi

permeable membrane separated the water from the salt in the pore water, and salt ions were free to migrate into the water filling the pore pressure measuring system. In support of this statement Mitchell (1962) reported that no measurable osmotic pressure was detected across a 4 inch thick porous stone with 0.5 N NaCl solution and water placed on opposite sides for a period of 24 hours. The body of each triaxial specimen would have been subject to the full solute suction as well as the measured matrix suction.

5.4.3 Results of consolidated undrained triaxial strength measurements

The results of the consolidated undrained triaxial test carried out on the three granular soils are given in tables 5.4 (b), (c) and (d), in appendix pp. xvi-xxi.

5.5 Consolidated drained triaxial tests on saturated specimens

Specimens of 38 mm diameter and 76 mm height were made by compacting 150.0 g of mixed aggregates (limestone powder or quartz powder) in a cylindrical mould in three layers. These were sealed to the pedestal of a triaxial cell using a rubber membrane. The glass beads were sealed in a similar manner, with measured weights of the glass beads compacted (144 g) in a split mould mounted on the pedestal. A positive back pressure using the appropriate distilled water, 1M NaCl solution, or 2g/l detergent solution, was applied through the triaxial base till saturation was achieved in the sample. Once a B-value of about 0.9 was achieved in the back-pressured specimen, it was sheared with the back pressure maintained constant and at a rate of 2 % per hour. These tests were intended to find if solute suction has any effect on shear strength when the matrix suction is completely absent.

5.5.1 Results of consolidated drained triaxial strength measurements.

The results of the consolidated drained tests performed on the soil samples mixed with distilled water, 1 M NaCl solution and 2g/l detergent with the back pressure being either water, 1 M NaCl solution or 2g/l detergent are given in tables 5.5 (a), (b) and (c) in appendix pp. xxviii-xxx.

5.6 Consolidated undrained triaxial strength measurements on limestone specimens dried in salt solutions.

Specimens from limestone powder were moulded at 6% water content from mixes made with distilled water, 1M NaCl and 2g/l detergent solutions. These were made by compacting 150 g of moist limestone powder in a cylindrical mould to dimensions of 38 mm diameter and 76 mm long. These specimens were oven dried to a constant mass, at a temperature of 50°C for 24 hours. Thereafter, they were dried over saturated solutions of $ZnSO_4$ (90% RH), Na_2SO_4 (93% RH), and K_2SO_4 (98% RH) in desiccators for three months. After this, some of the specimens were tested in consolidated undrained compression using a confining stress, σ_3= 300 kPa, at a constant rate of 2% per hour. Those specimens which were not sheared were re-exposed to atmospheres over distilled water, 1M NaCl and 2g/l detergent solutions for another three months, making a total of six months. After the expiration period of six months, the specimens were sheared as in the case above.

5.6.1 Results of consolidated undrained triaxial strength measurements on specimens dried in salt solutions.

The results of consolidated undrained triaxial strength measurements on limestone powder are summarized in table 5.6 in appendix pp. xxxii.

CHAPTER SIX
DISCUSSIONS OF RESULTS

6.0 Introduction

The various tests results obtained are discussed in this chapter.

6.1 Discussion of surface tension measurements

The results of the surface tension measurements for distilled water, water diluted with ionic solute (NaCl) and water diluted with a non-ionic solute (detergent) are given in the Table 5.2 (b) and (c) on appendix pages (iii) and (iv). The corresponding graphs are given in figures 6.1(a) and 6.2(b) respectively.

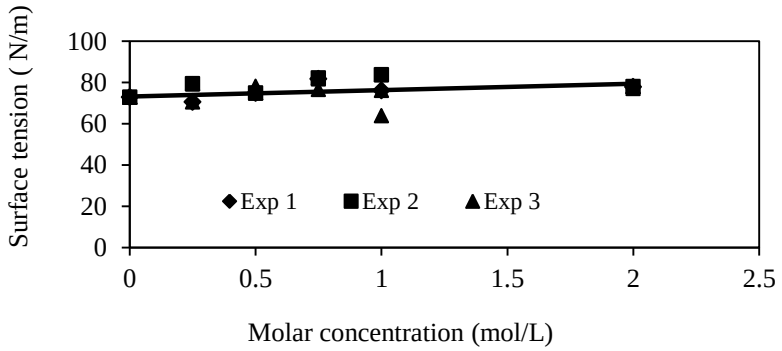


Figure 6.1(a) Effects of concentration of ionic solute (NaCl) on the surface tension.

Increasing NaCl concentration causes a very slight increase (10 %) in surface tension while detergent at a concentration of 2g/L causes a 50 % reduction of surface tension. This observation implies that dissolving sodium chloride in the water had virtually no effect on the capillary rise and hence on surface tension and so capillarity is a purely physical

surface effect and does not depend on the internal stresses in a solution that gives rise to solute or osmotic suction.

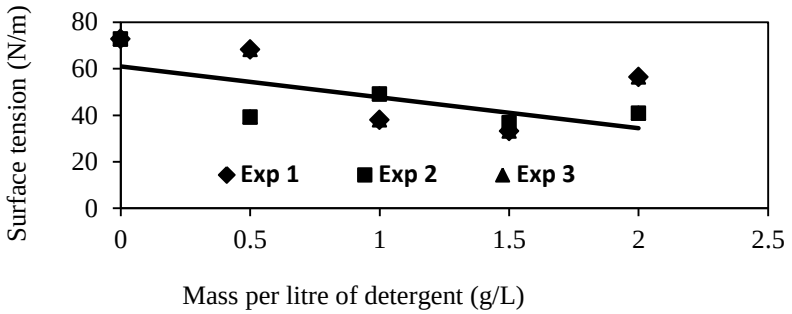


Figure 6.1(b) Effects of concentration of non-ionic solute (detergent) on the surface tension

This appears to contradict the assumptions of Raoult's law, which implies that, as more solute is dissolved in a fluid a lower relative humidity is obtained which consequently translates to a higher value of suction which, if the Kelvin equation is taken at face value, ought to translate to a higher meniscus rise in a thin capillary.

From Raoult's law, the relative humidity, H, in equilibrium with an aqueous solution is given by:

$$\mathbf{H} = \frac{\mathbf{n_w}}{\mathbf{n_w}+\mathbf{n_s}} \qquad \mathbf{6.1}$$

where n_w = number of moles of solvent and

n_s = number of moles of solute.

Also according to Kelvin's equation (Aitchison, 1965), the corresponding total suction is given by the equation:

$$\mathbf{h\gamma_w = \frac{R\theta}{m_w} \log_e [H]} \qquad \mathbf{6.2}$$

where h = height to which a solution in equilibrium with a relative humidity, H, would rise in a capillary of given radius,

R = universal gas constant,

θ = absolute temperature and

m_w = molecular mass of water.

Substituting for H in 6.2 gives:

$$\mathbf{(u_a - u_w)total = \frac{R\theta}{m_w} \log_e \left[\frac{n_w}{n_w + n_s}\right]} \qquad \mathbf{6.3}$$

The results obtained when NaCl was dissolved in water were different and show that capillary rise depends on a static balance between the upward surface tension forces and the downward weight of the column of liquid. It is representative of matrix suction and is not affected by the solute suction of the liquid column. In other words, equation 6.2 does not seem to be correct.

The capillary rises did not change in either case when near-identical capillary tubes were set up side by side as described above. Further, upon swapping the two containers of liquid, again the rises were unchanged. Both of these observations show that the height of capillary rise in a capillary tube is governed by the value of the surface tension and the radius of the capillary, as shown by equation 6.2, and not by the relative humidity above the meniscus. In other words, capillary rise is governed by the intermolecular forces of cohesion and adhesion and not by the relative humidity above the meniscus.

6.2 Discussion of results of total suction measurements

The results of thermocouple psychrometer measurements carried out on limestone powder, quartz powder and glass beads at a range of solution contents of (1-10%) using distilled water (control), 0.25 M, 0.50 M, 0.75 M, 1 M NaCl solutions and 2g/l detergent are given in Tables 5.3 (b), (c) and (d) in appendix pp. viii-x. The resultant graphs for these are given in Figures 6.2 (a), (b), and (c).

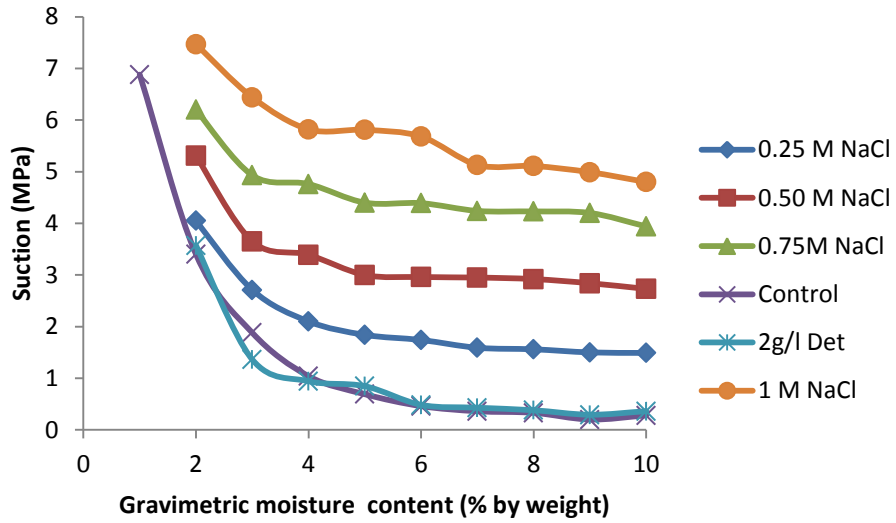


Figure 6.2 (a) Water content- total suction curves for Limestone Powder

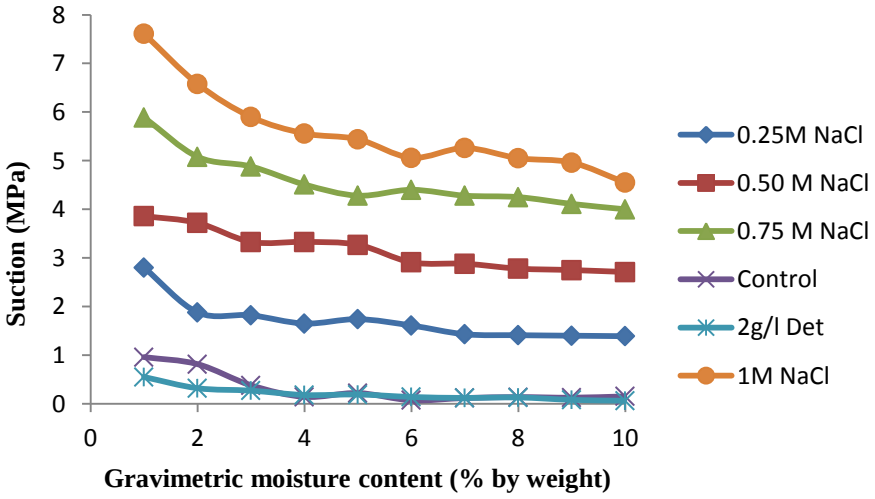


Figure 6.2 (b) Water content- total suction curves for Quartz Powder

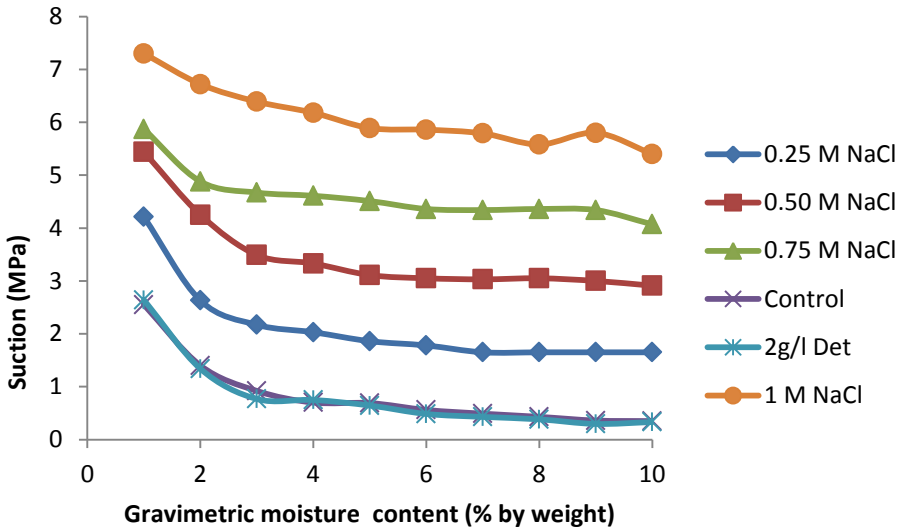


Figure 6.2 (c) Water content- total suction curves for Fine Glass Beads

In these graphs, the suctions were calculated from equation 6.3. It is evident that the curves for water and 2g/l detergent are almost coincident, i.e. 50 % reductions in surface tension have little effect on matrix suction.

When distilled water is the pore fluid the suction values obtained must be entirely matrix suction and the addition of detergent makes very little difference. For 1M NaCl, the suction must be entirely solute suction at higher water contents, with a significant matrix suction component at low water contents. At high water contents where matrix suction is low, the measured solute suction is very close to that calculated from Equation 6.3 i.e. 4.812 MPa. The calculation is as follows.

For every mole of sodium chloride added to water we have two moles of solute. Therefore the solute suction contribution of 1 M NaCl solution at 25 °C is given below:

$$NaCl(s) \rightarrow Na^{+}(aq) + Cl^{-}$$

Number of moles of water in 1 litre n_{water} = 55.56 moles

Sodium chloride dissociates into Na^+ (aq) + Cl^- (two moles of solute)

Number of moles of solute n_{solute} = 2*1 =2

$$\mathbf{H} = \frac{\mathbf{n_{water}}}{\mathbf{n_{water}} + \mathbf{n_{solute}}} = \mathbf{0.965}$$

$$\Delta \mathbf{P} = -\mathbf{311000} \log_{\mathbf{10}}(\mathbf{0.965})$$

$$= -\mathbf{4812\ kPa}$$

Using the Kelvin equation, the effect of dissolving 1M NaCl has been calculated. The effect of the solute corresponds to a lower vapour pressure above the air-water interface and hence a lower relative humidity. This corresponds to an increase in (u_a-u_w) from solute or osmotic suction. However the readings we often obtain from the psychrometer are often attributed to total suction which therefore creates a problem with the fundamental assumption already established from the Kelvin equation. Total suction should therefore be higher taking that total suction is matrix suction plus solute suction.

6.3 Discussion of results of consolidated undrained triaxial strength measurements

The results of the consolidated undrained triaxial test carried out on the three granular soils are given in tables 5.4 (b), (c) and (d) on appendix pp. xvi-xxi. The maximum peak deviator stresses versus water content at failure and the suctions obtained at failure versus water content are given in figures 6.3 (a), (b) and (c) for limestone powder, quartz powder and fine glass beads respectively.

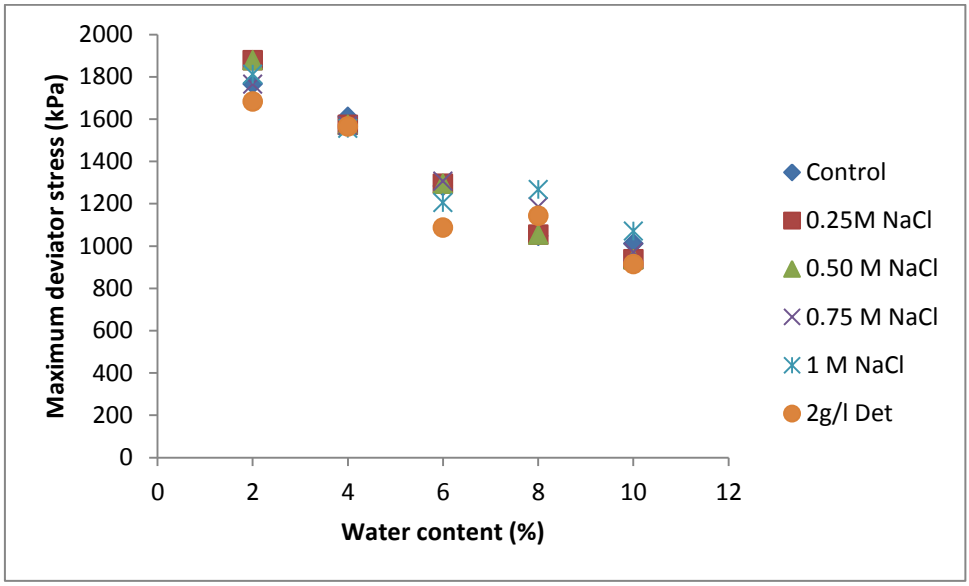


Figure 6.3 (a) i Maximum peak deviator stress versus water content for consolidated undrained triaxial tests on limestone powder.

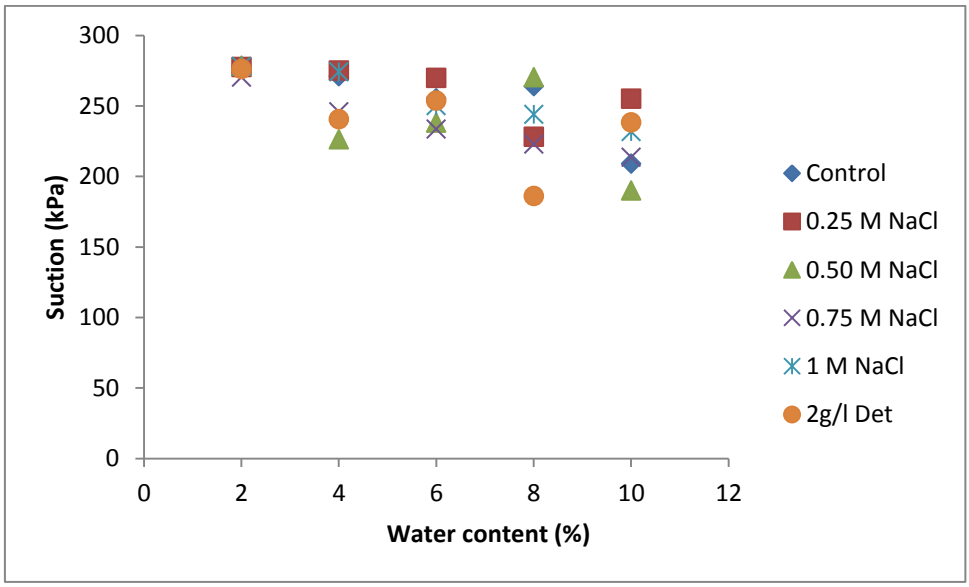


Figure 6.3 (a) ii Matrix Suction at failure versus water content for consolidated undrained triaxial tests on limestone powder.

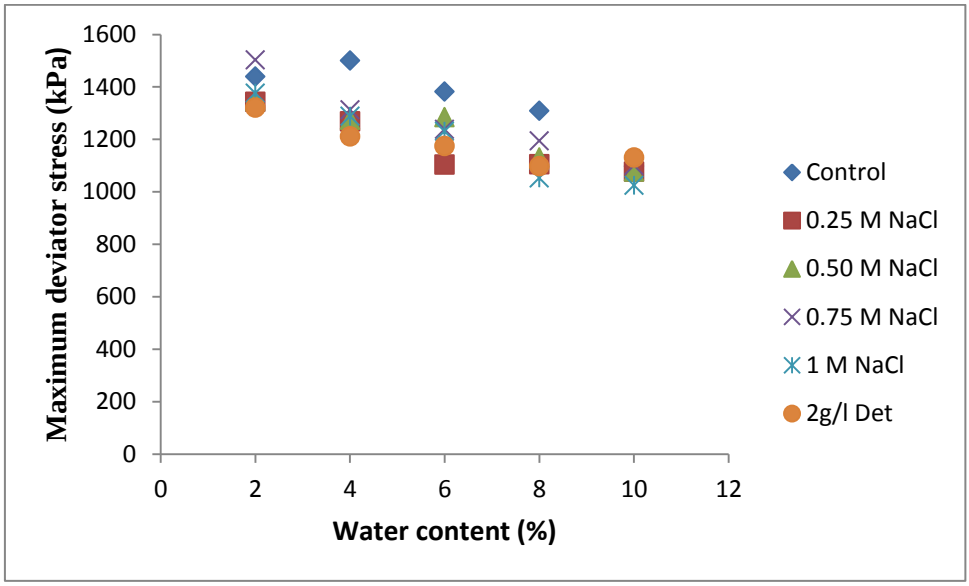


Figure 6.3 (b) i Maximum peak deviator stress versus water content for consolidated undrained triaxial tests on quartz powder.

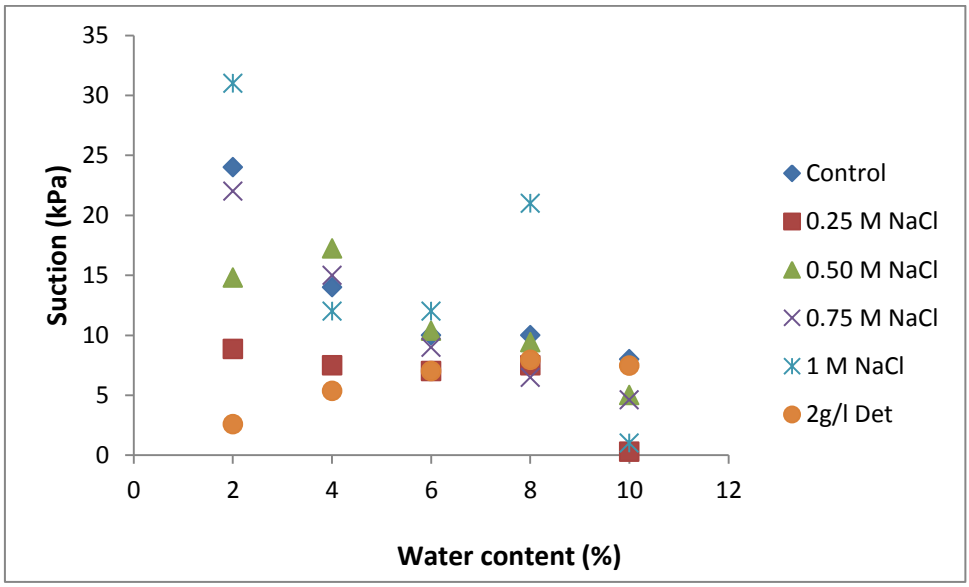


Figure 6.3 (b) ii Matrix Suction at failure versus water content for consolidated undrained triaxial tests on quartz powder.

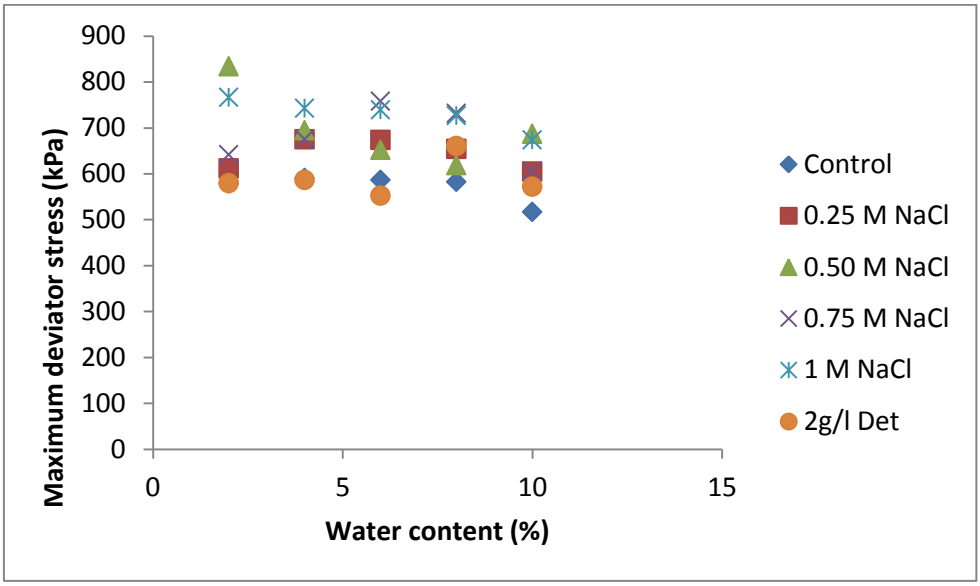


Figure 6.3 (c) i Maximum peak deviator stress versus water content for consolidated undrained triaxial tests on fine glass beads.

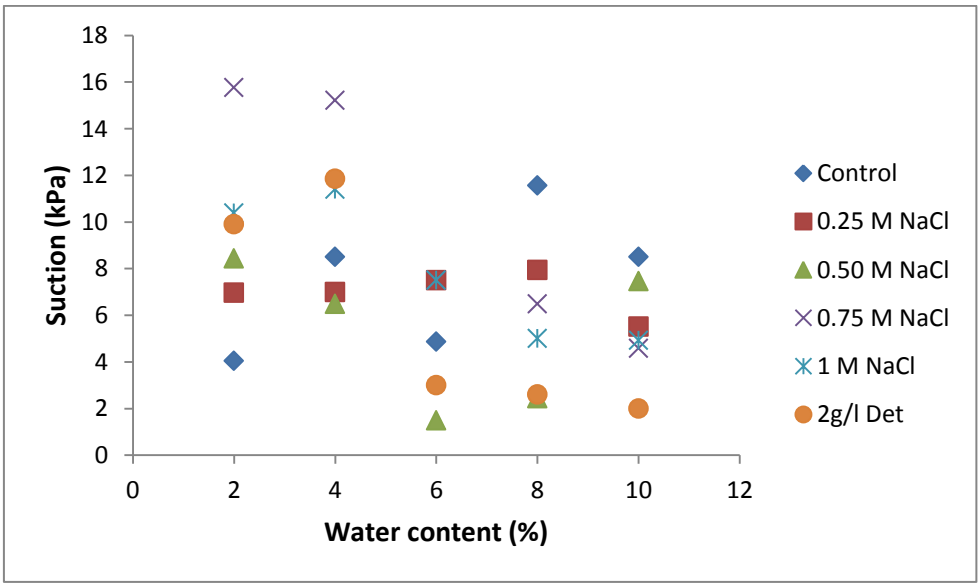


Figure 6.3 (c) ii Matrix Suction at failure versus water content for consolidated undrained triaxial tests on fine glass beads.

From figure 6.3 it can be seen that the suction at failure in the soils was little affected by the presence of sodium chloride or detergent. The

suction values obtained in the fine glass bead specimens were very low and so had very little effect on shear strength. The maximum peak deviator stresses show similar characteristics, with the effect of increasing water content being relatively little affected by the presence of dissolved substances.

Figures 6.3 (d), (e) and (f) show s'- t' strength diagrams for t'= ½(σ_1- σ_3), and upper and lower limits of s' i.e ½(σ_1+σ_3)-u_a and ½(σ_1+σ_3)-u_w compiled from figures 6.3 (a), (b) and (c), for 1 M NaCl at 2 % and 10 % water content. The t'-s' diagrams are perfectly normal for fairly dense granular materials, and show no signs of having been affected or distorted by the effect of the sodium chloride solution which, in the 1M NaCl specimens, amounted to a solute suction of 4.81 MPa. (see section 6.2 page 110)

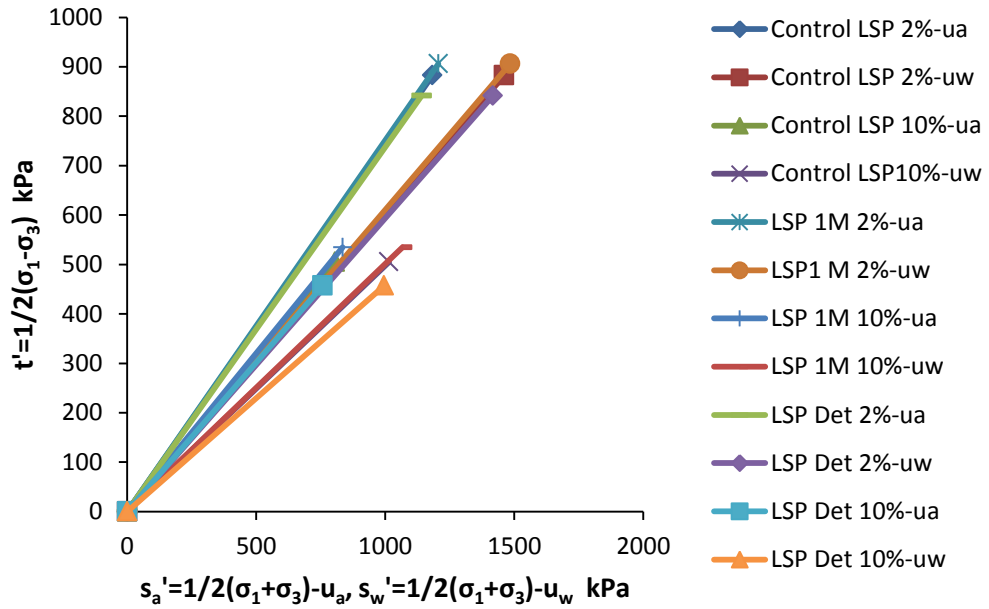


Figure 6.3 (d) s'- t' strength diagram showing the limits of measured strength for limestone powder

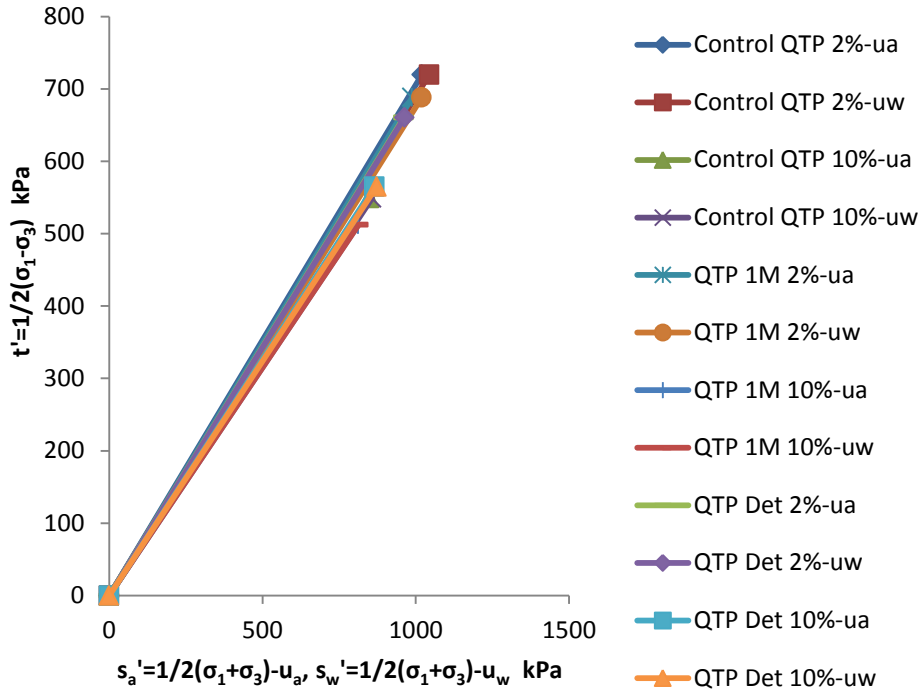


Figure 6.3 (e) s'- t' strength diagram showing the limits of measured strength for quartz powder

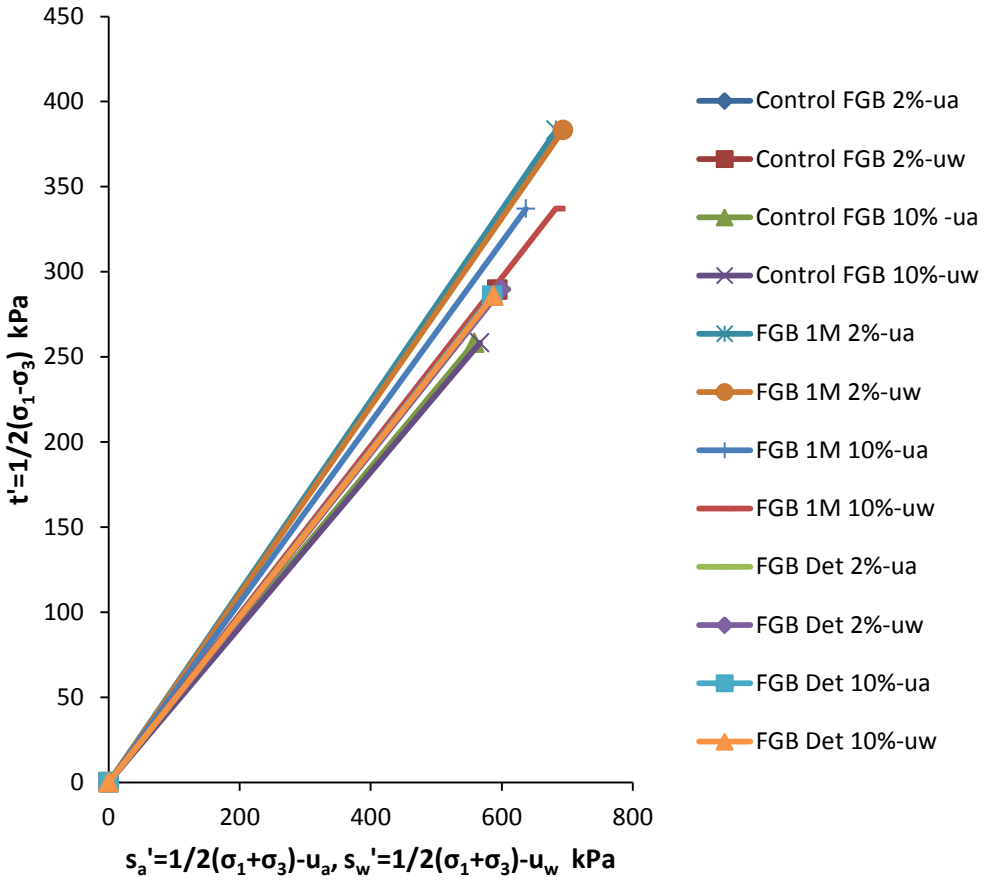


Figure 6.3 (f) s'- t' strength diagram showing the limits of measured strength for fine glass beads

Plotting the s'- t' diagram for upper and lower limits of the strength diagrams for the three soils at 2 % water content for the 1M NaCl mixes is shown in figure 6.3 (g)

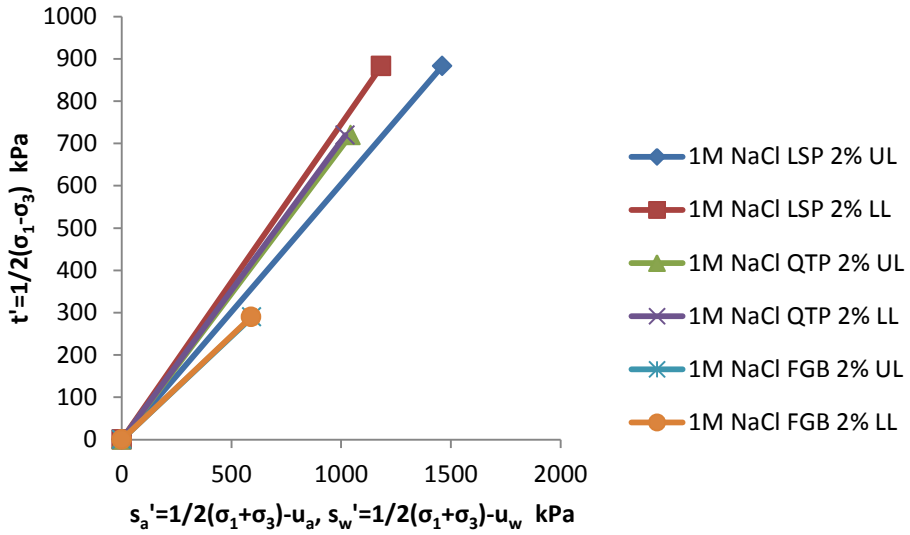


Figure 6.3(g) s'- t' strength diagram showing the limits of measured strength for the soils mixed with 1 M NaCl at 2 % water content

6.4 Discussion of results of consolidated drained triaxial strength measurements.

The results of the consolidated drained tests performed on the soil samples mixed with distilled water, 1 M NaCl solution and 2g/l detergent with the back pressure being either water, 1 M NaCl solution or 2g/l detergent are given in tables 5.5 (a), (b) and (c) in appendix pp. xxviii-xxx. The constant back pressures and maximum peak deviator stresses obtained are also indicated in the tables and an s'-t' diagram for these is shown in figures 6.4 (a), (b) and (c). The results obtained show that the presence of solutes had no systematic effect on the shear strength of specimens. Also, no change is seen if the solute suction of the solution mixed with the soil differs from that of the back pressure solution.

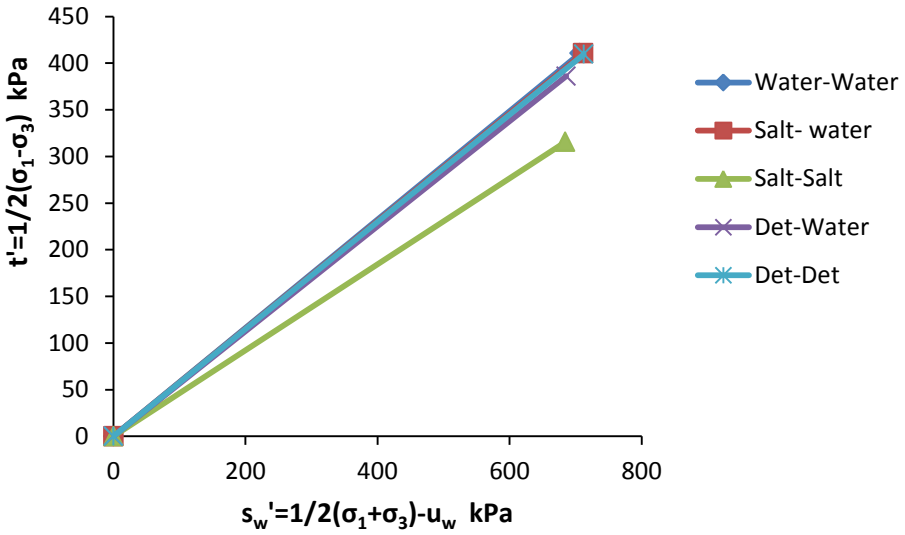


Figure 6.4 (a): s'- t' diagram for Limestone Powder in the CD test

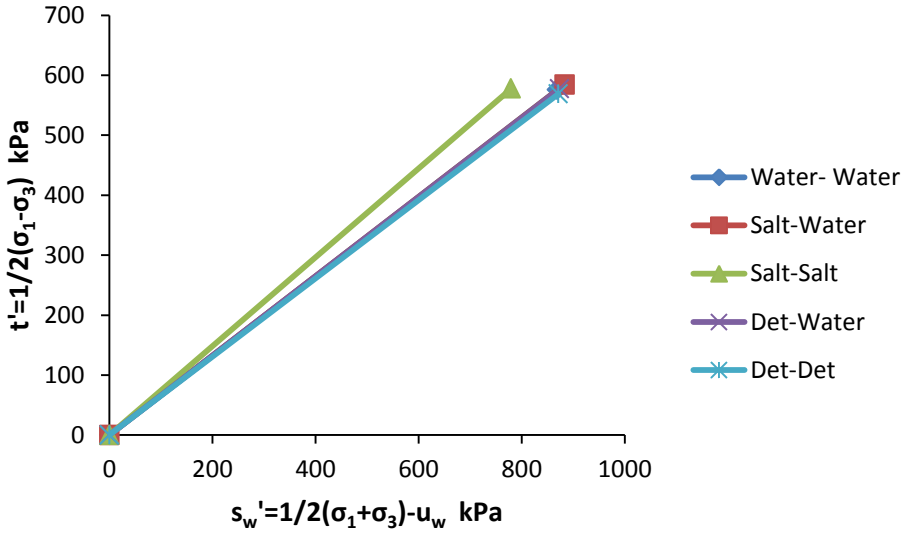


Figure 6.4 (b): s'- t' diagram for Quartz Powder in the CD test

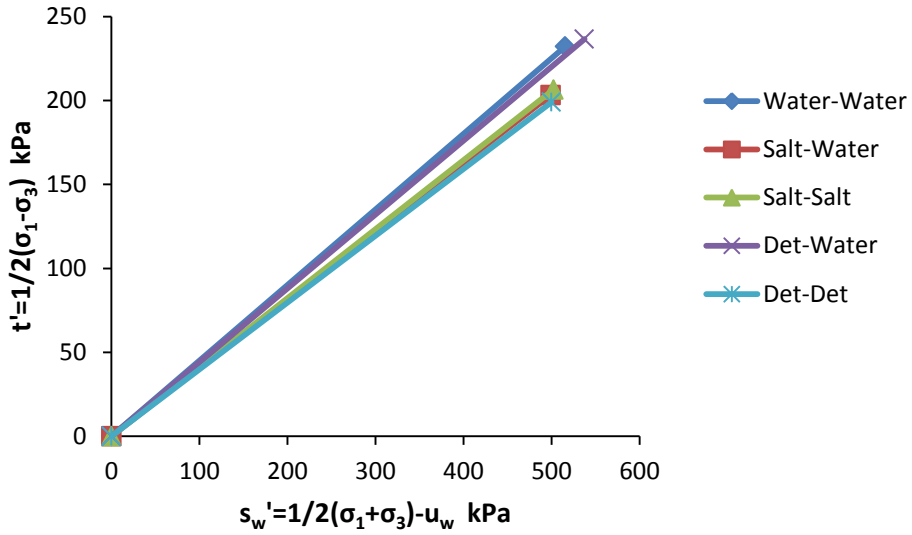


Figure 6.4 (c): s'- t' diagram for Fine Glass Beads in the CD test

The φ´ values of the soils obtained are given in Table 5.5 (d) in appendix pp. xxxi. The following notations are used to differentiate the specimens: the first word denotes the solution mixed with the soil and the second denotes the back pressure solution. For example: water-water denotes the specimen mixed with distilled water with the back pressure being distilled water.

For each of the respective soil mixes, the difference in the φ´ values from those of water-water specimens is minimal. The only exceptions were quartz powder mixed with salt solution and back pressure being salt; and glass beads mixed with detergent and back pressured with detergent, which can be considered as outliers. The difference within each granular material was less than 2º. This is indicative that solutes had little or no effect on the shear strength of the saturated samples. In these specimens once the B value was attained then all the pore air must have gone into solution and whatever remains of solute suction did not affect shear strength.

6.5 Discussion of results of consolidated undrained triaxial strength measurements on specimens dried in salt solutions.

The results are summarized in Table 5.6 in appendix pp xxxii. Figure 6.5 (a) shows plots of the strengths of specimens dried over saturated salt solutions then re-exposed to solutions of water, 1M NaCl and detergent solutions. Figure 6.5 (b) shows total suctions for limestone powder mixed with water (i.e. matrix suction) and 1M NaCl solutions (matrix + solute suction) respectively.

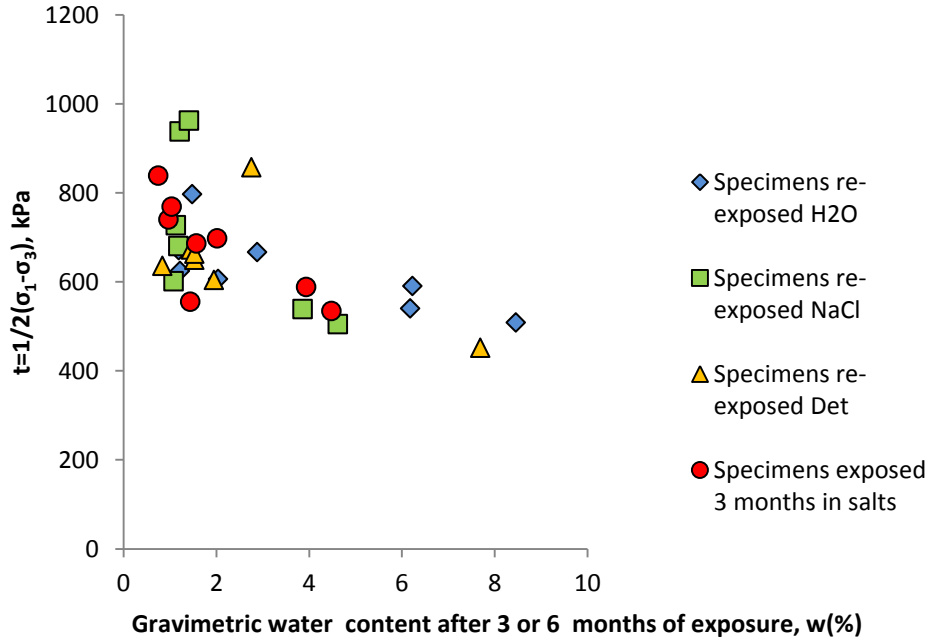


Figure 6.5 (a) Plots of specimens dried over saturated salts, re- exposed to solutions of water, 1 M NaCl and detergent.

Because the specimens were all compacted, they will display no hysteresis as their water content is either reduced or increased (Blight, 2013). Therefore, at any stage of their exposure treatment, if the water content is known, the matrix suction will be given by the matrix suction – water content curve shown in figures 6.5 (b) or 6.2 (a).

Figure 6.5 (c) shows the data of table 5.6 plotted as a strength (or K_f) diagram. ½(σ_1-σ_3) has been plotted vertically against ½(σ_1+ σ_3)-u_w horizontally. For these, σ_3 = 300 kPa and u_w = the matrix suction corresponding to water content when tested in triaxial shear. I.e. ½(σ_1+ σ_3) - u_w = ½(σ_1-σ_3) + σ_3 - u_w. As the specimens were relatively rigid with dry densities of 1700-1800 kg/m^3, the undrained application of σ_3 = 300 kPa would have generated negligible pore air and water pressures. (In fact the largest pore water pressure response to the application of σ_3 was 14 kPa for a specimen with a water content of 8.5 %, but only about 1 kPa per 1% water content for drier specimens).

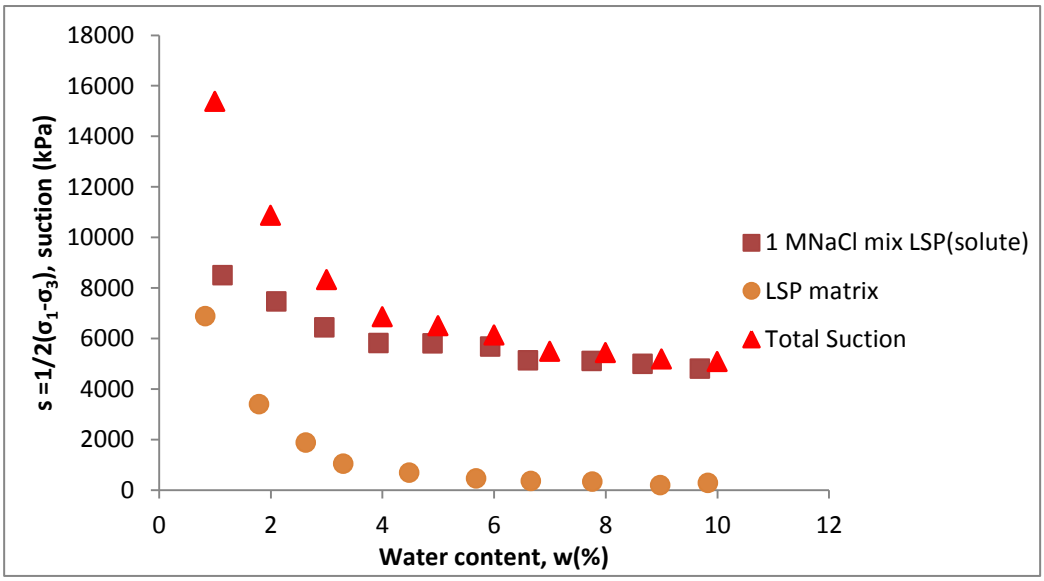


Figure 6.5 (b) Plots of total suction curves for limestone powder mixed with water (matrix suction) and limestone powder mixed with 1M NaCl (matrix + solute suction)

Fig 6.5 (c) shows points plotted for the first 3 months of exposure for all specimens originally mixed with water, 1M NaCl solution and 2g/L detergent solution as well as all specimens exposed for the second 3 months of exposure. All points, whether for specimens originally mixed with water, 1M NaCl or detergent, cluster about a common line. In other

words, their strength was controlled by matrix suction and solute suction played no direct part in contributing to strength. It is noteworthy that there is a cluster of points about ½(σ_1+ σ_3) - u_w =1000 kPa that are specimens mixed with 1 M NaCl. These specimens all gained their moisture when exposed to either water or detergent in the second three month period indicating that their strength had been indirectly affected by an increase in water content drawn by the NaCl from the water-saturated atmospheres of the water or detergent.

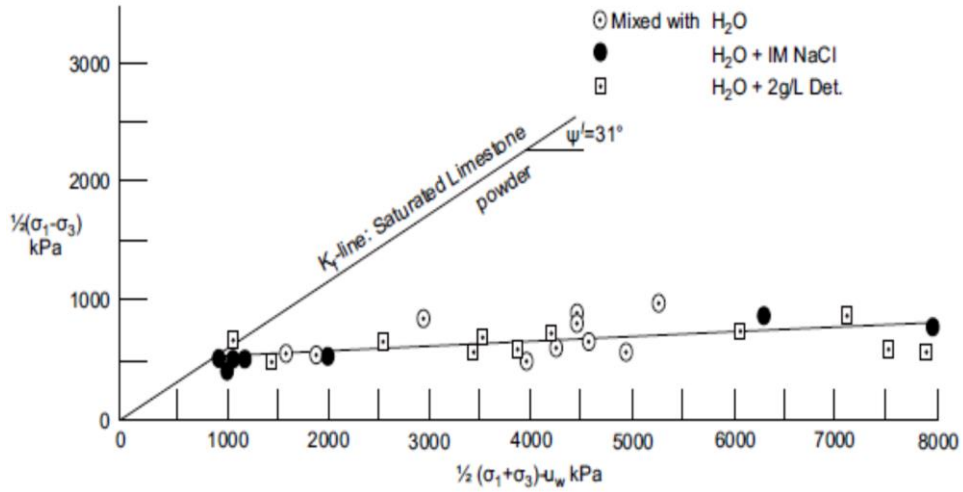


Figure 6.5 (c) Strength diagram plotted for Limestone powder in terms of ½(σ_1- σ_3) and ½(σ_1+σ_3) –u_w where σ_3 = 300 kPa and u_w = matrix suction for water content when tested.

In essence, the shear strengths of the specimens are dependent on the matrix suction developed within the pores of the material and are independent of the solute suction.

CHAPTER SEVEN

SUMMARY, CONCLUSIONS AND RECOMMENDATIONS

7.0 Summary

The findings from this thesis arise from the experimental work which was designed to find the separate contributions of matrix and solute suction to the shear strength of granular soils. This entailed altering the suction characteristics of the pore matrix in granular soils by mixing it with various solutions in order to generate matrix and solute suction in these soils respectively. The suction characteristics of the mixing fluids were determined and the shear strengths of the granular soils mixed at various water contents. The shear strengths obtained were interpreted in terms of the measured matrix and solute suctions.

7.1 Conclusions

The hypothesis of this study is that 'Osmotic suction significantly contributes to the shear strength of unsaturated soils'. In this study some reasons were suggested why the contributions of matrix and osmotic suctions independently to the shear strength of soils have not been investigated. The greatest single reason may be attributed to oversight. Osmotic suction is a borrowed concept from soil sciences and since there has been no problem encountered with it in soil sciences it pre supposes that the same might be true for geotechnical engineering. However the two disciplines have different objectives, with geotechnical engineering focusing on shear strength and volume change of soils and soil sciences focusing on the availability of water for plant survival. Casagrande's 1965 investigation of the Utah salt lake clays reveals that despite the solute suction of about 40 MPa, the clays have low shear strength. Since then, no or possibly very little research has been carried

out to explain why their shear strengths are that small. Sridharan & Venkatappa Rao (1973) also have asserted that osmotic suction plays a role in determining the behaviour of soils, alluding that current formulations of the effective stress equation do not account for osmotic suction. They advocated for the inclusion of both suctions as well as the contribution of the contractile skin stress to the effective stress equation. The work carried out here concludes that osmotic or solute suction does not contribute to the shear strength of granular aggregates directly. The following experimental outcomes support this conclusion:

1. Upon dissolving an ionic solute (NaCl) or a non-ionic solute (detergent) in water that will eventually be the pore fluid in the soil matrix, we expected to find a drastic change in surface tension from change in vapour pressure over the fluid. As a consequence of this, we would have expected a corresponding change in shear strength. The results were, however, contrary to expectation, since the increases or decreases in surface tension and consequently the effects on shear strength were marginal (Katte & Blight, 2012).

2. Solute suction also had no effect on the shear strength of saturated soils in which the pore fluid contained dissolved NaCl or detergent. In a saturated soil, matrix suction is non-existent and experiments revealed that the shear strength of the granular materials tested were the same, irrespective of the nature of the pore fluid. The pore fluid containing 1M NaCl had an osmotic suction as high as 4.812 MPa, but despite that the shear strengths were only slightly different from each other when a non- ionic detergent or distilled water were used. Therefore solute suction does not contribute to the shear strength of granular materials (Katte & Blight, 2013). In essence shear

strengths are dependent on the matrix suction developed in the pores of the material and independent of solute suction (Katte & Blight, 2014).

Though the presence of solutes does not contribute to shear strength directly, they may, however, affect shear strength indirectly. Ionic solutes attract and retain moisture in soil, which may have an indirect effect on the shear strength and volume change because of the reduction in the matrix suction. However the presence of solute suction cannot be accounted for in the shear strength equation. In other words, the value of χ_s in equation 3.9 is zero for shear strength, although it may have a non-zero value for volume change. Also another indirect way in which solutes contribute to soil behaviour is that change of the pore fluid chemistry may influence whether a soil will be dispersive or not. If a sodic soil, which is high in exchangeable sodium comes in contact with non-saline water, the platelets are separated from the aggregates resulting in dispersion by an hydraulic gradient and loss of strength of the soil mass.

An important outcome from this experimentation is that the psychrometric readings obtained from dissolving an ionic solute in water are solute suction readings and not total suction as could be easily believed. The readings obtained are similar to those calculated from the Kelvin equation and Raoult's law. The total suction in this case should be of a much higher value.

7.2 Scientific relevance

Since much of the research interest in unsaturated soil mechanics revolves around the formulation of an effective stress equation for these

materials, going forward any formulation that does include the contribution of osmotic suction is irrelevant. Based upon these experimental evidences, the shear strength of unsaturated soils can be said to be entirely controlled by the effective stress equation proposed by Bishop in 1959.

7.3 Recommendations

Examination of current geotechnical literature shows that very little work has been carried out in this area. The effective stress equation and its derivation have been linked with the capillary model. From these experiments it is evident that surface tension has at least a minor role in the shear strength of soils. But the exact nature of this role has not been entirely clarified. Further areas of research could be;

- The nature of the contribution of solute suction to volume change behavior of unsaturated soil.

- The nature of the surface tension and associated capillary phenomena on the behavior of unsaturated soil.

REFERENCES

ADAMSON, A. W. & GAST, A. P. 1997. *Physical chemistry of surfaces,* New York, John Wiley & Sons.

AITCHISON, G. D. 1961. Relationship of moisture and effective stress functions in unsaturated soils *Pore pressure and suction in soils, .* Butterworth, London.

AITCHISON, G. D. 1964. Engineering concepts of moisture equilibria and moisture changes in soils Statement of the review panel *Moisture equilibria and moisture changes in soils beneath covered areas* Butterworths Australia.

AITCHISON, G. D. 1965. Moisture equilibria and moisture changes in soils beneath covered areas. Sydney: Butterworths.

AITCHISON, G. D. 1969. Soil suction in foundation design *7th International conference on Soil Mechanics and Foundation Engineering. Volume 2.* Mexico.

AITCHISON, G. D. & DONALD, I. B. 1956. Effective stress in unsaturated soils. 2nd Aust-N.Z. Conf. Soil Mech., Sydney, Australia, 192-199.

AL-KHAFAF, S. & HANKS, R. J. 1974. Evaluation of the filter paper method for estimating soil-water potential. Soil Science, 117(4):194-199.

ALLAM, M. M. & SRIDHARAN, A. 1987. Stresses present in unsaturated soils. Journal of Geotechnical Engineering. ASCE . Vol. 113, 11, 1395-1399

ALONSO, E. E., GENS, A. & JOSA, A. 1990. A constitutive model for partially saturated soils. *Geotechnique,* 40**,** 405-430.

ALONSO, E. E., ROMERO, E., HOFFMANN, C & GARCIA-ESCUDERO, E. 2005. Expansive bentonite-sand mixtures in cyclic controlled-suction drying and wetting. Engineering Geology, 81(3): 213-226.

AMENTE, G., BAKER, J. M., & REECE, F. C. 2000. Estimation of soil solution electrical conductivity from bulk soil electrical conductivity in sandy soils. Soil Science Society of America Journal, 64(6): 1931-1939.

BARBOUR, S. L. 1999. The soil water characteristic curve: a historical perspective . Canadian Geotechnical Journal, 35,, 873-894.

BARBOUR, S., FREDLUND, D. & PUFAHL, D. 1992. The osmotic role in the behaviour of swelling clay soils. *NATO ASI SERIES H CELL BIOLOGY***,** 97-97.

BARBOUR, S. L. & FREDLUND, D. G. 1989. Mechanisms of osmotic flow and volume change in clay soils, . *Canadian Geotechnical Journal,* 26**,** 551-562.

BENSON, C. H. & BOSSCHER, P. J. 1999. Time-domain reflectometry (TDR) in geotechnics: a review, nondestructive and automated testing for soil and rock properties. ASTM SPT 1350(Eds. W.A. Marrand C.E. Fairhurst), ASTM, West Conshohochen,PA.

BISHOP, A. W. 1954. The use of pore pressure coefficients in practice. Geotechnique, 4, No 4,148-152.

BISHOP, A. W. 1959. The principle of effective stress. *Teknisk Ukeblad Oslo Norway,* 106**,** 859-863.

BISHOP, A. & BLIGHT, G. 1963. Some aspects of effective stress in saturated and partly saturated soils. *Géotechnique,* 13**,** 177-197.

BISHOP, A. W. & DONALD, I. B. 1961. The experimental study of partly saturated soil in the triaxial apparatus. In Proceedings of the 5th International conference of soil mechanics and foundation Engineering, Paris, Vol. 1, pp.13-21.

BISHOP, A. W. & HENKEL, D. J. 1962. The measurement of soil properties in in the triaxial test. 2nd ed. London, U.K. Edward Arnold

BISHOP, A. W. & ELDIN, G. 1950. Undrained triaxial tests and their significance in the general theory of shear strength. *Geotechnique,* 2**,** 13-22.

BLATZ, J. & GRAHAM, J. 2000. A system for controlled suction in triaxial tests. *Géotechnique* **50** (4). 465-469.

BLIGHT, G. E. 1965. A study of effective stress for volume change. *Symposium on Moisture Equilibria and Moisture changes in the Soils Beneath Covered Areas.* Sydney, Australia: Butterworths.

BLIGHT, G. E. 1982. Aspects of the capillary model for unsaturated soils. *Asian Regional conference* International Society for Soil Mechanics & Foundation Engineering.

BLIGHT, G. E. 2007. Hysteresis during drying and wetting of soils. *Asian Conf. Unsat. Soils.* Nanjing China: Science Press.

BLIGHT, G. E. 2013. *Unsaturated Soil Mechanics in Geotechnical Practice,* Leiden The Netherlands, CRC Press/Balkema.

BOCKING, K. A. & FREDLUND, D. G. 1979. Use of the Osmotic Tensiometer to measure Negative pore water pressure. Geotechnical Testing Journal. Vol. 2 No. 1 pp. 3-10.

BOSO, M., TARANTINO, A .& MONGIOVI, L. 2005. A direct shear box improved with the osmotic technique. In. Proceedings of advanced experimental unsaturated soil mechanics , Trento, pp. 85-91.

BRACKLEY, I. 1971. Partial collapse in unsatBurated expansive clay. COUNCIL FOR SCIENTIFIC AND INDUSTRIAL RESEARCH PRETORIA (SOUTH AFRICA) INFORMATION DIV.

BRENNER, R.P., GARGA, V.K. & BLIGHT, G. E. 1997. The mechanics of Residual soils, 1st edition, Rotterdam, Netherlands, Balkema.

BROWN, R. W. 1970. Measurement of water potential with thermocouple psychrometers: construction and applications. USDA. Forest Service Research Paper INT-80.

BULUT, R. & LEONG, E. C. 2008. Indirect measurement of suction. Geotech Geol Eng 26:633-644

BULUT, R., PARK, S. W., LYTTON, R. L. 2000.Comparison of total suction values from psychrometer and filter paper methods. In Unsaturated soils for Asia. Proceedings of the Asian conference on unsaturated soils, UNSAT-ASIA 2000 Singapore, 18-19 May, pp. 269-273.

CAMPBELL, G. S. & GARDNER, W. H. 1971. Psychrometric measurement of soil potential: Temperature and bulk density effects. *Soil Science Society of America,* 35**,** 8-12.

CASAGRANDE, A. 1965. Role of calculated risk in earthwork and foundation engineering. *Journal of Soil Mechanics and Foundation Engineering, ASCE,* 91**,** 1-40.

CHANDLER, R. J., CRILLY, M. S. & MONTGOMERY-SMITH, G. 1992. A low cost method of assessing clay desiccation for low-rise buildings. Proceedings of the Institution of Civil Engineer, 92 (2):82-89.

CHANDLER, R. J. & GUTIERREZ, C. I. 1986. The filter paper method of suction measurement. Geotechnique, 36: 265-268.

CHÁVEZ, C., ROMERO, E. & ALONSO, E.E. 2009. A Rockfill Triaxial Cell with Suction Control. *Geotechnical Testing Journal* **32** (3). 219-231.

COLEMAN, J. D. 1962. Stress strain relations for partly saturated soils. *Geotechnique,* 12**,** 348-350.

COLMENARES, J. E. & RIDLEY, A. M. 2002. Stress-strain and strength relationships for a reconstituted clayey silt. *Proceedings of the Third International Conference on Unsaturated Soils. Unsat 2002,*Vol. **2**. Jucá J.F.T., de Campos T.M.P. and Marinho F.A.M.

(eds.), Balkema Publishers, Netherlands. 481-484.

CRONEY, D. & COLEMAN, J. D. 1948. Soil thermodynamics applies to the movement of moisture in road foundations. *In Proc 7th int. Cong. Appl. Mech.*

CRONEY, D., COLEMAN, J. D. AND. LEWIS, W. A. 1950. Calculation of moisture distribution below structures, . *Cov. Eng. L.,* 45.

CRONEY, D., COLEMAN, J. D. & BRIDGE, P. M. 1952. *The Suction of Moisture Held in Soils and Other Porous Materials,* London UK, H M Stationary Office.

CRONEY, D., COLEMAN, J. D. & BRIDGE, P. M. 1952. *The Suction of Moisture Held in Soils and Other Porous Materials,* London UK, H M Stationary Office.

CUI, Y. J. & DELAGE, P. 1996. 1958. Yielding and plastic behaviour of an unsaturated compacted silt. *Geotechnique* **46** (2). 291-311.

CUNNINGHAM, M. R RIDLEY, A. M., DINEEN, K. & BURLAND, J. B 2003. The mechanical behaviour of a reconstituted unsaturated silty clay. Geotechnique 53(2): 183-194.

DALTON, F. N., HERKELRATH, W. N., RAWLINS, D. S. & RHOADES, J. D. 1984. Time-domain reflectometry: simultaneous measurement of soil water content and electrical conductivity with a single probe. Science, 224(4652): 989-990.

DONALD, I. B 1956. Shear strength measurements in unsaturated non cohesive soils with negative pore pressures. In: Proc..of 2nd Aust. NZ. Conf. Soil Mech. & Found. Eng., Christchurch, New Zealand pp. 200-205.

DAVIS, J. & RIDEAL, E. 1963. Interface phenomena. New York: Academic Press.

DELAGE, P. 2002. Experimental unsaturated soil mechanics : State of the art report . 3rd International conference on unsaturated soils, vol 3, Recife.

DELAGE, P., HOWAT, M. D. & CUI, Y. J. 1998. The relationship

between suction and swelling properties in a heavily compacted unsaturated clay. Engineering Geology, 50, 31-48.

DELAGE, P., SURAJ DE SILVA, G. P. R. & DE LAURE, E. 1987. Un nouvel appareil triaxial pour les sols non satures. vol 1 9e European conference on soil mechanics and foundation engineering, Dublin, pp. 26-28.

DELAGE, P., SURAJ DE SILVA, G. P. R. & VICOL, T. 1992. Suction controlled testing of non saturated soils with an osmotic consolidometer. 7th International conference of expansive soils, Dallas, pp. 206-211.

DINEEN, K & BURLAND, J. B. 1995. A new approach to osmotically controlled oedometer testing. Proceedings of the 1st conference on unsaturated soils Unsat 95, vol.2 Balkema Paris, pp. 459-465.

DUECK, A. 2004. Hydro-Mechanical Properties of a Water Unsaturated Sodium Bentonite-Laboratory Study and Theoretical Interpretation. PhD thesis, Lund University, Sweden.

EDLEFSEN, N. E. & ANDERSON, A. 1943. Thermodynamics of soil moisture.

ESCARIO, V. 1980. Suction control penetration and shear test. In: Proc. Of 4th Inter. Conf. on Expansive soils. Denver, CO, Vol. 2. pp. 781-797

ESTERBAN, V. & SAEZ, J. 1998. A device to measure swelling characteristics of rock samples with control of the suction up to very high values. In ISRM Symposium on Rock Mechanics and Power Plants, Madrid, Spain. pp. 2.

FAWCETT, R. G. AND COLLIS-GEORGE, N. 1967. A filter paper method for determining the moisture characteristics of soil. Australian Journal of Experimental Agriculture and Animal Husbandry, 7:162-167.

FENG, G., MEIRI, A. & LETEY, J. 2003. Evaluation of a model for irrigation management under saline conditions: I. Effects on plant growth. *Soil Science Society of America Journal,* 67**,** 71-76.

FREDLUND, D. G. 1975. A diffused air volume indicator for unsaturated soils. Canadian Geotechnical Journal, 12, 533-539.

FREDLUND, D. G. 1989. Soil suction monitoring for roads and airfields. Symposium on the state-of-the Art of Pavement Response Monitoring Systems for Roads and Airfields, sponsored by the U.S. Army Corps of Engineers, Hannover, NH.

FREDLUND, D. G. & MORGENSTERN, N. R. 1977. Stress state variables for unsaturated soils. *Journal of Geotechnical and Geoenvironmental Engineering,* 103, 447-466.

FREDLUND, D. G., MORGENSTERN, N. R. & WIDGER, R. A. 1978. Shear strength of unsaturated soils. Canadian Geotechnical Journal, 15, 313-321.

FREDLUND, D. G. & RAHARDJO, H. 1993. *Soil Mechanics for Unsaturated Soils,* New York., John Wiley and Sons, Inc., .

FREDLUND, D. G. & XING, A. 1994. Equations of the soil water characteristic curve. Can. Geotech. J., 31(4) 521-532.

GALLEN, H. B. 1965 Thermodynamics and an Introduction to Thermostatistics, John Wiley & Sons, New York.

GALLIPOLI, D., GENS, A., SHARMA, R. & VAUNAT, J. 2003. An elasto-plastic model for unsaturated soil incorporating the effects of suction and degree of saturation on mechanical behaviour. *Géotechnique.,* 53**,** 123-136.

GAN, J. K. M, FREDLUND, D. G. & RAHARDJO, H. 1988. Determination of the shear strength parameters of an unsaturated soil using the direct shear tests. Canadian Geotechnical journal, 25, 3, 500-510.

GUAN, Y. & FREDLUND, D. G. 1997. Use of the tensile strength of water for the direct measurement of high soil suction. Can.

Geotech. J. 34, No. 4, 604–614.

GARDNER, R. 1937. Evaluation of the filter paper method for es timating soil-water potential. Soil Science, 117(4): 194-199.

GARDNER, W. R 1958. Some steady state solutions of unsaturated moisture flow equation with application to evaporation from a water table. Soil Sci., 85(4), 228-232.

HANSEN, H.C 1926. The water retaining power of the soil. J. Ecology 14, pp. 111-119

HENKEL, D. J. 1960. The shear strength of saturated remoulded clays. *Research conf. on shear strength of cohesive soils***,** 533-554.

HILF, J. W 1956. An Investigation of Pore Water pressure in Compacted Cohesive Soils. Technical Memo No. 654, US Bureau of Reclamation, Denver, Co.

HO, D. Y. F. 1979. Measurement of soil suction using filter paper technique. Internal report, IR-11, Transportation and Geotech group. Department of Civil Engineering, University of Saskatchewan, Saskatoon, Canada.

JENNINGS, J. 1961. A revised effective stress law for use in the prediction of the behavior of unsaturated soils. *Pore Pressure and Suction in Soils***,** 26-30.

JOTISANKASA, A., COOP, M. & RIDLEY, A. 2007. The development of a suction control system for a triaxial apparatus. Geotechnical testing Journal, 30, 1, 1-7.

KALINSKI, R. J. & KELLY, W. E. 1993. Estimating water content of soils from electrical resistivity. Geotechnical Testing Journal, 16(3):323-329.

KASSIFF, G. AND BEN SHALOM A. 1971. Experimental relationship between swell pressure and suction. Géotechnique, 21: 245-255.

KATTE, V. Y. & BLIGHT, G. E. 2012. The roles of solute suction and surface tension in the strength of unsaturated soil. *Unsaturated Soils: Research and Applications.* Mancuso, C., Jommi, C. &

D'Onza, F.(eds), Heidelberg, Germany, Springler, 2, 431-438.

KATTE, V. Y. & BLIGHT, G. E. 2013. Solute suction and shear strength in saturated soils. *1st Panam. Conf. Unsat. Soils*, Cartagena, Columbia, Taylor & Francis.

KATTE, V. Y. & BLIGHT, G. E. 2014. Fundamental concepts of the mechanics of unsaturated soils. *Unsaturated Soils: Research & Applications,* Sydney.

KAYE, G. W. C. & LABY, T. H. 1973. Tables of physical and chemical constants. Longman, London.

KHALILI, N., GEISER, F. & BLIGHT, G. 2004. Effective stress in unsaturated soils: review with new evidence. *International Journal of Geomechanics,* 4**,** 115.

KHALILI, N. & KHABBAZ, M. 1998. A unique relationship of chi for the determination of the shear strength of unsaturated soils. *Géotechnique,* 48.

KRAHN, J. AND FREDLUND, D. G. 1972. On total, matric and osmotic suction. Soil Science, 115(5):339-348.

LAMBE, T. W. 1960. A mechanistic picture of the shear strength of clay. *Conf. on shear strength of cohesive soils.* New York: ASCE.

LANG, A. 1967. Osmotic coefficients and water potentials of sodium chloride solutions from 0 to 40 C. *Australian Journal of Chemistry,* 20**,** 2017-2023.

LEONG, E. C., HE, L. & RAHARDJO, H. 2002. Factors affecting the filter paper method for total and matric suction measurements. Geotechnical Testing Journal, 25 (3):321-332.

LEONG, E. C., TRIPATHY, S. & RAHARDJO, H. 2003. Total suction measurement of unsaturated soils with a device using the chilled mirror dew-point technique. Geotechnique, 53(2): 173-182.

LLORET, A., VILLAR, M. V., SANCHEZ, M., GENS, A., PINTADO, X & ALONSO E.E 2003. Mechanical behaviour of heavily compacted

bentonite under high suction changes. Geotechnique 53(1): 27-40.

LU, N. 2008. Is matric suction a stress variable? *Journal of Geotechnical and Geoenvironmental Engineering,* 1123**,** 899.

LU, N., GODT, J. W. & WU, D. T. 2010. A closed-form equation for effective stress in unsaturated soil. *Water Resources Research,* 46**,** W05515.

LU, N. & LIKOS, W. J. 2006. Suction stress characteristic curve for unsaturated soil. *Journal of Geotechnical and Geoenvironmental Engineering,* 132**,** 131.

LU, N. & LUKOS, W. J. 2004. Unsaturated soil mechanics. John Wiley & Sons, Inc., Hoboken, New Jersey.

LYKLEMA, J. 1990. *Fundamental of interface and colloid science,* New York, Academic Press.

LYKLEMA, J. 2000. *Fundamentals of Interface and Colloid Science,* San Diego, Academic Press.

MANHEIM, F. T. 1996. A hydraulic squeezer for obtaining interstitial water from consolidated and unconsolidated sediments. U.S. Geological Survey professional paper 550-C, pp. 256-261.

MARSHALL, T. J. 1959. Relations Between Water and Soil. Harmondsworth, UK: Commonwealth Bureau of soils.

MATYAS, E. L. & RADHAKRISHNA, H. S. 1968. Volume change characteristics of partially saturated soils. *Geotechnique,* 18**,** 432-448.

MCQUEEN, I. S. & MILLER, R. F. 1974. Approximating soil moisture characteristics from limited data: empirical evidence and tentative model. *Water Resources Research,* 10**,** 521-527.

MCQUEEN, I. S. & MILLER, R. F. 1968. Calibration and evaluation of wide range gravimetric method for measuring soil moisture stress. Soil Sci. Vol. 106, pp. 225-231.

MEILANI, I., RAHARDJO, H., LEONG, E. C. & FREDLUND, D.G. 2002. Mini suction probe for suction measurement. Canadian Geotechnical Journal, 39 (6) 1427-1432.

MITCHELL, J. K. 1962. *Components of pore water pressure and their engineering significance*, Institute of Transportation and Traffic Engineering, University of California.

MORGENSTERN N, R. 1976. Constitutive relations for volume change in unsaturated soils. *Can. Geotech. J,* 13**,** 261.

MURRAY, E. J. & SIVAKUMAR, V. 2010. Unsaturated soils: a fundamental interpretation of soil behaviour. Wiley Blackwell

NOORANY, I. 1984. Phase relations in marine soils. *Journal of Geotechnical Engineering, ASCE,* 110**,** 539-543.

NG, C. W. W., CUI, Y., CHEN, R & DELAGE, P. 2007. The axis translation and osmotic techniques in shear testing of unsaturated soils: a comparison. Soils and Foundations, 47(4), 678-684.

NUTH, M. & LALOUI, L. 2008. Effective stress concept in unsaturated soils: clarification and validation of a unified framework. *International journal for numerical and analytical methods in Geomechanics,* 32**,** 771-801.

OBERG, A. L. & SALFORS, G. 1997. Determintaion of shear strength parameters of unsaturated silts and sands based on the water retention curve. Geotech. Testing J. 20,1, 40-48.

OLDECOP, L. A & ALONSO, E. E. 2004. Testing rockfill under relative humidity control. Geotechnical testing journal ASTM 27(3): 10. Paper ID: GTJ11847

PECK, A. J. & RABBIDGE, R.M. 1969. Design and performance of an osmotic tensiometer for measuring capillary potential. *Soil Science Society American Proceedings*, 33: 196-202.

POWER, K. C., VANAPALLI, S. K & GARGA, V. K. 2008. A revised contact filter method. Geotech. Testing J., 31, 6, 461-469.

RAHARDJO, H. & LEONG, E. C. 2006. Suction measurements. In:

Unsaturated soil, Vol 1 Geotechnical special Publication No. 147. ASCE Reston, VA, pp. 81-104 Proceedings of the fourth International conference on unsaturated soils UNSAT 2006, Carefree, AZ.

RENDULIC, L. 1936. Relation between void ratio and effective principal stresses for a remoulded silty clay *Proc. 1st International Conf. on Soil Mechanics.*

RICHARDS, B. G. 1966. The significance of moisture flow and equilibria in unsaturated soils in relation to the design of structures built on shallow foundations in Australia. *In:* ASTM (ed.) *symposium on permeability and capillarity.* Atlantic City, USA.

RICHARDS, L. & OGATA, G. 1958. Thermocouple for vapor pressure measurement in biological and soil systems at high humidity. *Science,* 128**,** 1089.

RIDLEY A.M & BURLAND J.B. 1993. Indirect Measurement of Suction Geotechnical and Geological Engineering Volume 26, Issue 6, pp 633-644.

SHAW, B. & BAVER, L.D. 1939. An electro-thermal method for following moisture changes of the soil insitu. *In* Proceedings of Soil Science Society of America, 4:78-83.

SHENG, D., SMITH, D. W, SLOAN, S. W. & GENS, A. 2002. An explicit stress intergration scheme for unsaturated soil models. 3rd Int. Conf. Unsat. Soils, Recife, Brazil 1, 125-131.

SKEMPTON, A. W. (ed.) 1960. *Significance of Terzaghi's concept of effective stress.,* New York: Wiley.

SIVAKUMAR, V. 1993. A Critical State Framework for Unsaturated soils PhD thesis submitted to the University of Sheffield, UK.

SOILMOISTURE EQUIPMENT CORPORATION. 1998. Catalogue, Santa Barbara, CA.

SPANNER, D. 1951. The Peltier effect and its use in the measurement of suction pressure. *Journal of Experimental Botany,* 2**,** 145-168.

SREEDEEP, S. & SINGH, D. 2006. Methodology for determination of osmotic suction of soils. *Geotechnical and Geological Engineering,* 24**,** 1469-1479.

SRIDHARAN, A. & VENKATAPPA RAO, G. 1973. Mechanism controlling volume change in saturated clays and the role of the effective stress concept. Geotechnique 23, 2, 359-382

TANG, R .K. W. 1978. The measurement of soil suction by the filter paper method, phases I-V. Laboratory reports. Department of Civil Engineering, University of Saskatchewan, Saskatoon, Canada.

TANG, G. X., GRAHAM, J., BLATZ, J., GRAY, M., & RAJAPAKSE, R.K.N.D. 2002. Suctions, stresses and strengths in unsaturated sand-bentonite. Engineering Geology, 64: 147-156.

TARANTINO, A. & MONGIOVI, L. 2001. Design and construction of a tensiometer for direct measurement of matric suction. In: Proceedings of the Third international conference on Unsaturated soils UNSAT 02 Recife Brazil Vol 1, Juca, J.F.T., deCampos, T.M.P and Marinho, F.A.M (eds), pp 319-324.

TAYLOR, D.W. 1948. Fundamentals of soil mechanics. John Wiley & Sons, New York.

TERZAGHI, K. 1926. *Principles of Soil Mechanics,* New York, USA, McGraw-Hill.

TERZAGHI, K. 1936. The shearing resistance of saturated soils and the angle between the planes of shear. *1st International Conference on Soil Mechanics and Foundation Engineering.*

TERZAGHI, K. 1943. *Theoretical Soil Mechanics,* New York, USA, Wiley.

THOM, R., SIVAKUMAR, R., BROWN, J. L. & HUGHES, D. A. 2008. A simple triaxial system for evaluating the performance of unsaturated soils under repeated loading. Geotechnical Testing Journal, ASTM, 31(2), 107-114.

TOKER, N. K., GERMAINE, J. T., SJOBLOM, K. J. & CULLIGAN, P. J. 2004. A new technique for rapid measurement of continuous soil moisture characteristic curves Geotechnique 54 (3) 179-186.

TOPP, G. C., DAVIS, J. L & ANNAN, A. P 1980. Electromagnetic determination of soil water content: Measurements in coaxial transmission lines Water resources research, Vol. 16, No. 3, pp. 574-582.

VAN GENUCHTEN, M. T. 1980. A closed-form equation for predicting the hydraulic conductivity of unsaturated soils. *Soil Science Society of America Journal,* 44**,** 892-898.

WHEELER, S. & SIVAKUMAR, V. 1995. An elasto-plastic critical state framework for unsaturated soil. *Géotechnique,* 45**,** 35-53.

WHITE, R. L. 1979 *Introduction to the principles and practice of soil science*, Blackwell Scientific, ed. 1.

WIEBE, H. H., BROWN, R. W., DANIEL, T. W. & CAMPBELL, E. 1970. Water potential measurements in trees. BioScience 20:225–226.

YU, X. & DRNEVICH, V.P. 2004 Soil water content and dry density by time domain reflectometry. Journal of Geotechnical and Geoenvironmental Engineering, 130(9):922-934.

ZUR, B. 1966. Osmotic control the matric soil water potential. Soil Sci 102: 394-398.

Appendix

Table 5.1 Particle size distribution of granular materials

Limestone powder				
Sieve No	**Mass retained**	**Percent retained**	**Cum percent. ret.**	**Percent. passing**
0.6	0.00	0.00	0.00	100
0.425	0.25	0.1666670	0.167	99.833
0.3	0.08	0.053333	0.22	99.78
0.15	45.22	30.14667	30.37	69.63
0.075	21.27	14.18	44.55	55.45
0.053	77.08	51.3667	95.94	4.06
pan	6.1	4.066667	100	0

Quartz powder				
Sieve No	**Mass retained**	**Percent retained**	**Cum percent. ret.**	**Percent. passing**
0.6	1.4	0.35	0.35	99.65
0.425	5.1	1.27	1.62	98.38
0.3	24.6	6.15	7.77	92.23
0.15	208.1	52.02	59.79	40.21
0.075	102.8	25.7	85.49	14.51
0.053	57.4	14.35	99.84	0.16
pan	0	0	100	0

Fine Glass Beads				
Sieve No	**Mass retained**	**Percent retained**	**Cum percent. ret.**	**Percent. passing**
1.18	0	0		100
0.6	0.03	0.02	0.02	99.98
0.425	0.35	0.23333	0.253	99.747
0.3	0.74	0.493333	0.746	99.254
0.15	6.67	4.446667	5.192	94.808
0.075	112.44	74.96	80.152	19.948
0.053	27.22	18.14667	98.3	1.7
pan	2.55	1.7	100	0

Table 5.2 (a) Measurement of the radius of glass capillary

Capillary 1	1	2	3
Mass of syringe before (g)	8.433	8.413	7.450
Mass of syringe after (g)	8.292	8.299	7.274
Mass of water injected (g)	0.1412	0.1138	0.176
Temperature of water ºC	20	20	20
Density of water (g/ml)	0.998	0.998	0.998
Capillary length (cm)	16.6	16.0	23.4
RH (%)	84	84	84
Radius (cm)	0.05208	0.04768	0.04899
Average Radius (cm)	0.04958		

Capillary 2	1	2	3	4
Mass of syringe before (g)	4.413	7.540	5.216	5.386
Mass of syringe after (g)	4.312	7.427	5.085	5.285
Mass of water injected (g)	0.101	0.113	0.131	0.101
Temperature of water ºC	20	22	25	25
Density of water g/ml	0.997	.997	0.994	0.994
Capillary length (cm)	15.9	17.4	20.2	16
RH (%)	84	84	84	84
Radius (cm)	0.0450	0.04554	0.04558	0.04497
Average Radius (cm)	0.04527			

Table 5.2(b) Surface tension measurements for distilled water and water diluted with ionic solute (NaCl).

Molarity M	Surface tension (N/m)
0.0	72.84
0.25	70.51
0.50	74.80
0.75	81.67
1.0	76.03
2.0	77.87
0.0	72.84
0.25	79.28
0.50	74.80
0.75	82.16
1.0	83.76
2.0	77.88
0.0	72.84
0.25	79.28
0.50	78.17
0.75	76.52
1.0	63.77
2.0	77.00

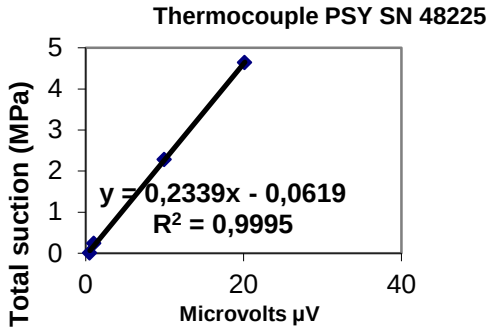
Table 5.2 (c) Surface tension measurements for distilled water and water diluted with a non- ionic solute (detergent)

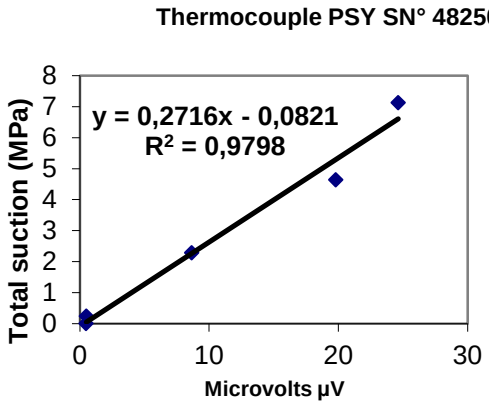
Detergent (g/l)	Surface tension (N/m)
0.0	65.95
0.5	61.84
1.0	34.41
1.5	29.97
2.0	51.06
0.0	65.95
0.5	35.53
1.0	44.91
1.5	33.32
2.0	37.03
0.0	69.77
0.5	65.84
1.0	63.29
2.0	44.74
0.0	65.94
0.5	61.84
1.0	34.41

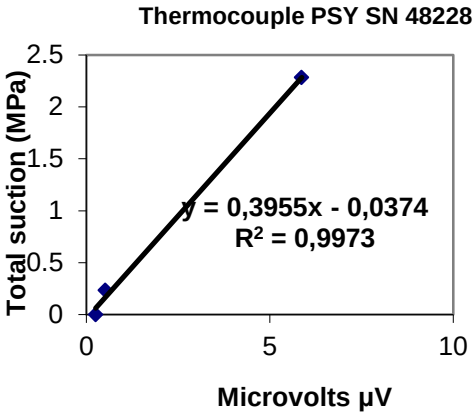
Table 5.3 (a) Results of calibration of psychrometer tips

Molar solution	**48274**		**48250**		**48228**	
	Voltage	**Suction**	**Voltage**	**Suction**	**Voltage**	**Suction**
0	0	0	0.493	0	0.55	
0.05	0.793	0.234	0.517	0.234	0.518	
0.5	10.14	2.281	8.656	2.281	5.87	0
1.0	21.14	4.64	19.82	4.64	-	0.234
1.5	26.42	7.134	24.64	7.134	-	2.281
						-
						-

Molar solution	**48255**		**48114**	
	Voltage	**Suction**	**Voltage**	**Suction**
0	0,529	0	0.5	0
0.05	1.028	0.234	0.67	0.234
0.5	9.954	2.281	9.846	2.281
1.0	20.141	4.64	20.87	4.64
1.5			27.826	7.134


Thermocouple PSY SN 48225
Total suction (MPa)
Microvolts µV
y = 0,2339x - 0,0619
R² = 0,9995
0
1
2
3
4
5
0
20
40


Thermocouple PSY SN° 48250
Total suction (MPa)
Microvolts µV
y = 0,2716x - 0,0821
R² = 0,9798
0
1
2
3
4
5
6
7
8
0
10
20
30


Thermocouple PSY SN 48228
Total suction (MPa)
Microvolts µV
y = 0,3955x - 0,0374
R² = 0,9973
0
0.5
1
1.5
2
2.5
0
5
10

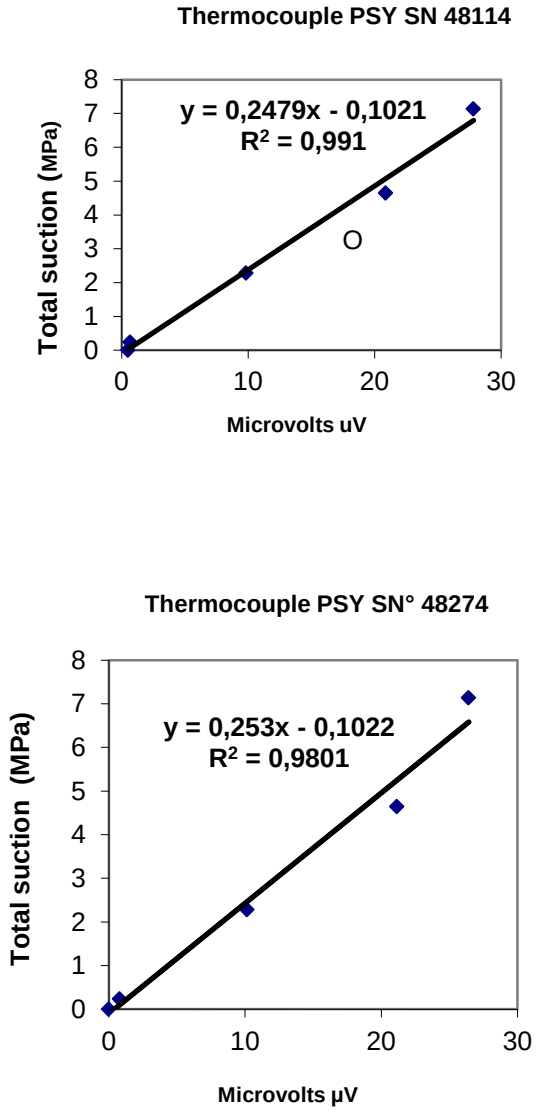


Figure 5.3 Calibration curves of psychrometers

Table 5.3 (b) Total suction values for Limestone Powder

Limestone Powder								
0.25 M NaCl			**0.50 M NaCl**			**0.75 M NaCl**		
Real Mc (%)	**Lab Mc (%)**	**Suction (MPa)**	**Real Mc (%)**	**Lab Mc (%)**	**Suction (MPa)**	**Real Mc (%)**	**Lab Mc (%)**	**Suction (MPa)**
1.00	1	ND	1.00	1.22	ND	1.00	1.05	ND
2.00	2.03	4.05	2.00	2.03	5.31	2.00	2.06	6.20
3.00	2.87	2.71	3.00	2.99	3.65	3.00	3.08	4.93
4.00	4.00	2.10	4.00	4.04	3.39	4.00	4.07	4.76
5.00	4.89	1.84	5.00	4.86	3.00	5.00	4.93	4.40
6.00	5.75	1.74	6.00	5.86	2.96	6.00	5.86	4.39
7.00	6.78	1.59	7.00	6.70	2.95	7.00	6.84	4.24
8.00	7.74	1.56	8.00	7.81	2.92	8.00	7.84	4.23
9.00	8.86	1.50	9.00	8.91	2.84	9.00	8.88	4.20
10.00	9.41	1.49	10.00	9.52	2.73	10.00	9.65	3.94
Limestone Powder								
1 M NaCl			**Control**			**2g/l Detergent**		
Real Mc (%)	**Lab Mc (%)**	**Suction (MPa)**	**Real Mc (%)**	**Lab Mc (%)**	**Suction (MPa)**	**Real Mc (%)**	**Lab Mc (%)**	**Suction (MPa)**
1.00	1.14	ND	1.00	0.83	6.88	1.00	1.14	ND
2.00	2.10	7.47	2.00	1.79	3.40	2.00	1.81	3.57
3.00	2.96	6.44	3.00	2.63	1.88	3.00	2.86	1.36
4.00	3.93	5.82	4.00	3.30	1.04	4.00	3.80	0.942
5.00	4.90	5.81	5.00	4.48	0.69	5.00	4.68	0.846
6.00	5.93	5.68	6.00	5.68	0.46	6.00	5.71	0.484
7.00	6.61	5.13	7.00	6.66	0.36	7.00	6.90	0.429
8.00	7.75	5.11	8.00	7.76	0.33	8.00	7.59	0.38
9.00	8.66	4.99	9.00	8.98	0.20	9.00	8.73	0.293
10.00	9.69	4.80	10.00	9.83	0.28	10.00	9.66	0.361

Lab Mc: Moisture content of specimen measured in the laboratory
Real Mc: Target moisture content

Table 5.3 (c) Total suction values for Quartz Powder

Quartz Powder								
0.25 M NaCl			0.50 M NaCl			0.75 M NaCl		
Real Mc (%)	Lab Mc (%)	Suction (MPa)	Real Mc (%)	Lab Mc (%)	Suction (MPa)	Real Mc (%)	Lab Mc (%)	Suction (MPa)
1.00	0.79	2.80	1.00	0.90	3.86	1.00	0.81	5.89
2.00	1.80	1.88	2.00	1.81	3.72	2.00	1.84	5.08
3.00	2.95	1.82	3.00	2.76	3.33	3.00	2.83	4.88
4.00	3.76	1.65	4.00	3.59	3.33	4.00	2.77	4.51
5.00	4.75	1.74	5.00	4.62	3.27	5.00	4.78	4.28
6.00	5.88	1.61	6.00	5.63	2.91	6.00	5.55	4.40
7.00	6.73	1.43	7.00	6.72	2.88	7.00	6.58	4.28
8.00	7.61	1.41	8.00	7.63	2.78	8.00	7.47	4.25
9.00	8.72	1.40	9.00	8.50	2.75	9.00	8.52	4.11
10.00	9.82	1.39	10.00	9.63	2.71	10.00	9.42	4.00
Quartz Powder								
1 M NaCl			Control			2g/l Detergent		
Real Mc (%)	Lab Mc (%)	Suction (MPa)	Real Mc (%)	Lab Mc (%)	Suction (MPa)	Real Mc (%)	Lab Mc (%)	Suction (MPa)
1.00	0.85	7.61	1.00	0.69	0.960	1.00	0.90	0.55
2.00	1.76	6.58	2.00	1.70	0.815	2.00	1.95	0.32
3.00	2.78	5.90	3.00	2.61	0.380	3.00	2.96	0.27
4.00	3.88	5.56	4.00	3.51	0.140	4.00	3.97	0.18
5.00	4.60	5.44	5.00	4.72	0.220	5.00	4.50	0.19
6.00	5.55	5.06	6.00	5.48	0.072	6.00	5.60	0.14
7.00	6.62	5.26	7.00	6.42	0.118	7.00	6.80	0.12
8.00	7.57	5.05	8.00	7.37	0.137	8.00	7.78	0.13
9.00	8.53	4.96	9.00	8.65	0.125	9.00	8.76	0.08
10.00	9.23	5.55	10.00	9.32	0.152	10.00	9.87	0.062

Lab Mc: Moisture content of specimen measured in the laboratory
Real Mc: Target moisture content

Table 5.3 (d) Total suction values for Fine Glass Beads

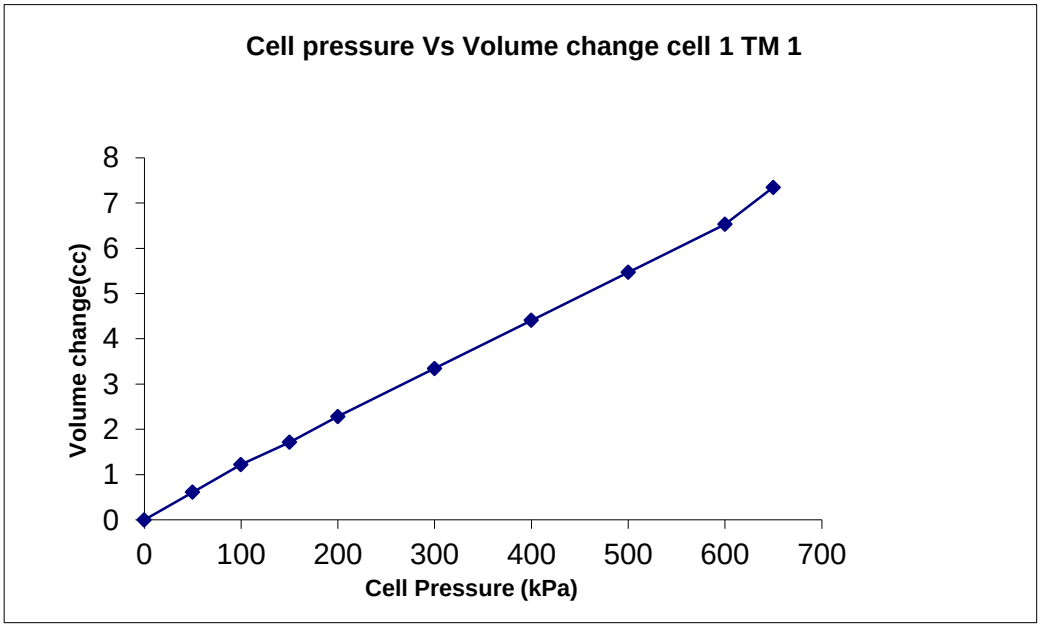
Fine Glass Beads								
0.25 M NaCl			**0.50 M NaCl**			**0.75 M NaCl**		
Real Mc (%)	**Lab Mc (%)**	**Suction (MPa)**	**Real Mc (%)**	**Lab Mc (%)**	**Suction (MPa)**	**Real Mc (%)**	**Lab Mc (%)**	**Suction (MPa)**
1.00	0.91	4.21	1.00	0.89	5.44	1.00	1.08	5.87
2.00	1.90	2.63	2.00	1.80	4.25	2.00	1.83	4.88
3.00	2.92	2.17	3.00	2.82	3.49	3.00	2.63	4.67
4.00	3.82	2.03	4.00	3.75	3.33	4.00	3.77	4.61
5.00	4.71	1.86	5.00	4.62	3.11	5.00	4.56	4.51
6.00	5.74	1.78	6.00	5.61	3.05	6.00	5.59	4.36
7.00	6.59	1.65	7.00	6.58	3.03	7.00	6.56	4.34
8.00	7.71	1.65	8.00	7.51	3.05	8.00	7.60	4.36
9.00	8.54	1.65	9.00	8.30	3.00	9.00	8.39	4.34
10.00	9.60	1.65	10.00	9.48	2.91	10.00	9.23	4.07
Fine Glass Beads								
1 M NaCl			**Control**			**2g/l Detergent**		
Real Mc (%)	**Lab Mc (%)**	**Suction (MPa)**	**Real Mc (%)**	**Lab Mc (%)**	**Suction (MPa)**	**Real Mc (%)**	**Lab Mc (%)**	**Suction (MPa)**
1.00	0.98	7.30	1.00	0.98	2.55	1.00	0.90	2.64
2.00	1.79	6.72	2.00	1.87	1.40	2.00	2.03	1.34
3.00	2.67	6.39	3.00	2.83	0.92	3.00	2.75	0.767
4.00	3.61	6.18	4.00	3.92	0.70	4.00	3.77	0.749
5.00	4.52	5.89	5.00	4.88	0.69	5.00	4.69	0.644
6.00	5.52	5.86	6.00	5.77	0.56	6.00	5.79	0.485
7.00	6.33	5.79	7.00	6.98	0.49	7.00	6.62	0.429
8.00	7.41	5.58	8.00	7.78	0.43	8.00	7.68	0.383
9.00	8.36	5.80	9.00	8.86	0.36	9.00	8.59	0.296
10.00	9.07	5.40	10.00	9.96	0.35	10.00	9.43	0.332

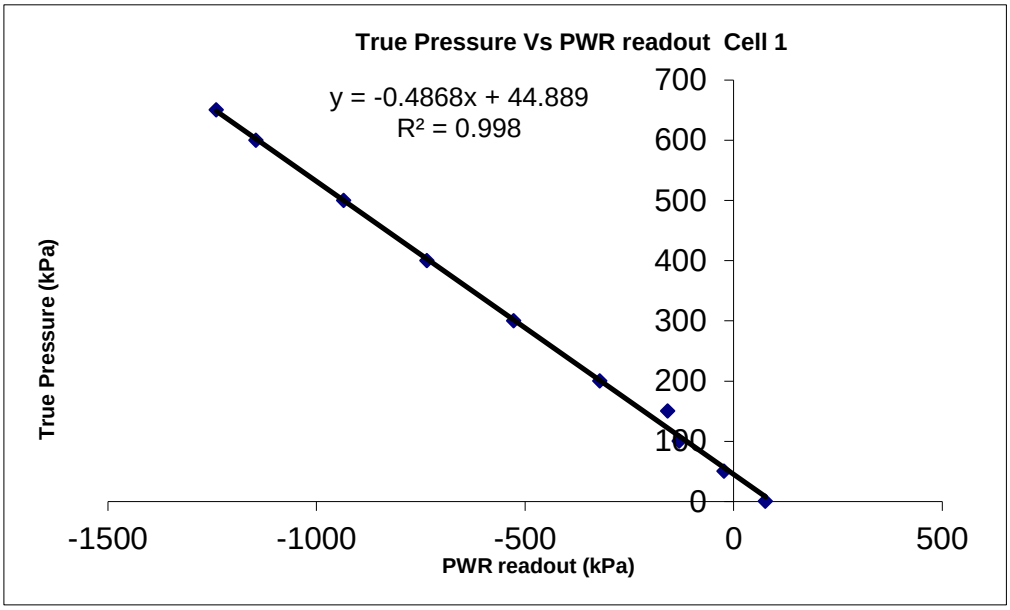
Lab Mc: Moisture content of specimen measured in the laboratory
Real Mc: Target moisture content

Table 5.4 (a) (i) Calibration of triaxial cell and pore pressure transducers

Cell 1

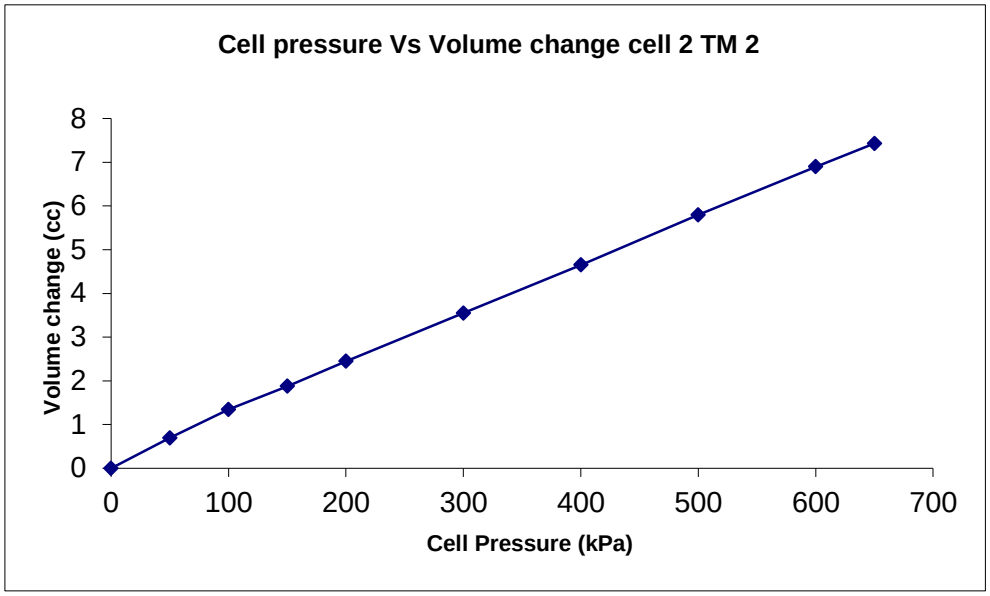
Cell	Height	Actual	Difference	Volume Change	PWR
0	81.0	78.5	0.0	0.0	76
50	79.5	77.0	1.5	0.612	-23
100	78.0	75.5	3.0	1.224	-130
150	76.8	74.3	4.2	1.7136	-158
200	75.4	72.9	5.6	2.2848	-321
300	72.8	70.3	8.2	3.3456	-527
400	70.2	67.7	10.8	4.4064	-735
500	67.6	65.1	13.4	5.4672	-935
600	65.0	62.5	16.0	6.528	-1145
650	63.0	60.5	18.0	7.344	-1240

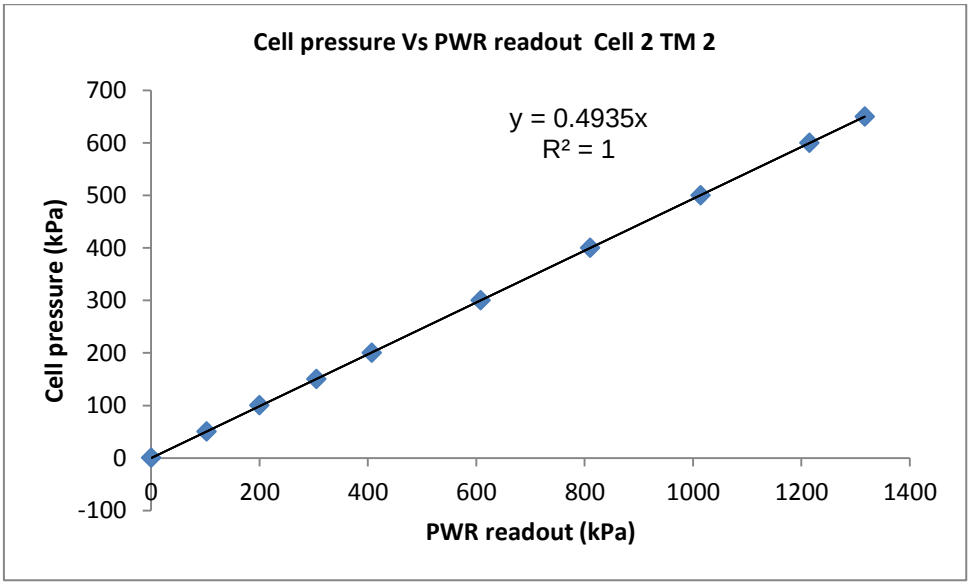




Cell 2

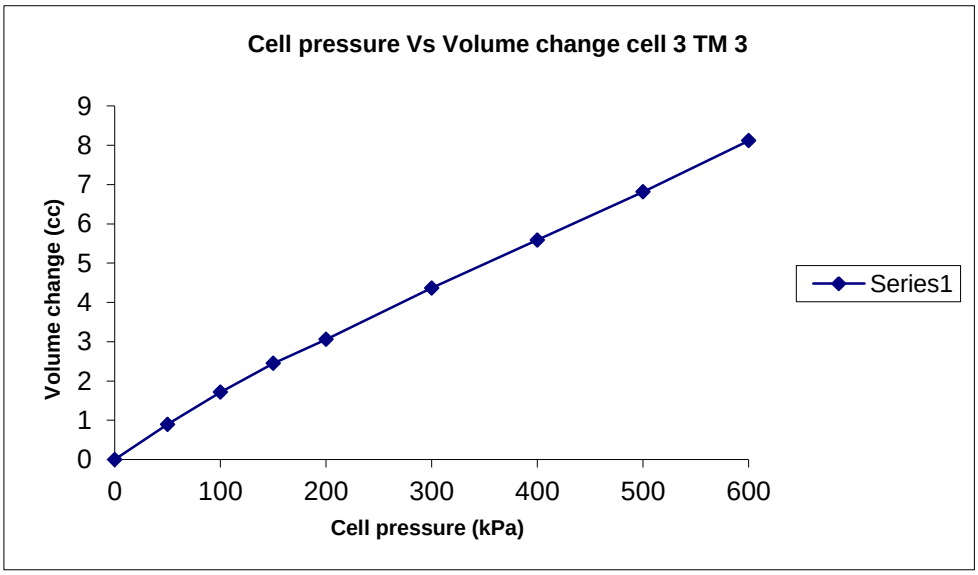
Cell	Height	Actual	Difference	Volume Change	PWR
0	82.1	69.8	0.0	0.0	0
50	80.4	68.1	1.7	0.6936	102
100	78.8	66.5	3.3	1.3464	200
150	77.5	65.2	4.6	1.8768	305
200	76.1	63.8	6.0	2.448	407
300	73.4	61.1	8.2	3.5496	608
400	70.7	58.4	11.4	4.6512	810
500	67.9	55.6	14.2	5.7936	1014
600	65.2	52.9	16.9	6.8952	1215
650	63.9	51.6	18.2	7.4256	1317


Cell pressure Vs Volume change cell 2 TM 2
Volume change (cc)
0
1
2
3
4
5
6
7
8
0
100
200
300
400
500
600
700
Cell Pressure (kPa)


Cell pressure Vs PWR readout Cell 2 TM 2
y = 0.4935x
R² = 1
Cell pressure (kPa)
-100
0
100
200
300
400
500
600
700
0
200
400
600
800
1000
1200
1400
PWR readout (kPa)

Cell 3

Cell	Height	Actual	Difference	Volume Change	PWR
0	86.9	63.3	0.0	0.0	10
50	85.4	62.8	1.5	0.612	50
100	84.0	60.4	2.9	1.836	100
150	82.4	58.8	4.5	1.7136	150
200	81.0	57.4	5.9	2.4072	200
300	78.0	54.4	8.9	3.6312	300
400	75.0	51.4	11.9	4.8552	400
500	72.0	48.4	14.9	6.0792	500
600	69.0	45.4	17.9	7.3032	600.5



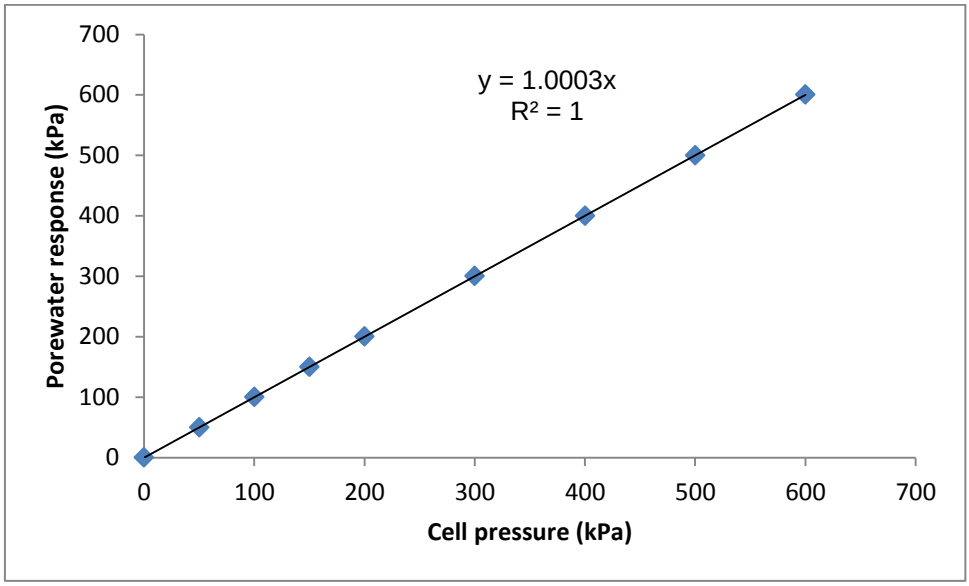


Table 5.4 (a-ii) Calibration of Triaxial Machines

Limestone powder	TM 1	TM2	TM3
Water content (%)	1.91	1.91	1.90
Bulk density (kg/m^3)	1778	1820	1747
Dry density (kg/m^3)	1744	1786	1714
Max Dev. Stress (kPa)	1786.2	1796.2	1786.8
Pore Water R response (kPa)	-78.27	-78.4	-78.5

Table 5.4(b) Results of triaxial strength tests and suctions for limestone powder

Limestone Powder Control					
Moisture content (%)	**PWR (kPa)**	**Suction (kPa)**	**Max. Dev. Stress (kPa)**	**Bulk Density (kg/m^3)**	**Dry Density (kg/m^3)**
2	-78.03	278.03	1765.51	1868	1834
4	-71.00	271.00	1609.00	1954	1882
6	-55.27	255.27	1283.30	1838	1741
8	-63.87	263.87	1047.01	1784	1667
10	-8.97	208.97	1010.36	1801	1642
0.25 M NaCl Limestone Powder					
Moisture content (%)	**PWR (kPa)**	**Suction (kPa)**	**Max. Dev. Stress (kPa)**	**Bulk Density (kg/m^3)**	**Dry Density (kg/m^3)**
2	-77.55	277.55	1876.87	1885	1832
4	-75.00	275.00	1571.51	1874	1797
6	-69.73	269.73	1293.76	1852	1711
8	-28.00	228.00	1053.73	1818	1679
10	-55.16	255.16	936.51	1840	1669
0.50 M NaCl Limestone Powder					
Moisture content (%)	**PWR (kPa)**	**Suction (kPa)**	**Max. Dev. Stress (kPa)**	**Bulk Density (kg/m^3)**	**Dry Density (kg/m^3)**
2	-78.52	278.52	1845.30	1854	1812
4	-26.26	226.26	1448.14	1875	1775
6	-38.00	238.00	1367.52	1902	1796
8	-70.22	270.22	1053.63	1784	1658
10	10.00	190.00	952.80	1762	1593
0.75 M NaCl Limestone Powder					
Moisture content (%)	**PWR (kPa)**	**Suction (kPa)**	**Max. Dev. Stress (kPa)**	**Bulk Density (kg/m^3)**	**Dry Density (kg/m^3)**
2	-70.22	270.22	1763.72	1867	1832
4	-45.74	245.74	1569.29	1859	1785
6	-33.50	233.50	1304.88	1834	1725
8	-22.79	222.79	1184.68	1884	1743
10	-13.50	213.50	969.89	1848	1684

Continuation Table 5.4(b) results of triaxial strength tests and suctions for Limestone Powder

1 M NaCl Limestone Powder					
Moisture content (%)	**PWR (kPa)**	**Suction (kPa)**	**Max. Dev. Stress (kPa)**	**Bulk Density (kg/m^3)**	**Dry Density (kg/m^3)**
2	-78.03	278.03	1811.66	1872	1829
4	-74.13	274.13	1554.52	1899	1825
6	-50.00	250.00	1204.91	1812	1700
8	-44.00	244.00	1265.76	1830	1699
10	-31.62	231.62	1069.16	1783	1628
2g/l Detergent Limestone Powder					
Moisture content (%)	**PWR (kPa)**	**Suction (kPa)**	**Max. Dev. Stress (kPa)**	**Bulk Density (kg/m^3)**	**Dry Density (kg/m^3)**
2	-78.08	276.08	1683.06	1921	1868
4	-40.60	240.60	1564.04	1898	1821
6	-53.61	253.61	1085.85	2017	1821
8	14.00	186.00	1143.00	1758	1618
10	-38.27	238.27	914.11	1754	1592

PWR: Pore water response
Max. Dev. Stress: Maximum deviator stress

Table 5.4 (c) results of triaxial strength tests and suctions for Quartz Powder

Quartz Powder Control					
Moisture content (%)	**PWR (kPa)**	**Suction (kPa)**	**Max. Dev. Stress**	**Bulk Density (kg/m^3)**	**Dry Density (kg/m^3)**
2	176	24.00	1439	1834	1803
4	186	14.00	1500	1994	1926
6	190	10.00	1382	1939	1836
8	190	10.00	1308	1843	1705
10	192	08.00	1098	1847	1689
0.25 M NaCl Quartz Powder					
Moisture content (%)	**PWR (kPa)**	**Suction (kPa)**	**Max. Dev. Stress**	**Bulk Density (kg/m^3)**	**Dry Density (kg/m^3)**
2	191.14	08.86	1342.20	1811	1760
4	192.50	07.50	1268.59	1821	1742
6	193.00	07.00	1103.38	1830	1720
8	192.50	07.50	1105.40	1808	1683
10	199.70	00.30	1076.70	1898	1681
0.50 M NaCl Quartz Powder					
Moisture content (%)	**PWR (kPa)**	**Suction (kPa)**	**Max. Dev. Stress**	**Bulk Density (kg/m^3)**	**Dry Density (kg/m^3)**
2	185.21	14.79	1256.14	1990	1892
4	182.77	17.23	1274.66	1832	1632
6	189.62	10.38	1283.79	1869	1752
8	190.59	09.41	1130.59	1815	1677
10	195.00	05.00	1077.37	1722	1546
0.75 M NaCl Quartz Powder					
Moisture content (%)	**PWR (kPa)**	**Suction (kPa)**	**Max. Dev. Stress**	**Bulk Density (kg/m^3)**	**Dry Density (kg/m^3)**
2	178.00	22.00	1502.70	1832	1799
4	192.06	15.00	1311.63	1884	1816
6	191.00	9.00	1237.32	1830	1725
8	193.53	6.47	1193.47	1760	1632
10	195.4	5.41	1099.78	1862	1711

Continuation Table 5.4 (c) results of triaxial strength tests and suctions for Quartz Powder.

1 M NaCl Quartz Powder					
Moisture content (%)	**PWR (kPa)**	**Suction (kPa)**	**Max. Dev. Stress**	**Bulk Density (kg/m^3)**	**Dry Density (kg/m^3)**
2	169.00	31.00	1376.00	1827	1799
4	188.00	12.00	1288.00	1785	1816
6	188.00	12.00	1230.34	1805	1725
8	179.00	21.00	1052.36	1770	1632
10	199.00	1.00	1024.53	1749	1570
2g/l Detergent Quartz Powder					
Moisture content (%)	**PWR (kPa)**	**Suction (kPa)**	**Max. Dev. Stress**	**Bulk Density (kg/m^3)**	**Dry Density (kg/m^3)**
2	197.42	2.58	1320.80	2075	1841
4	194.63	5.37	1211.30	2083	2000
6	193.00	7.00	1174.17	1844	1748
8	192.05	7.95	1097.72	1749	1628
10	192.53	7.47	1129.96	185 6	1697

PWR: Pore water response
Max. Dev. Stress: Maximum deviator stress

Table 5.4(d) results of triaxial strength tests and suctions for Fine Glass Beads

Fine Glass Beads Control					
Moisture content (%)	**PWR (kPa)**	**Suction (kPa)**	**Max. Dev. Stress**	**Bulk Density (kg/m^3)**	**Dry Density (kg/m^3)**
2	195.96	4.04	578.90	1776	1741
4	191.50	8.50	590.34	1780	1719
6	195.13	8.47	586.16	1670	1587
8	188.43	11.57	582.30	2070	1920
10	191.50	8.50	516.60	1768	1622
0.25 M NaCl Fine Glass Beads					
Moisture content (%)	**PWR (kPa)**	**Suction (kPa)**	**Max. Dev. Stress**	**Bulk Density (kg/m^3)**	**Dry Density (kg/m^3)**
2	193.03	6.97	611.22	1776	1742
4	193.00	7.00	674.69	1727	1664
6	192.50	7.50	673.41	1697	1601
8	192.05	7.95	654.33	2067	1928
10	194.48	5.52	604.38	1783	1627
0.50 M NaCl Fine Glass Beads					
Moisture content (%)	**PWR (kPa)**	**Suction (kPa)**	**Max. Dev. Stress**	**Bulk Density (kg/m^3)**	**Dry Density (kg/m^3)**
2	191.56	8.44	833.86	1732	1700
4	193.51	-6.49	694.63	1723	1661
6	198.50	1.50	651.68	1690	1611
8	197.56	2.44	618.47	1692	1579
10	192.54	7.46	687.14	1678	1520
0.75 M NaCl Fine Glass Beads					
Moisture content (%)	**PWR (kPa)**	**Suction (kPa)**	**Max. Dev. Stress**	**Bulk Density (kg/m^3)**	**Dry Density (kg/m^3)**
2	184.24	15.76	641.35	1790	1755
4	184.79	15.21	675.00	1782	1724
6	192.5	7.50	757.61	1690	1611
8	193.52	6.48	731.22	1750	1629
10	195.42	4.58	605.63	1708	1562

Continuation Table 5.4(d) results of triaxial strength tests and suctions for Fine Glass Beads

1 M NaCl Fine Glass Beads					
Moisture content (%)	**PWR (kPa)**	**Suction (kPa)**	**Max. Dev. Stress**	**Bulk Density (kg/m^3)**	**Dry Density (kg/m^3)**
2	189.61	10.39	766.45	1872	1829
4	188.59	11.41	**742.28**	1899	1825
6	192.50	7.50	739.24	1812	1700
8	195.00	5.00	726.27	1830	1699
10	155.07	44.93	673.83	1783	1628
2g/l Detergent Fine Glass Beads					
Moisture content (%)	**PWR (kPa)**	**Suction (kPa)**	**Max. Dev. Stress**	**Bulk Density (kg/m^3)**	**Dry Density (kg/m^3)**
2	190.10	9.90	579.36	1715	1686
4	188.14	11.86	586.26	1698	1641
6	197.00	3.00	551.99	1671	1582
8	197.40	2.60	660.39	1813	1694
10	198.00	2.00	571.83	1656	1546

PWR: Pore water response
Max. Dev. Stress: Maximum deviator stress

Table 5.4 (e) Results of s-t parameters Limestone Powder

Limestone Powder- Control						
Mc (%)	**½(σ_1-σ_3) (kPa)**	**½(σ_1+σ_3) (kPa)**	**½(σ_1+σ_3)-u_a (kPa)**	**½(σ1+σ3)-u_w (kPa)**	**φ**	**φ'**
2	882.76	1382.76	1182.76	1460.79	48.30	37.20
4	804.50	1304.50	1104.50	1375.50	46.77	35.81
6	641.65	1141.65	941.65	1196.92	42.98	32.43
8	523.51	1023.51	823.51	1087.38	39.49	28.79
10	505.18	1005.18	805.18	1014.15	38.88	29.89
Limestone Powder- 0.25 M NaCl						
Mc (%)	**½(σ_1-σ_3) (kPa)**	**½(σ_1+σ_3) (kPa)**	**½(σ_1+σ_3)-u_a (kPa)**	**½(σ1+σ3)-u_w (kPa)**	**φ**	**φ'**
2	938.43	1438.43	1238.43	1515.98	49.29	38.26
4	785.76	1285.76	1085.76	1360.76	46.38	35.29
6	646.88	1146.88	946.88	1216.61	43.11	32.14
8	526.86	1026.86	826.86	1054.86	39.60	29.98
10	468.26	968.26	768.26	1023.42	37.57	27.24
Limestone Powder- 0.50 M NaCl						
Mc (%)	**½(σ_1-σ_3) (kPa)**	**½(σ_1+σ_3) (kPa)**	**½(σ_1+σ_3)-u_a (kPa)**	**½(σ1+σ3)-u_w (kPa)**	**φ**	**φ'**
2	922.65	1422.65	1222.65	1501.17	49.02	37.94
4	724.07	1224.07	1024.07	1250.33	45.02	35.41
6	683.76	1183.76	983.76	1221.76	44.05	34.05
8	526.82	1026.82	826.82	1097.04	39.60	28.71
10	476.40	976.40	776.40	966.40	37.87	29.55
Limestone Powder- 0.75 M NaCl						
Mc (%)	**½(σ_1-σ_3) (kPa)**	**½(σ_1+σ_3) (kPa)**	**½(σ_1+σ_3)-u_a (kPa)**	**½(σ1+σ3)-u_w (kPa)**	**φ**	**φ'**
2	881.86	1381.86	1181.86	1452.08	48.28	37.41
4	784.65	1284.65	1084.65	1330.38	46.36	36.16
6	652.44	1152.44	952.44	1185.94	43.26	33.39
8	592.34	1092.34	892.34	1115.12	41.61	32.10
10	484.95	984.95	784.95	998.45	38.18	29.07
Limestone Powder- 1M NaCl						
Mc (%)	**½(σ_1-σ_3) (kPa)**	**½(σ_1+σ_3) (kPa)**	**½(σ_1+σ_3)-u_a (kPa)**	**½(σ1+σ3)-u_w (kPa)**	**φ**	**φ'**
2	905.83	1405.83	1205.83	1483.86	48.72	37.64
4	777.26	1277.26	1077.26	1351.39	46.20	35.13
6	602.45	1102.45	902.45	1152.45	41.90	31.53
8	632.88	1132.88	932.88	1176.88	42.74	32.55
10	534.58	1034.58	834.58	1066.20	39.85	30.11

Continuation of Table 5.4 (e) Results of s-t parameters Limestone Powder

Limestone Powder-2g/l Detergent						
Mc (%)	**½(σ_1-σ_3) (kPa)**	**½(σ_1+σ_3) (kPa)**	**½(σ_1+σ_3)-u_a (kPa)**	**½(σ1+σ3)-u_w (kPa)**	**φ**	**φ'**
2	841.53	1341.53	1141.53	1417.61	47.52	36.43
4	782.02	1282.02	1082.02	1322.62	46.30	36.27
6	542.92	1042.92	842.92	1096.54	40.12	29.69
8	571.50	1071.50	871.50	1057.50	41.00	32.73
10	457.05	957.05	757.05	995.32	37.16	27.35

Table 5.4 (f) Results of s-t parameters Quartz Powder

Quartz Powder- Control						
Mc (%)	**½(σ_1-σ_3) (kPa)**	**½(σ_1+σ_3) (kPa)**	**½(σ_1+σ_3)-u_a (kPa)**	**½(σ1+σ3)-u_w (kPa)**	**φ**	**φ'**
2	719.50	1219.50	1019.50	1043.50	44.91	43.61
4	750.00	1250.00	1050.00	1064.00	45.61	44.84
6	691.00	1191.00	991.00	1001.00	44.23	43.68
8	654.00	1154.00	954.00	964.00	43.30	42.74
10	549.00	1049.00	849.00	857.00	40.31	39.86
Quartz Powder- 0.25 M NaCl						
Mc (%)	**½(σ_1-σ_3) (kPa)**	**½(σ_1+σ_3) (kPa)**	**½(σ_1+σ_3)-u_a (kPa)**	**½(σ1+σ3)-u_w (kPa)**	**φ**	**φ'**
2	671.10	1171.10	971.10	979.96	43.74	43.24
4	634.29	1134.29	934.29	941.79	42.78	42.36
6	551.69	1051.69	851.69	858.69	40.39	40.00
8	552.70	1052.70	852.70	860.20	40.42	40.00
10	538.35	1038.35	838.35	838.65	39.97	39.96
Quartz Powder- 0.50 M NaCl						
Mc (%)	**½(σ_1-σ_3) (kPa)**	**½(σ_1+σ_3) (kPa)**	**½(σ_1+σ_3)-u_a (kPa)**	**½(σ1+σ3)-u_w (kPa)**	**φ**	**φ'**
2	628.07	1128.07	928.07	921.66	42.61	42.98
4	637.33	1137.33	937.33	954.56	42.86	41.91
6	641.89	1141.89	941.89	933.37	42.98	43.47
8	565.29	1065.29	865.29	874.71	40.81	40.28
10	538.68	1038.68	838.68	843.68	39.98	39.70
Quartz Powder- 0.75 M NaCl						
Mc (%)	**½(σ_1-σ_3) (kPa)**	**½(σ_1+σ_3) (kPa)**	**½(σ_1+σ_3)-u_a (kPa)**	**½(σ1+σ3)-u_w (kPa)**	**φ**	**φ'**
2	751.35	1251.35	1051.35	1073.35	45.64	44.45
4	655.81	1155.81	955.81	963.76	43.35	42.90
6	618.66	1118.66	918.66	927.66	42.35	41.85
8	596.73	1096.73	896.73	903.20	41.74	41.37
10	550.12	1050.12	850.12	843.72	40.34	40.71
Quartz Powder- 1M NaCl						
Mc (%)	**½(σ_1-σ_3) (kPa)**	**½(σ_1+σ_3) (kPa)**	**½(σ_1+σ_3)-u_a (kPa)**	**½(σ1+σ3)-u_w (kPa)**	**φ**	**φ'**
2	688.00	1188.00	988.00	1019.00	44.16	42.49
4	644.00	1144.00	944.00	956.00	43.04	42.37
6	615.17	1115.17	915.17	927.17	42.26	41.59
8	526.18	1026.18	826.18	847.18	39.58	38.42
10	512.27	1012.27	812.27	813.27	39.12	39.06

Continuation of Table 5.4(f) Results of s-t parameters Quartz Powder

Quartz Powder-2g/l Detergent						
Mc (%)	**½(σ_1-σ_3) (kPa)**	**½(σ_1+σ_3) (kPa)**	**½(σ_1+σ_3)-u_a (kPa)**	**½(σ1+σ3)-u_w (kPa)**	**φ**	**φ'**
2	660.40	1160.40	960.40	962.98	43.46	43.32
4	605.65	1105.65	905.65	911.02	41.99	41.69
6	587.09	1087.09	887.09	894.09	41.46	41.06
8	548.8	1048.86	848.86	856.81	40.31	39.86
10	564.98	1064.98	864.98	857.97	40.80	41.21

Table 5.4 (g) Results of s-t parameters Fine Glass Beads

Fine Glass Beads- Control						
Mc (%)	**½(σ_1-σ_3) (kPa)**	**½(σ_1+σ_3) (kPa)**	**½(σ_1+σ_3)-u_a (kPa)**	**½(σ1+σ3)-u_w (kPa)**	**φ**	**φ'**
2	289.45	789.45	589.45	593.49	29.42	29.20
4	295.17	795.17	595.17	603.67	29.75	29.29
6	293.08	793.08	593.08	597.95	29.63	29.36
8	291.15	791.15	591.15	602.72	29.52	28.90
10	258.30	758.30	558.30	566.80	29.57	27.12
Fine Glass Beads - 0.25 M NaCl						
Mc (%)	**½(σ_1-σ_3) (kPa)**	**½(σ_1+σ_3) (kPa)**	**½(σ_1+σ_3)-u_a (kPa)**	**½(σ1+σ3)-u_w (kPa)**	**φ**	**φ'**
2	305.61	805.61	605.61	612.58	30.32	29.94
4	337.35	837.35	637.35	644.35	31.97	31.59
6	336.70	836.70	636.70	644.20	31.94	31.53
8	327.17	827.17	627.17	635.12	31.46	31.02
10	302.19	802.19	602.19	596.38	30.14	30.46
Fine Glass Beads - 0.50 M NaCl						
Mc (%)	**½(σ_1-σ_3) (kPa)**	**½(σ_1+σ_3) (kPa)**	**½(σ_1+σ_3)-u_a (kPa)**	**½(σ1+σ3)-u_w (kPa)**	**φ**	**φ'**
2	416.93	916.93	716.93	725.37	35.58	35.10
4	347.32	847.32	647.32	431.02	32.47	*
6	325.84	825.84	625.84	627.34	31.39	31.31
8	309.24	809.24	609.24	611.68	30.52	30.38
10	343.57	843.57	643.57	651.03	32.28	31.87
Fine Glass Beads - 0.75 M NaCl						
Mc (%)	**½(σ_1-σ_3) (kPa)**	**½(σ_1+σ_3) (kPa)**	**½(σ_1+σ_3)-u_a (kPa)**	**½(σ1+σ3)-u_w (kPa)**	**φ**	**φ'**
2	320.68	820.68	620.68	636.44	31.12	30.27
4	337.50	837.50	637.50	652.71	31.98	31.15
6	378.80	878.80	678.80	686.30	33.94	33.52
8	365.61	865.61	665.61	672.09	33.33	32.97
10	302.81	802.81	602.81	423.70	30.17	45.64
Fine Glass Beads - 1M NaCl						
Mc (%)	**½(σ_1-σ_3) (kPa)**	**½(σ_1+σ_3) (kPa)**	**½(σ_1+σ_3)-u_a (kPa)**	**½(σ1+σ3)-u_w (kPa)**	**φ**	**φ'**
2	383.23	883.23	683.23	693.62	34.14	33.56
4	371.14	871.14	671.14	682.54	33.59	32.96
6	369.62	869.62	669.62	677.12	33.52	33.1
8	363.14	863.14	663.14	668.14	33.22	32.94
10	336.92	836.92	836.92	681.85	31.95	29.63

Continuation of Table 5.4 (g) results of s-t parameters Fine Glass Beads

Fine Glass Beads -2g/l Detergent						
Mc (%)	**½(σ_1-σ_3) (kPa)**	**½(σ_1+σ_3) (kPa)**	**½(σ_1+σ_3)-u_a (kPa)**	**½(σ1+σ3)-u_w (kPa)**	**φ**	**φ'**
2	289.68	789.68	589.68	559.58	29.44	28.91
4	293.13	793.13	593.13	604.99	29.63	29.00
6	275.99	755.99	575.99	578.99	28.65	28.48
8	330.19	830.19	630.19	623.48	31.61	31.99
10	285.92	785.92	585.92	587.92	29.22	29.11

Table 5.5 (a) Consolidated drained tests for Limestone powder

Limestone powder					
	Control with pure water	1M NaCl mix Water **BP**	1M NaCl mix. Salt **BP**	Detergent mix. Water **BP**	Detergent mix. Detergent **BP**
Peak Max. Deviator stress **(kPa)**	821	821	763	772	819
Cell Pressure **(kPa)**	450	450	500	500	500
Back pressure **(kPa)**	150	150	200	200	200
PWR **(kPa)**	154	149	197	197.5	197
Bulk density **(kg/m^3)**	1919	1815	1791	1746	1752
Dry density **(kg/m^3)**	1573	1504	1481	1450	1453

BP: Backwater Pressure
PWR: Porewater Response

Table 5.5 (b) Consolidated drained tests for Quartz powder

Quartz powder					
	Control with pure water	1M NaCl mix Water BP	1M NaCl mix. Salt BP	Detergent mix. Water **BP**	Detergent mix. Detergent **BP**
Peak Max. Deviator stress **(kPa)**	1151	1168.5	1155.2	1155	1138
Cell Pressure **(kPa)**	400	400	400	450	400
Back pressure **(kPa)**	100	100	100	150	100
PWR **(kPa)**	106.5	100.5	198	153.5	97.5
Bulk density **(kg/m^3)**	2050	1771	1783	1827	1742
Dry density **(kg/m^3)**	1622	1490	1516	1493	1451

BP: Backwater Pressure
PWR: Porewater Response

Table 5.5 (c) Consolidated drained tests for Fine Glass beads

Fine Glass beads					
	Control with pure water	1M NaCl mix Water BP	1M NaCl mix. Salt BP	Detergent mix. Water **BP**	Detergent mix. Detergent **BP**
Peak Max. Deviator stress **(kPa)**	464.32	406.32	412.83	473	398
Cell Pressure **(kPa)**	400	400	400	400	400
Back pressure **(kPa)**	100	100	100	100	100
PWR **(kPa)**	116.5	104	104	99	99
Bulk density **(kg/m^3)**	1582	1559	1593	1529	1662
Dry density **(kg/m^3)**	1263	1229	1271	1177	1308

BP: Backwater Pressure
PWR: Porewater Response

Table 5.5 d. The φ´ values of the consolidated drained tests.

Soil	Mix	φ'
Limestone Powder	water-water	35.5°
	salt-salt	35.9°
	salt-water	35.3°
	det-det	35.1°
	det-water	34.2°
Quartz powder	water-water	41.5°
	salt-salt	47.8°
	salt-water	41.4°
	det-det	40.8°
	det-water	41.4°
Glass beads	water-water	26.8°
	salt-salt	24.3°
	salt-water	24.0°
	det-det	23.5°
	det-water	26.1°

Table 5.6 Shear strength test results of limestone powder in different saturated solutions then exposed to atmospheres of distilled water, 1M NaCl and detergent. Initial water content 6%.Total exposure time 6 months

		After 3 months exposure					After 6 months exposure			
Soil Mixed with	Dried over saturated solutions	Peak Max. dev. Stress (kPa)	Water content (%)	ρ_b (kg/m^3)	ρ_d (kg/m^3)	Re-Exposed to	Max dev. Stress (kPa)	Water content (%)	ρ_b (kg/m^3)	ρ_d (kg/m^3)
Water	K_2SO_4	1480	0.97	1794	1776	water	-	-	-	-
						NaCl	1876	1.21	1754	1734
						Det	1345	1.45	1755	1730
	$ZnSO_4$	1111	1.44	1816	1790	Water	1593	1.48	1771	1745
						NaCl	-	-	-	-
						Det	1714	2.76	1773	1725
	Na_2SO_4	1176	3.97	1869	1770	Water	1342	1.19	1775	1754
						NaCl	1924	1.41	1742	1723
						Det	1299	1.53	1754	1728
1 M NaCl	K_2SO_4	1068	4.48	1931	1848	Water	1181	6.23	2024	1905
						NaCl	-	-	-	-
						Det	903	7.69	1866	1733
	$ZnSO_4$	-	-	-	-	Water	1080	6.18	1879	1786
						NaCl	1078	3.86	1812	1739
						Det	1034	10.6	2094	1894
	Na_2SO_4	1395	2.02	1774	1739	Water	1017	8.46	1923	1773
						NaCl	1203	1.08	1851	1782
						Det	-	-	-	-
2g/L Detergent	K_2SO_4	1538	1.04	1753	1735	Water	1213	2.04	1793	1757
						NaCl	1010	4.62	1873	1790
						Det	1271	0.84	1744	1730
	$ZnSO_4$	1372	1.57	1798	1770	Water	1334	2.88	1828	1777
						NaCl	1361	1.18	1759	1873
						Det	1208	1.95	1738	1712
	Na_2SO_4	1677	0.75	1729	1716	Water	1248	1.22	1749	1728
						NaCl	1454	1.13	1731	1712
						Det	1326	1.53	1738	1712